MUTATIONAL AND FUNCTIONAL STUDIES ON PROTEINS OF THE FERREDOXIN/THIOREDOXIN REGULATORY SYSTEM

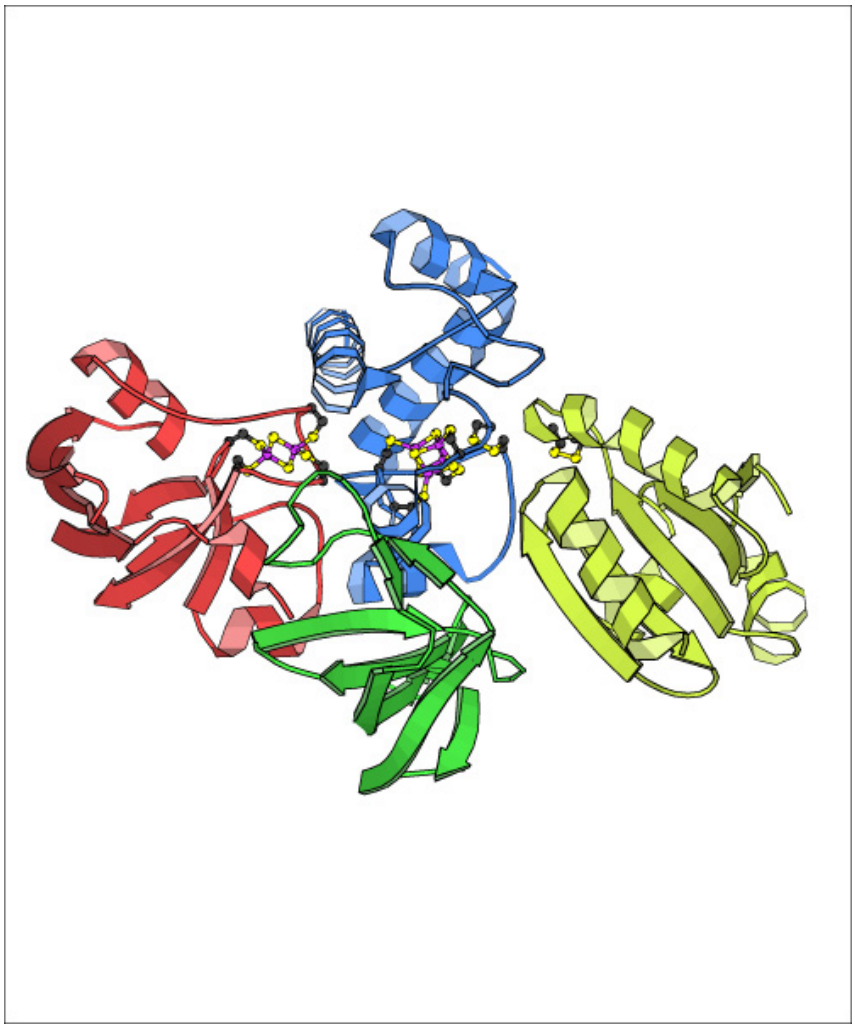

Wanda Manieri

Neuchâtel 2002

IMPRIMATUR POUR LA THESE

Mutational and functional studies on proteins of the ferredoxin/thioredoxin regulatory system

de Mme Wanda Manieri

UNIVERSITE DE NEUCHATEL

FACULTE DES SCIENCES

La Faculté des sciences de l'Université de Neuchâtel sur le rapport des membres du jury,

Mme M. Miginiac-Maslow (Paris),
MM. P. Schürmann (directeur de thèse) et
J.-M. Neuhaus

autorise l'impression de la présente thèse.

Neuchâtel, le 19 novembre 2002

Le doyen:

F. Zwahlen

Remerciements

Je voudrais exprimer ma profonde gratitude au Professeur Peter Schürmann de m'avoir accueillie dans son groupe et dirigé mon travail. Je lui suis très reconnaissante de la disponibilité qu'il a eu à mon égard, de son aide, de la confiance et les libertés qu'il m'a accordés durant ces quatre année de recherche et surtout de la possibilité qu'il m'a donné de découvrir «le fabuleux monde de la FTR».

Je tiens égalment à remercier le Dr Miroslawa Miginiac-Maslow et le Professeur Jean-Marc Neuhaus pour avoir accepté de faire partie du jury de ma thèse.

Je remercie très fortement Nadine Paris, Sophie Marc-Martin et Anne-Lise Stritt-Etter pour les excellents moments professionnels passés ensemble et surtout pour leur amitié, leur disponibilité et leur bonne humeur très communicative.

Mes remerciements s'adressent également à tous les membres du laboratoire de Biochimie Végétale, avec une pensée particulière pour Wassila Ghedamsi, Coralie Gigon et Ian Cuesta qui, dans le cadre de leur formation, ont contribués à ce travail.

Je remercie tous mes collègues de biologie et de chimie, spécialement Jean-François Dumas pour les nombreux conseils d'ordre informatique qu'il m'a donnés.

Enfin je remercie toute ma famille: «Colgo l'occasione di esprimervi di tutto cuore la mia riconoscenza per il vostro sostegno, per la fiducia che mi avete incondizionatamente dimostrato in tutti questi anni e per il vostro grande amore. Grazie per essermi sempre stati vicini.»

Abbreviations

ATP	adenosine-5'-triphosphate
bp	base pair
°C	Celsius degree
Cyt	cytochrome
cm	centimeter
Da	Dalton
Dth	dithionite
DTT	dithiothreitol
EDTA	ethylenediamino-tetraacetic acid
FBPase	fructose 1,6-bisphosphatase
Fd	ferredoxin
Fd/Trx	ferredoxin/thioredoxin
FPLC	fast protein liquid chromatography
FTR	ferredoxin:thioredoxin reductase
FNR	ferredoxin:NADP reductase
IgG	immunoglobuline G
HMW	high molecular weight
IM	phosphoglucose isomerase
IPTG	isopropyl-β-D-thiogalactoside
L	liter
LB	Luria-Bertani medium
M	molar
mA	milliamper (10^{-3} A)
mBBr	Thiolite® Monobromobimane Reagent
MDH	malate dehydrogenase
2-MET	2-mercapto-ethanol
mg	milligramme
min	minute
mV	millivolt
PCR	polymerase chain reaction
PMSF	phenylmethylsulfonyl fluoride
PRK	phosphoribulokinase
rpm	revolutions per minute
RUBISCO	ribulose 1,5-bisphosphate carboxylase
SBPase	sedoheptulose 1,7-bisphosphatase
SDS	sodium dodecylsulfate
SUA	variable subunit of FTR
SUB	catalytic subunit of FTR
TEA	triethanolamine
TEMED	N,N,N',N'-tetramethyl-ethylendiamine

Trx	thioredoxin
Tris	tris-(hydroxymethyl)-aminomethane
V	volt

Index

1 Introduction

1.1 An Overview of Photosynthesis

Photosynthesis is the process by which light energy is converted to the chemical energy of a phosphoanhydride bond in ATP and to reducing power in the form of NADPH and stored in the chemical bonds of carbohydrates. The overall reaction of oxygen-generating photosynthesis, namely

$$6CO_2 + 6H_2O \longrightarrow 6O_2 + C_6H_{12}O_6$$

is the reverse of the reaction by which carbohydrates are oxidized to CO_2 and H_2O. In plants this process occurs in the chloroplasts.
The main products of photosynthesis are polymers of six-carbon sugars, usually sucrose or starch. Leaf starch, an insoluble polymer of glucose, is stored in the chloroplast. Sucrose, a water-soluble disaccharide, is synthesized in the cytosol from three-carbon precursors generated in the chloroplast and then transported from the leaf through the phloem to other parts of the plants; nonphotosynthetic (nongreen) plant tissues like roots and seeds metabolize sucrose for energy.
Oxygen is also formed during photosynthesis in plants, in eukaryotic single-celled algae, and in two groups of photosynthetic prokaryotes, the *cyanobacteria* (formerly called the *blue-green algae*) and the *prochlorophytes*.

1.1.1 Photosynthesis consists of both "Light" and "Dark" reactions

It is convenient to divide the processes of photosynthesis into four stages, each occuring in a defined area of the chloroplast:

1 *Absorption of Light.* The initial step in Photosynthesis is the absorption of light by chlorophyll attached to proteins in the thylacoid membranes. The energy of the absorbed light is used first to remove electrons from water, in green plants, forming oxygen and then to transfer the electrons to a primary acceptor. All these reactions occur in a complex of proteins, termed a *photosystem,* in the thylakoid membrane.

2. *Electron Transport.* Electrons move from the primary electron acceptor through a chain of electron transport molecules in the thylakoid membrane until they reach the ultimate electron acceptor, usually $NADP^+$, reducing it to NADPH. The transport of electrons is coupled to the movement of protons across the membrane from the stroma to the thylakoid lumen, forming a pH gradient across the thylakoid membrane (Fig.1).

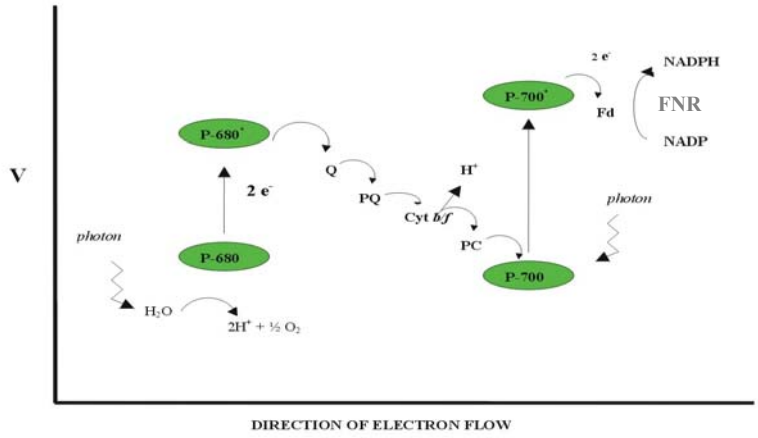

Fig.1. Scheme of electron transport chain of photosynthesis

3. *Generation of ATP.* Protons move down their concentration gradient from the thylakoid lumen to the stroma through a set of transport proteins, the CF_0CF_1 complex that couples proton movement to the synthesis of ATP from ADP and P_i.

4. *CO_2 Fixation - the Conversion of CO_2 into Carbohydrates.* The ATP^{4-} and NADPH generated by the second and third stages of photosynthesis provide the energy and the electrons to drive the synthesis of polymers of six-carbon sugars from CO_2 and H_2O.

All four stages of phosynthesis are tightly coupled and controlled so as to produce the amount of carbohydrate required by the plant. Almost all reactions involving the absorption of light and the formation of NADPH and ATP (stages 1-3) are catalyzed by proteins in the thylakoid membrane. The enzymes that incorporate CO_2 into chemical intermediates (the process of CO_2 fixation) and then convert it to starch are soluble constituents of the chloroplast stroma. The enzymes that form sucrose from three-carbon intermediates are in the cytosol.
The reactions that generate ATP and NADPH are *directly* dependent on light energy and thus stages 1-3 are called the *light reactions* of photosynthesis.

The reactions in stage 4, although still often called the *dark reactions*, are not independent of light since several of the enzymes involved in these reactions need to be activated by light.

1.1.2 Plants utilize two photosystems, PSI and PSII, with different functions in photosynthesis

Higher plants and algae generate oxygen. To do this they utilize two photosystems, termed PSI and PSII. Both PSII and PSI contain chlorophyll *a* and *b* and both support light-driven transport of an electron across the thylakoid membrane. More importantly, the two photosystems differ significantly in their functions.
PSII splits water: the absorption of a photon causes an electron to move from P_{680} on the lumen side to an acceptor quinone on the stromal side of the membrane and the resultant positive charge on the P_{680} strips an electron from water, forming O_2 as well as protons that remain in the thylakoid lumen and form part of the proton-motive force (see Fig. 1).
The electrons in the acceptor quinone move, via a series of carriers, to the electron donor site on the luminal surface of the PSI reaction center; during this movement, additional protons are transported into the thylakoid lumen.
PSI uses the energy of an absorbed photon to transfer the electron to ferredoxin, on the stromal surface, and from there electrons are passed to the ultimate acceptor, $NADP^+$ forming NADPH via ferredoxin:NADP reductase (FNR).

1.2 The ferredoxin/thioredoxin system

1.2.1 Link to oxygenic photosynthesis

The ferredoxin/thioredoxin system, consisting of ferredoxin (Fd), ferredoxin:thioredoxin reductase (FTR), thioredoxin and target enzyme, functions as a general mechanism of light-mediated enzyme regulation. In eukaryotes, this system is located in chloroplasts and it is directly linked to the absorption of light.
Light plays a regulatory role in carbon reduction (Buchanan,1980; Scheibe, 1991) and related processes in oxygenic photosynthetic organism. Key photosynthetic

enzymes functional in assimilation are light-activated whereas degradative enzymes are light-deactivated. Since these enzymes, and the opposing pathways, coexist in the same cell compartment, a regulatory light-dark system is indispensable to chloroplasts to maintain an enzyme order by assuring that carbon dioxide assimilation is enhanced during the day, and carbohydrate degradation occurs primarily at night (Fig. 2).

Fig. 2. Activation scheme of Calvin-Benson enzymes by light and their deactivation in the dark

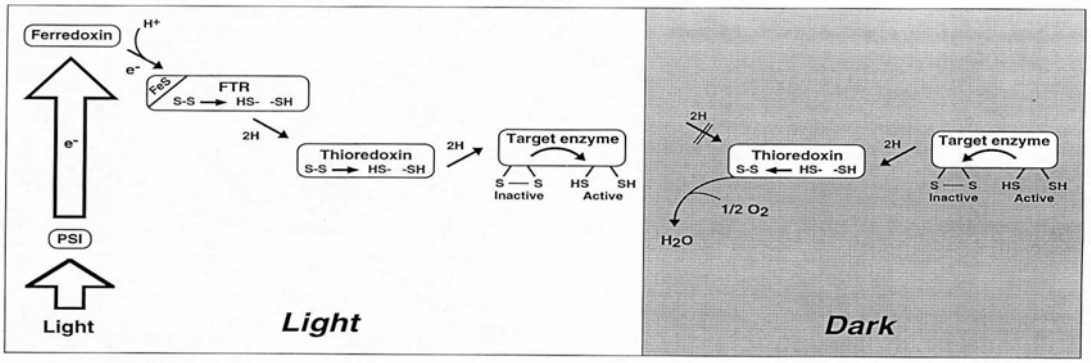

This light-dark regulation is accomplished by the ferredoxin/thioredoxin system. The mechanism is simple (see Fig. 2): upon illumination, sunlight photons captured by chlorophyll pigments in the photosystems are used to oxidize water and reduce ferredoxin. The reducing power of ferredoxin is then transferred via FTR to thioredoxin that interacts with selected target enzymes. As a consequence of the reduction of regulatory disulfides, this interaction brings about structural changes in the active site of the target enzymes.

1.2.2 Ferredoxin

Plant-type Fds are one-electron-carrier proteins containing one iron-sulfur cluster [2Fe-2S] with a very low oxidation-reduction potential of typically –400 mV. *In vivo,* Fd distributes electrons coming from PSI to several enzymes which are ferredoxin-dependent like FNR, sulfite reductase, nitrite reductase, acetyl CoA carboxylase, ferredoxin-dependent glutamate synthase (GOGAT) and FTR. Ferredoxin thus plays a key role in chloroplast metabolism in dispatching the reducing power to different metabolic pathways.

Amino acid sequences of over 70 plant-type ferredoxins are highly homologous and three-dimensional structures of five plant-type ferredoxins from cyanobacteria (Fukuyama *et al.*, 1995) to higher plants (Binda *et al.*, 1998) are also conserved in terms of backbone and side chain structures.
Ferredoxin and each ferredoxin-dependent enzyme form a 1:1 protein-protein complex. This specific interaction is considered to be important for efficient electron transfer between the two proteins. Among the physical and chemical forces involved in protein interactions, such as hydrophobic interactions, electrostatic forces and hydrogen bonding, several lines of evidence (chemical modification experiments, cross-linking experiments, and computer modeling studies) indicate that the complex is mainly formed as a result of electrostatic forces through the negative charges of ferredoxin and the positive charges of each enzyme. Ionic strength affects the transient kinetics of electron transfer from ferredoxin to FNR also indicating that the complementary electrostatic charges influence complex formation (Walker, M. C. *et al.*, 1991).
In the spinach protein, a cluster of three acidic residues (namely Glu92-94) has been suggested to be involved in the binding with positively charged residues of FTR (de Pascalis *et al.*, 1994). In the chloroplast-type ferredoxins, the acidic cluster is fairly well conserved. In more details: Glu92 is strictly conserved, Glu93 is conservatively substituted by Asp in two cases or changed to Gln and Glu94 is more variable but in such a way that at least one acidic residue is present at the position 93 or 94.
The three-dimensional structure has been determined for spinach ferredoxin (Binda *et al.*, 1998). The structure shows a fold with three α-helices, a five-stranded β-sheet and a long loop containing four cysteine ligands to the iron atoms (Fig. 3). The iron-sulfur cluster is located towards the outer edge of the molecule in the loop. The two irons are tetrahedrally coordinated by inorganic sulfide ions and cysteine residues.

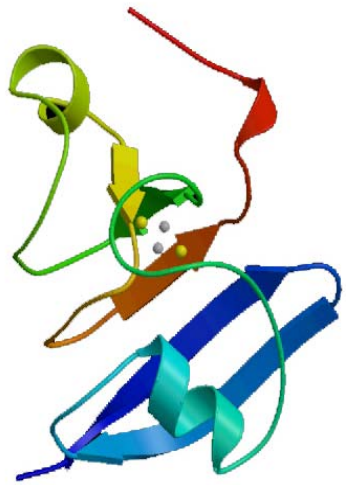

Fig. 3. Spinach Ferredoxin structure. Fd structure is characterized by a central core formed by a five-stranded β-sheet (arrows) and three α-helices (in green, red and light blue in picture) and a long loop containing the cluster (yellow/grey balls). The orientation of the cluster is such that the Fe1 atom is more exposed to solvent whereas Fe2 is positioned within the protein interior.

1.2.3 Ferredoxin:thioredoxin reductase

Chloroplast FTRs are soluble, heterodimeric proteins with M_r of about 25 kDa and are localized in the chloroplast stroma.
FTR, which transduces the general redox signal from ferredoxin to thioredoxin, is a unique iron-sulfur enzyme composed of two dissimilar subunits, designated the catalytic and variable subunit. The catalytic subunit of the enzyme from different organism has a constant size of about 13 kDa, whereas that of the variable subunit ranges from 8 to 13 kDa.
FTR has been purified and characterized from different organisms: spinach (Schürmann, 1981; Droux *et al*., 1987), maize (Iwadate *et al*., 1996, 1998; Droux *et al*., 1987) and *Nostoc* (Droux *et al*., 1987), soybean (Schürmann, unpublished data) and *Chlamydomonas reinhardtii* (Huppe *et al*., 1990). The FTRs from spinach (Gaymard & Schürmann, 1995; Gaymard *et al*., 2000) and *Synechocystis* (Schwendtmayer *et al*., 1998) have been cloned and expressed as perfectly functional enzymes in *E.coli*, and the three-dimensional structure of FTR from *Synechocystis* has been determined (Dai, 1998; Dai *et al*., 2000).

1.2.3.1 Variable and catalytic subunits of spinach ferredoxin:thioredoxin reductase

The variable subunit of spinach FTR, which appears to have only a structural function, is a polypeptide of 112 amino acids with an isoelectric point of 5.4. It is a heart-shaped molecule with a β-barrel constituting the main body, two loops forming the upper and outer part of the heart on the top of which sits the essentially α-helical catalytic subunit.
Sequence alignment of known precursor of the variable subunit from different organism shows, disregarding the transit peptides, a rather low conservation (Fig. 4).

Fig. 4. Sequence alignment of known variable subunits of FTRs. The transit peptide of spinach FTR is in italics. Alignement data: red-identity; green-strongly similar; blue-weakly similar; black-different.

```
Spinacia        --------MTTGVAVMSSATAASTATATAAATARIPLFLSRNNSSATVCSTLRCRTITRT
Zea mays        ------------------------------------------------------------
Solanum         ----------MTASTSAFFSSSILNIPNSKNQSLIIPSHKNILNPN-PFTQIKIHKSRNP
Synechocystis   ------------------------------------------------------------
Arabidopsis     MSSQIALSPAIAAAIRRPSSHDCLSASATTATATPMALKSCIVAPLSLFTSQSQIKHSSS

                          1         10        20        30        40
                          |         |         |         |         |
Spinacia        RTRERLAICCEVALKSDSSTGFDSSSSSSPPEEDEELKKNLEKVGCKVKVKSPLKVYH--
Zea mays        ------------------EVAS--------DDVAAEEAAAAPKIGRRVRVTAPLRVYH--
Solanum         QKPNGYFISKSVTVDNPSTVSSTSSLSVD-EGVDEKDAAAMGKVGSKVRVTVPLKVYH--
Synechocystis   ----------------------------------------MNVGDRVRVTSSVVVYHHP
Arabidopsis     RKTSRTTIRCDVAIKSADSINADANPSSSPSSEEEIEAEAKAKIGSRVRVTAPLKVYH--

                  50        60        70        80        90          100
                  |         |         |         |         |           |
Spinacia        VPKLPEVELTPDMVGVIKQYVGFWKGKYISPNYPFKVEYRIDVPDRGS--VKLVVHLKEE
Zea mays        VLKAPDLDIQG-MEGVVKQYVCVWKGKRVTANFPFKVEFELA-VEGQPKPVRFFAHLRED
Solanum         EPKVPELDLDG-RIGTVKQYVAVHKGKQISANLPYKVQFVVDDLEGRSTPVKFSAHLKED
Synechocystis   EHKKTAFDLQG-MEGEVAAVLTEWQGRPISANLPVLVKFEQR----------FKAHFRPD
Arabidopsis     VNRVPEVDLEG-MEGKLKDYVAVWKGKRISANLPYKIEFFKE-IEGRG-LVKFVSHLKED

                    110
                    |
Spinacia        EFEIIAE
Zea mays        EFEFVDG
Solanum         EFEFLD-
Synechocystis   EVTLIED
Arabidopsis     EFEFIDQ
```

The mature catalytic subunit of spinach FTR is a polypeptide of 113 amino acids (Fig. 5) with an isoelectric point of 5.3 and an overall α-helical structure containing five helices. The catalytic subunits of different species have, in contrast to their variable counterparts, a highly conserved primary structure and among the strictly conserved residues are seven Cys, six of them are organized in two CPC and one CHC motifs.

Fig. 5. **Sequence alignment of known catalytic subunits of FTRs.** The transit peptide of spinach FTR is not given and the one from *Zea mays* is in italics. Alignement data: red-identity; green-strongly similar; blue-weakly similar; black-different.

```
                                                  1            10        20
                                                  |            |         |
Spinacia        ------------------------------------AD----PSDKSMEVMRKFSEQFCRK
Solanum         MRTLQASTSYSVGFGISSFATRPKPSTHRCLTVAKME----PSEKSVEIMRKFSEQYARR
Arabidopsis     -MNLQA-VSCSFGFLSSPLGVTPRTSFRRFVIRAKTE----PSEKSVEIMRKFSEQYARR
Zea mays        MTSTVTTTVGCGGLPVRPLSTATRGRPRRCAVRAQAAGADASNDKSVEVMRKFSEQYARR
Synechocystis   ------------------------------MTSSDTQ-----NNKTLAAMKNFAEQYAKR

                        30        40        50        60        70        80
                        |         |         |         |         |         |
Spinacia        SDTYFCVDKSVTAVVIKGLADHRDTLGAPLCPCRHYDDKEAEAKQGFWNCPCVPMRERKE
Solanum         SETYFCMDKGVTSVVIKGLAEHKDTLGAPLCPCRHYDDKAAEAQQGFWNCPCVPMRERKE
Arabidopsis     SGTYFCVDKGVTSVVIKGLAEHKDSYGAPLCPCRHYDDKAAEVGQGFWNCPCVPMRERKE
Zea mays        SNTFFCADKTVTAVVIKGLADHRDTLGAPLCPCRHYDDKAAEVAQGFWNCPCVPMRERKE
Synechocystis   TDTYFCSDLSVTAVVIEGLARHKEELGSPLCPCRHYEDKEAEVKNTFWNCPCVPMRERKE

                        90        100       110
                        |         |         |
Spinacia        CHCMLFLTPDNDFAGKEQTITLDEIREVTSNM-
Solanum         CHCMLFLTPDNDFAGEEQTISMEEIKETTANM-
Arabidopsis     CHCMLFLTPDNDFAGKDQTITSDEIKETTANM-
Zea mays        CHCMLFLTPDNDFAGKDQVISFEEIKEATSKF-
Synechocystis   CHCMLFLTPDNDFAGDAQDIPMETLEEVKASMA
```

1.2.3.2 The iron-sulfur center and the active site disulfide bridge of FTR

The iron-sulfur center and the disulfide bridge from the active site are both located in the catalytic subunit. The crystallization of recombinant *Synechocystis* FTR (Dai, 1998) allowed to well understand the protein structure of FTR.
The disulfide is composed of Cys57 and Cys87 and it is in van der Waals contact with the iron center. The irons of the iron-sulfur center are coordinated by cysteines 55,74,76 and 85 in a normal cubane type geometry (Fig. 6).

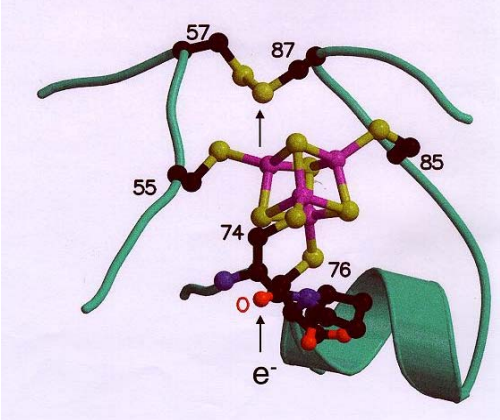

Fig. 6. The active site of *syn* FTR. The irons of the iron-sulfur center are coordinated by Cys55, Cys74, Cys76 and Cys85. The active site disulfide bridge is made between Cys57 and Cys87 and it is in van der Waals contact with the iron center, primarily the sulfur atom of Cys87. Beside the active site cysteines, Pro75 is also shown as ball and stick model and the oxygen atom in the *cis*-peptide bond between Cys74 and Pro75 is labeled. Incoming electrons can pass from ferredoxin to the main chain of Cys74 to the disulfide bridge via the iron center.

In spinach FTR Cys54 and Cys84 form the disulfide active site. Cys54 is accessible to the solvent whereas Cys84 is protected. The four remaining cysteines, Cys52, Cys71, Cys73 and Cys82 are ligands to the iron center in a normal cubane type geometry and this arrangement places the redox-active disulfide bridge adjacent to the cluster. In addition, His83 in this geometry is very close to the disulfide bridge and might increase the nucleophilicity of the Cys54 in the active site.

1.2.3.3 Interaction with ferredoxin and thioredoxin

The transformation of the redox signal from an electron to a disulfide signal is accomplished by FTR. This transformation necessitates simultaneous interaction of FTR with Fd and thioredoxin for the transfer of electrons from Fd to the disulfide. The structure of the FTR is ideally suited for this task since it is an unusually thin molecule. Its shape in a concave disc, where the [4Fe-4S] cluster is accessible from one side and the active site made of the disulfide bridge is accessible from the other side, allows simultaneous docking of ferredoxin and thioredoxin (Fig. 7).

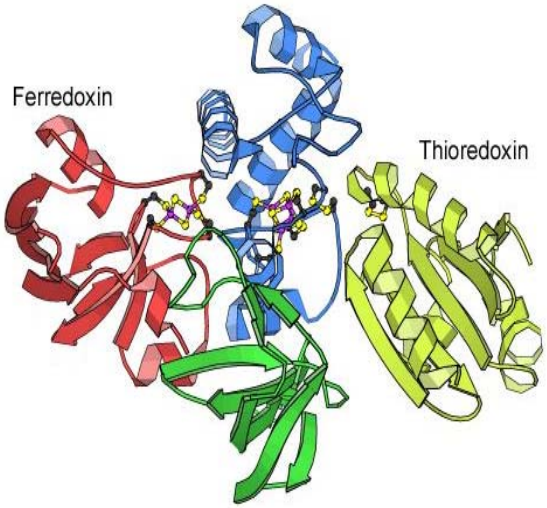

Fig. 7. Modelling of the interaction between ferredoxin, FTR and thioredoxin. The disc-shaped structure of the FTR allows docking of a ferredoxin (red, to the left) on one side of the molecule, while thioredoxin (yellow, to the right) binds to the other side and forms a mixed-disulfide with the enzyme.
The iron-sulfur centers and disulfide bridges are shown in a ball and stick representation.

Differential chemical modification studies (De Pascalis *et al.*,1994) have identified five acidic amino acid residues (Asp34, Asp65, Glu92, Glu93 and Glu94) and the carboxyl group of the C-terminal Ala97 on ferredoxin to be involved in binding to FTR. The negatively charged residues of ferredoxin lie largely in one of the two negative surface potential domains that surround the [2Fe-2S] cluster, but do not include residues in the helical region that runs from residues 24-31. These residues lie in the second domain of negative surface potential of ferredoxin, which appears to be involved in the interaction between ferredoxin and FNR. On the other hand, four positively charged residues (Lys9, Lys23, Lys47 and Arg80) are conserved on the Fd-interaction surface of FTR. These are thought to be responsible for the correct orientation of ferredoxin.
The thioredoxin docking area contains mainly hydrophobic residues and is less charged containing only one positive (Lys63) and one negative (Glu84) charge. The absence of other charged groups makes the thioredoxin interaction area less selective. This seems to be important *in vivo*, where FTR reduces different thioredoxins.

1.2.3.4 The redox signal: mechanism of action

The reaction mechanism proposed for FTR combines results from spectroscopic studies on native and active-site modified FTR and from the structural analysis (Dai *et al.,*2000). It tries to explain how the [4Fe-4S] cluster, with a redox potential of +340 to +420 mV (De la Torre *et al.*, 1982; Salamon *et al.*, 1995; Staples *et al.*, 1996) participates in the two-electron reduction of the active site disulfide with a

redox potential of –320 mV (Hirasawa *et al.*, 1999). In the mechanism (summarized here in Fig. 8) the proximity of the active site disulfide bridge of FTR to the Fe-S cluster appears to be essential for the electron transfer from ferredoxin to thioredoxin.

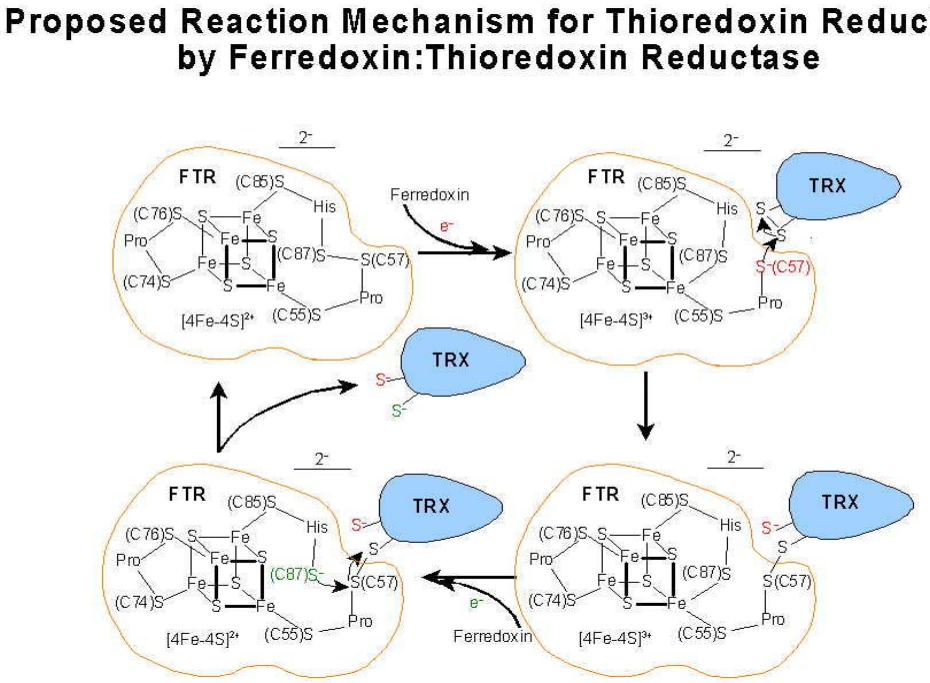

Fig. 8. Suggested mechanism of action for *Synechocystis* FTR (Dai *et al.*, 2000). Cys 87 one of the irons of the cluster in the FTR structure coordinates the iron in a five coordinated cluster.

The initial electron from a ferredoxin molecule can be transferred via the iron-sulfur center directly to the disulfide that is in close contact with one iron atom of the cluster. In this step, Cys87 (in *Synechocystis*) coordinates an iron in a five-coordinated cluster and this results in an oxidation of the $[4Fe\text{-}4S]^{2+}$ cluster to a $[4Fe\text{-}4S]^{3+}$ cluster. These penta-coordinated iron clusters show modified redox potentials (Staples *et al.* , 1996). For the FTR intermediate the redox potential of the [4Fe-4S] cluster is lowered from +420 mV to –210 mV, which is in the same region as the redox potential for the active site-disulfide (Hirasawa *et al.*, 1999).
The reduction of thioredoxin has been proposed to proceed via a mixed disulfide between thioredoxin and FTR. The one-electron reduced FTR, with its nucleophilic thiol Cys57 (in *Synechocystis;* or Cys54 in spinach), would be able to attack the disulfide bridge of thioredoxin to form a mixed disulfide. This intermediate complex covers one of the sides of the flat FTR molecule and the second electron for the reduction should be delivered by the next incoming ferredoxin which has to dock

on the opposite side of the flat disk-like heterodimer. The iron-sulfur ligands on the ferredoxin side of the FTR molecule are connected by Pro75 (in *Synechocystis*) in a CPC motif.
The second electron delivered by a new ferredoxin molecule reduces the iron-sulfur cluster back to its original 2+ oxidation state while Cys87 (in *Synecocystis*) becomes a nucleophilic thiol that can attack the heterodisulfide bridge between FTR and thioredoxin and in this way release the reduced thioredoxin.

1.2.4 The oxidation-reduction properties of the ferredoxin/thioredoxin system components

The oxidation-reduction properties of the ferredoxin/thioredoxin system components play an essential role in the activation step of redox-regulated enzymes although there has been little systematic investigation of the oxidation-reduction properties of the proteins of the chloroplast thioredoxin regulated system. Measurements of the midpoint potentials of some of the proteins in the ferredoxin/thioredoxin system had been reported by cyclic voltammetry that provided the first published E_m values for spinach thioredoxin *f* and *m* and for spinach FTR (Salamon *et al.*,1995). Although cyclic voltammetry had proven to be useful for reliably measuring E_m values for the disulfide/dithiol couples of glutathione, *Escherichia coli* thioredoxin, the E_m values obtained by cyclic voltammetry for spinach thioredoxin *f* and *m* were significantly more positive than those previously obtained for maize thioredoxin *m* (Rebeille *et al*., 1986) and spinach thioredoxin *f* (Hutchison, 1994). However, the potential of the two thioredoxins is slightly more oxidizing than that of target enzymes like FBPase (-305 mV) (Balmer *et al.*, 2001) and NADP-MDH (-330 mV).

1.2.5 Thioredoxins

Thioredoxins belong to a family of proteins present in all living systems from eukaryotic to prokaryotic cells. A typical thioredoxin can be described as a small monomeric, heat-stable protein, with an acidic isoelectric point and with a disulfide oxidoreductase enzymatic function.
Its catalytic mechanism involves a conserved pentapeptide sequence, -Trp-Cys-Gly-Pro-Cys-, and occurs via a reversible disulfide-dithiol reaction of the SH groups. There are over 200 sequences known of different thioredoxins with lengths ranging from 105 to 120 amino acids and the location of the two cysteines in the

active site is conserved. The three-dimensional structures have a common fold consisting of a central β-sheet flanked by α-helices.
Thioredoxins are involved in a large number of important cellular processes such as deoxyribonucleotide biosynthesis, regeneration of oxidative damage, activation of transcription factors, life cycle of *Escherichia coli* phages, and regulation of photosynthetic events.

1.2.5.1 Chloroplast thioredoxins

Higher plant chloroplasts contain two types of thioredoxins, a prokaryotic type, thioredoxin *m*, and a eukaryotic type, thioredoxin *f*, also present in algae. In spinach leaf chloroplast thioredoxin *f* specifically activates FBPase, SBPase, PRK, NADP-GAPDH, rubisco activase, chloroplast H^+-ATPase and fatty acid metabolism, whereas reduced thioredoxin *m* is most effective for the activation of NADP-MDH, deactivation of G6PDH, and translation.
In chloroplasts, thioredoxins are the last members of the regulatory chain which transmit the light signal to the target enzymes.

1.2.5.2 Thioredoxin *f* and *m*

Both types of chloroplast thioredoxins are reduced by FTR, and this reduction seems to be equally efficient with both, although quantitative results are not available; however these two types can clearly be distinguished by their primary structures.

Thioredoxin *f*. Thioredoxin *f* is nuclear-encoded and has been purified from spinach (Wolosiuk *et al.*,1979) and pea (Prado *et al.*, 1992) chloroplasts and its primary structure determined (Aguilar *et al.*, 1989). Thioredoxin *f* has been cloned and overexpressed in *Escherichia coli* and the crystal structure of the spinach protein has been solved (Capitani *et al.*, 2000). The overall structure of thioredoxin *f* presents a central twisted β-sheet surrounded by α-helices (Fig. 9 A) and a main difference with thioredoxin *m* is the presence of a third cysteine (Cys73 in spinach) exposed on the surface and conserved in all *f*-type thioredoxins.

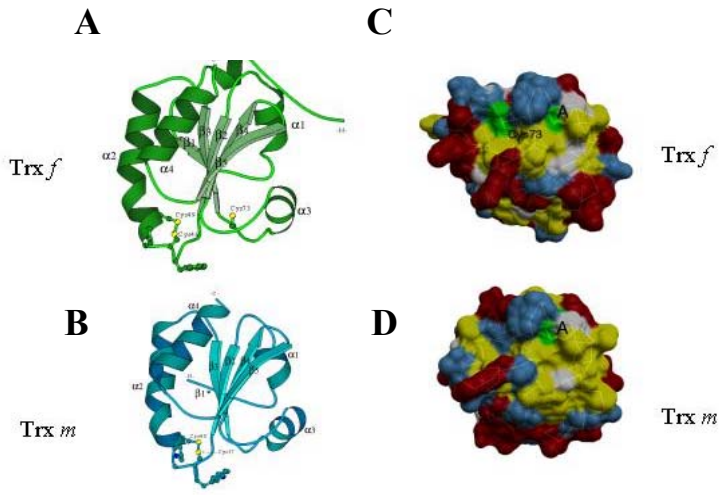

Fig 9. A.B. Cartoon representation of thioredoxin *f* and *m* structure. Thioredoxins are α/β-proteins with a central five-stranded β-sheet surrounded by four helices with a redox-active disulfide (yellow).
C.D. Surface views of thioredoxins *f* and *m*. Thioredoxin *f* (C), thioredoxin *m* (D). The colors represent the following residue types: green-Cys; red-charged; blue-polar; yellow-apolar; gray-back-bone.

This third cysteine residue is responsible for the appearence of a thioredoxin *f* dimer upon electrophoretic separation, a behavior not observed for spinach thioredoxin *m*, which has no additional cysteine residues.
Analysis of the surface topography of thioredoxin *f* shows a different distribution of polar, charged and hydrophobic residues compared to thioredoxin *m* (Fig. 9 C&D). The active site of thioredoxin *f* is surrounded by positive charges which may be essential in orienting thioredoxin *f* correctly in order to interact with its target proteins.
By contrast, the hydrophobic residues of thioredoxin *f* may be important in the interaction with FTR since the interaction site of FTR is rather hydrophobic.

Thioredoxin *m*. Thioredoxin *m* is nuclear encoded and synthesized on cytoplasmatic ribosomes as a precursor protein with a transit peptide that allows to pass the chloroplast membrane. After the import, the transit peptide is cut off by a processing enzyme. Recombinant *m*-type thioredoxins have been reported from *Chlamydomonas* (Lancelin *et al.*, 1993), spinach (P. Schürmann, 1995) and pea (López-Jaramillo *et al.*, 1997).
The eukaryotic *m*-type thioredoxins show high similarities between each other (~ 70-80%) and with the cyanobacterial (72%) and the *E.coli* proteins (59%); this suggests that the *m*-type thioredoxins of the eukaryotic cells are of bacterial origin. This conclusion is also supported by the fact that in the reactions where thioredoxin *m* is involved it can usually be replaced by thioredoxin from *E. coli* with good efficiency.

Fig. 9 B shows the overall structure of thioredoxin *m* that is locally quite different from thioredoxin *f*, especially in the N-terminal region; the Cys37 residue (in spinach) in the active-site is solvent accessible while the other (Cys40) is not.
Differences in charge distribution between thioredoxin *f* and *m* (Fig. 9 C&D) could explain the difference in activity and specifity of these proteins; hydrophobic effects correlated with surface complementarity, start playing an important role.
In spinach chloroplasts three functionally indistinguishable isoforms of thioredoxin *m* (m_b, m_c, and m_d) have been found (Maeda *et al.,* 1986) and these isoforms are caused by a N-terminal heterogeneity. Wedel *et al.* 1992, have demonstrated that these isoforms are the products of the processing after the import of the precursor protein in the chloroplast.

1.2.6 Chloroplast Target enzymes

Thioredoxins activate (or inactivate) target enzymes by a step-wise, thiol-disulfide exchange in which the regulatory disulfide of the enzyme undergoes nucleophilic attack by an active-site sulfhydryl of the thioredoxin (Cys46 in spinach thioredoxin *f*, and Cys37 in spinach thioredoxin *m*) to form a protein-protein mixed disulfide.
The proximal active-site sulfhydryl (Cys49 in thioredoxin *f*, and Cys40 in thioredoxin *m*) then intramolecularly attacks the mixed disulfide, generating reduced enzyme and oxidized thioredoxin (Fig. 10).
Thioredoxin *f* has been reported to selectively activate fructose-1,6-bisphosphatase (FBPase), while thioredoxin *m* appears more selective for NADP-dependent malate dehydrogenase (MDH).

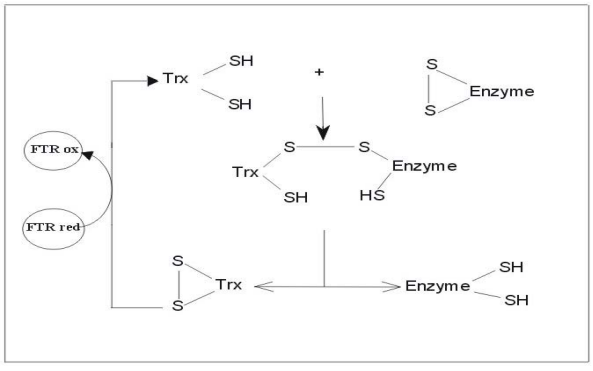

Fig. 10. Mechanism of thioredoxin (Trx) dependent enzyme activation comprising the re-reduction of Trx by FTR.

1.2.6.1 Fructose-1,6-bisphosphatase

Fructose-1,6-bisphosphatase (FBPase) is a tetrameric enzyme present in several cell compartments in plants. The reaction catalyzed by this enzyme is the cleavage of the substrate fructose-1,6-bisphosphate (FBP) to fructose-6-phosphate (F6P) and inorganic phosphate.
In higher plants, two principal forms are present, one in the cytosol and the other in the chloroplast. The cytosolic form takes part in gluconeogenesis and is activated by metabolites, while the chloroplast form participates in the regeneration of ribulosebisphosphate in the Calvin-Benson cycle and in the starch synthesis, and is activated by light-dependent processes.
The sequence of chloroplast FBPase compared to cytosolic FBPase revealed the presence of an insert in the middle of the primary structure compared to its cytosolic isoform. This insert contains three cysteines (Cys155, Cys174 and Cys179 in spinach); two separated by only four hydrophobic residues and the third, Cys155, by 18 residues upstream toward the N-terminus. Site-directed mutagenesis experiments suggested that all cysteines present in the insert are involved in regulation. Crystallographic analysis of the oxidized recombinant pea enzyme reveals a disulfide bond between Cys153 (Cys155 in spinach) and Cys173 (Cys174 in spinach), whereas the third cysteine in the loop is present as a free sulfhydryl and oriented towards the core of the protein (Chiadmi *et al.*, 1999).
Balmer & Schürmann have recently demonstrated that the Cys155 (in spinach) forms the transient heterodisulfide bond during reduction by thioredoxin *f*, which indicates that it must be surface exposed. In contrast, mutation of Cys179 probably induces some minimal structural change in the regulatory site which influences the catalytic site of FBPase (Balmer & Schürmann, 2001).
Prior to reduction, FBPase and thioredoxin *f* form an initial complex, and this first interaction involves electrostatic factors (Ocón *et al.*, 2001), where a negatively charged domain in the FBPase interacts with basic residues of thioredoxin *f* (Hermoso *et al.*, 1999).
The FBPase reduction by thioredoxin *f* is not the only activating factor, but also the alkalinisation and the Mg^{2+} concentration increase in the stroma during the dark-light transition influence the FBPase activity. It was demonstrated that, in vitro, a high concentration of magnesium and a pH above 8.0 can activate the enzyme (Gardemann *et al.*, 1986).

1.2.6.2 NADP-malate dehydrogenase (NADP-MDH)

NADP-dependent malate dehydrogenase (NADP-MDH) catalyzes the reduction of oxaloacetate to malate with concomitant oxidation of the cofactor NADPH. This

enzyme is involved in the C4 pathway, responsible for the primary fixation and transfer of CO_2 in a number of C4 plants. In C4 plants such as sorghum, the subunits of the dimeric enzyme are synthesized as precursors of 429 amino acids, imported into the chloroplasts of mesophyll cells and processed to the mature form with 389 amino acids per subunit. It is also present in C3 type plants such as spinach and pea, where it is implicated in a chloroplast shuttle mechanism which exports reducing power into the cytosol.
Among all the malate dehydrogenases, the chloroplastic NADP-dependent form exhibits the unique property of being strictly regulated by light: it is totally inactive in the dark and activated by the ferredoxin/thioredoxin system only when the chloroplasts are illuminated. The chloroplast enzyme is a homodimer of 85 kDa and differs from its NAD-dependent counterpart by the presence of N- and C-terminal extensions and eight cysteine residues at strictly conserved positions. Two of these are located in the N-terminal and two in the C-terminal extension where they form the two regulatory disulfides. The four remaining cysteines are located in the core part of the protein. Both N- and C-terminal extension contain one regulatory disulfide bridge.
Removal of the N-terminal disulfide by mutagenesis (Issakidis *et al.*, 1996) has yielded an inactive enzyme which still required thioredoxin activation but shows an altered activation kinetic. By contrast the removal of the C-terminal disulfide (Ruelland *et al.*, 1998) produced a mutant enzyme with activation properties similar to the wild-type. Finally, the removal of both disulfides provides a thioredoxin-insensitive, permanently active enzyme (Issakidis *et al.*, 1994). Cys377 (in sorghum) has been recently demonstrated to be involved in the interaction with thioredoxin (Goyer *et al.*, 2001) and the three-dimensional structures of sorghum (Johansson *et al.*, 1999) and *Flaveria* NADP-MDH (Carr *et al.*, 1999) were solved and confirmed the presence of two surface-exposed, thioredoxin-accessible disulfide bonds. There is, also, experimental evidence that the disulfide bridge involving the C-terminal residues is shielding access to the catalytic residues, and the N-terminal end is involved in the slow conformational change of the active site needed for activity.

2 Aim of this study

FTR from spinach has already been cloned and expressed in our laboratory when I started my PhD. However, key questions such as the stability of the spinach FTR and the relationship between structure and function of FTR (wild-type and/or mutant) in the interaction with ferredoxin and thioredoxin were still open. In addition the production of stable protein-protein complexes between FTR and its electron donor and acceptor proteins for structural analyses was still a long-range goal of our lab.
For this purpose, in the present study we further investigated: a) the redox properties of Ferredoxin/Thioredoxin system components; b) the role of the variable subunit in spinach FTR; c) the interaction between ferredoxin and FTR; d) the interaction between FTR and thioredoxins. We constructed mutants of FTR and Trx *m* which should allow the formation of stable mixed disulfide complexes between FTR and Trx suitable for structural analysis by X-ray crystallography.

Redox potentials

In order to understand the role of FTR in the regulatory pathway, it was interesting to define the redox potentials of the Ferredoxin/Thioredoxin system components and their dependence on pH which, in the chloroplast stroma, changes during the light-dark cycle (pH 7.0 in the dark and pH 8.0 in the light). Since the redox potentials measured earlier by cyclic voltammetry (Salamon *et al*., 1995) were more positive than the values reported by other groups applying different techniques (Rebeille *et al*., 1986; Hutchison *et al*., 1995) we have decided to re-determine the potentials of FTR and Trxs using the fluorescent probe mono-bromobimane.

Role of the variable subunit of spinach FTR

The FTR from spinach is unstable and turned out to be unsuitable for crystallization. This instability is due to the N-terminus of the variable subunit, which, compared to the FTR from maize or *Synechocystis*, is longer and breaks off small peptides. In order to produce a stable protein we removed part of the N-terminus on the variable subunit and compared this truncated FTR with the unmodified FTR in the capacity to interact with Fd and Trx (Manieri *et al*., in preparation).

Ferredoxin-FTR interaction

Ferredoxin forms ionic complexes with interacting proteins by providing the negative charges. For the interaction with spinach FNR an involvement of the acidic cluster Glu92-94 has been demonstrated (Piubelli *et al*., 1996; Aliverti *et al*., 1997) and in the interaction with *Chlamydomonas* FTR a direct involvement of Glu91, corresponding to spinach Glu92, in electron transfer was reported (Jacquot *et al*., 1997). We have used spinach ferredoxin mutants to assess the importance of the acidic cluster Glu92-94 in the interaction with FTR.

FTR-thioredoxin interaction

Chloroplasts contain both thioredoxins *f* and *m* which catalyze identical redox reactions via FTR. An open question still is whether FTR is capable of reducing both chloroplast thioredoxins with equal efficiency. We have tried to answer this question by comparing the affinities of FTR for the two thioredoxins under standardized conditions. In addition, in order to generate stable mixed-disulfide complexes between FTR and thioredoxins it was necessary to use site-directed mutagenesis to produce mutants which contain only the surface exposed, nucleophilic Cys of the active sites. Such mutants were avaible for the spinach thioredoxin *f*, but not for FTR nor thioredoxin *m*. We therefore constructed a C84S mutant of FTR as well as a C27S and C27/84S double mutant. Cys27, which is a well conserved residue, was removed because it is accessible on the Trx-interaction side of FTR and might disturb the formation of mixed-disulfides. To obtain a suitable thioredoxin *m* mutant, we replaced the inaccessible Cys40 by either Ser or Ala. The mutant proteins were produced and purified and, where possible, characterized.

3 Materials and methods

3.1 Materials

Companies	Equipments
Beckman	Centrifuge CS-6R, Ultracentrifuge XL-80
Bioengineering	Fermentor L 1523
Biorad	Minigel MiniProtean II, Gel Doc 1000, Dot-Blot
Dupont	Centrifuge RC-5B Plus, RC-5B, RMC 14
Eppendorf	Centrifuge 5417C
Fedegari	Autoclave Technoclav 50
Infors	Aquatron HT
LKB	Collector 7000 Ultrarac, Cellules UV 2238 Uvicord SII, 8300 Uvicord II
Metrohm	pH-meter 691, 744
Mettler	Balances AC 100, P 1200
Millipore	Milli RO plus, Milli Q
Miostar	DMR-703 micro-wave
MJ research	Thermocycle PTC-100
MWG-Biotech	LiCor 4000L sequencer
New Brunswick Scientific	Fermentor Multigen
Perkin Elmer	Spectrophotometer Lambda 17, Thermocycle Cetus
Pharmacia	Spectrophotometer Ultrospec 3000, FPLC, Collector Frac-300
Savant	Speed Vac Concentrator
Sartorius	Western blot semi-dry Sartoblot II

3.2 Molecular biology materials

3.2.1 Bacterial strains

- **XL1-Blue**-recA$^-$ strain: *E.coli* (recA1, lac$^-$, end A1,gyrA96,thi,hsdR17, supE44, relA1, [F', proAB,lac/q, LacZΔM15, Tn10](tet^r)).

XL-1 Blue *E.coli* strain was used to replicate pGEM®-T-Easy Vector (Promega) recombinant vector.

- **BL21 (DE3)** strain: *E.coli* B F^- dcm ompT hsdS(rB-mB-) gal (DE3).

BL21(DE3) *E.coli* strain was used for the expression of thioredoxin m_c wild type and thioredoxin m_c mutants : Trx m_c C40S and Trx m_c C40A.

- **BN103** strain: *E.coli* Delta (laclc^{q}2yA) v169, proA$^+$, lon$^-$, arw D139, strA, thi, hflA150,[chr : :Tn10],(strept^r,tetr).

BN103 Delta *E.coli* strain was used to produce thioredoxin *m* wild type in pKK233-MTTL vector. The strain is resistant to tetracycline and to streptomycine, but not to ampicilline.

- **BL21(DE3)pLysS** strain: *E. coli* B F^- dcm ompT hsdS (rB-mB-) gal (DE3) [pLysS Camr]a).

BL21(DE3)pLysS *E.coli* strain (Studier *et al*., 1986) (Stratagene) was used to express FTR mutants.
The strain provides tight control for the expression of toxic proteins by reducing the basal level of T7 RNA polymerase activity through the use of T7 lysozyme, a natural inhibitor of T7 RNA polymerase.

- **BL21-codon plus (DE3)-RIL** strain: *E.coli* B F^- ompT hsdS (r^-_B m^-_B) dcm$^+$ Tet^r gal λ(DE3) endA Hte [argU ileY leuW Cam^r].

BL21-Codon plus (DE3)-RIL, kindly provided by Dr. Agnes Massoneau, University of Neuchâtel, Department of Plant Physiology, was used in an attempt to increase the production of FTR WT and FTRΔ16 and FTRΔ24 mutants.

3.2.2 Vectors

3.2.2.1 Cloning vectors

- pGEM®-T Cloning Easy Vector (Promega). This vector is used with XL1-Blue-recA$^-$ strain.

- pBluescript II SK+ (Stratagene)**.** This vector (amp^r) of 2961 bp derives from pUC 19 and is used with XL1-Blue-recA$^-$ strain.

3.2.2.2 Expression vectors

The pET vectors were originally constructed by Studier and colleagues (Studier and Molfatt, 1986; Rosemberg *et al*.,1987; Studier *et al*.,1990).
The newer pET derivatives were designed with enhanced features to permit easier subcloning, detection and purification of target proteins.

- pET 3d (amp^r) used with BL21(DE3)pLysS strain.
- pET 3c (amp^r) used with BL21(DE3) strain.

The pET translation vector denotes the reading frame relative to the *Bam* HI cloning site recognition sequence, GGATCC and all vectors with the suffix "c" express from the ATC triplet of the *Bam* HI recognition sequence.
Vector with a "d" suffix also expresses from the "c" frame, but contains an upstream *Nco* I cloning site in place of the *Nde* I site in that series for insertion of target genes directly into the ATG start codon.

- pKK233-2 MTTL (amp^r & tet^r) used with BN103 strain.

3.2.3 Primers

All primers were synthesized by Microsynth (Balgach, Switzerland).

Specific vector primers

pET 3c and pET 3d	T7 T7 terminator	5'-tttaatacgactcactatataggg-3' 5'-cgatcaataacgagtcgcc-3'
pGEM®-T-Easy Vector	M13 reverse	5'-ggaaacagctatgaccatg-3'
pBluescript SK+	M13	5'-gtaaaacgacggccagt-3'

Primers for FTR mutants

SUAmin; N-terminal primer for variable subunit of FTR with a *Nco* I restriction site (underlined)	5'-ccatggaagtagctttgaaatccg-3'
SUAmeg; C-terminal primer for variable subunit of FTR with a *Eco* RI restriction site (underlined)	5'-ggtaccattagacttctactctgctatgatttcggaattc-3'
SUBmeg; N-terminal primer for catalytic subunit of FTR with a *Nde* I restriction site (underlined)	5'ggtaccataaggaaacagacatatggcagatccttctgacaaatct -3'
SUBmin; C-terminal primer for catalytic subunit of FTR with a *Bam* HI restriction site (underlined)	5'-ggatccttacatatttgatgtaacttctcg-3'
SUA∆16; upstream primer for FTR∆16 truncated mutant with a *Nco* I restriction site (underlined)	5'-atccatggcatcacctccagaagaagacgag-3'
SUA∆24; upstream primer for FTR∆24 truncated mutant with a *Nco* I restriction site (underlined)	5'-aattccatggaattgaagaagaatctggag-3'
FTR∆24 C27S; mutation of Cys 27 to Ser 27 (underlined), primer antisense	5'-cttttatcaacagaaaagtatgtatc-3'
FTR∆24 C84S; mutation of Cys 84 to Ser 84 (underlined), primer antisense	5'-gccactctatgctgtttctgac-3'

Primers for Thioredoxin m_c

Trx m_c*1*; N-terminal primer for Trx m_c with a *Nde* I restriction site (underlined)	5'-atatcattaacatatggctagtgaagctgtcaag-3'
Trx m_c *2*; C-terminal primer for Trx m_c with a *Bam* HI restriction site (underlined)	5'-taacattggatccttaaggagataagtatttctc-3'
Trx m_c *C40S*; mutation of Cys 40 to Ser 40 (underlined)	5'-tgagcttggagggtccaca-3'
Trx m_c *C40A*; mutation of Cys 40 to Ala 40 (underlined)	5'-tgagcttggcgggtccaca-3'

3.2.4 DNA digestion, ligation and transformation

Restriction enzymes were purchased either from New England Biolabs, Boehringer-Mannheim, Promega, Stratagene or Gibco-BRL. We used T4 DNA ligase by Gibco BRL for ligation; XL1-blue competent cells for cloning and BL21(DE3), BL21(DE3)pLysS, BL21-codon plus(DE3)-RIL competent cells for expression.

3.2.5 Sequencing

Sequencing was made with Amersham DNA labstation 625 kit and with an automatic sequencer Li-Cor 4000L.
Primers were M13 and M13 Reverse for pGEM®-T-Easy and pBluescript SK+ vectors and T7 and T7 term primers for pET 3c and 3d vectors. These primers are already modified in 5' by IRD 800 chromophore.

3.3 Molecular biology methods

3.3.1 Vector purification

All protocols of alcaline lysis and vector purification were set up according to Sambrook *et al.*,1989.

3.3.2 DNA digestion

The digestion was made in 20 μl following the manufacturer instructions at 37°C for two hours and fragments were separated on 0.8 and 1.5 % agarose gels by electrophoresis.

Fragments were purified with the QIAEX II Gel Extraction Kit (QIAEX II Handbook 02/99) and by a method developed in our laboratory, consisting of directly pipetting the bands from the gel.

3.3.3 Ligation

55 ng of digested, purified vectors and 50-80 ng of digested, purified fragments were ligated over night at 14 °C in a final volume of 15 μl.

3.3.4 Transformation

150 μl of competent cells were mixed with 2/3 of the ligation product and incubated 30 minutes in the ice. After 2 minutes of heat shock at 42 °C the cells were incubated 5 minutes in the ice and plated on solid LB-Agar medium with selective antibiotics (34 μg/ml of Chloramphenicol for BL21(DE3)pLysS), and X-Gal and IPTG and finally incubated overnight at 37 °C.
The selected white colonies were tested by PCR with pGEM®-T-Easy Vector primers:

PCR program				
1)	95 °C	1 min	Initial denaturation	
2)	95 °C	30 sec	Denaturation	
3)	**50 °C**	**30 sec**	Hybridization	
4)	72 °C	1 min	Elongation	Steps 2-4 34 cycles
5)	10 °C			

3.3.5 Site-directed mutagenesis by PCR

The general strategy is outlined in Figure 11. This procedure requires just one mutagenic primer and two universal primers (Barettino *et al.*,1994).

In the first PCR amplification, the mutagenic primer (M) is used together with the corresponding antiparallel universal primer (A) to yield a fragment that is subsequently used as a megaprimer in the second PCR reaction with the second universal primer (B). The resulting amplified fragment contains the mutation and can be cloned after digestion with the appropriate enzymes.

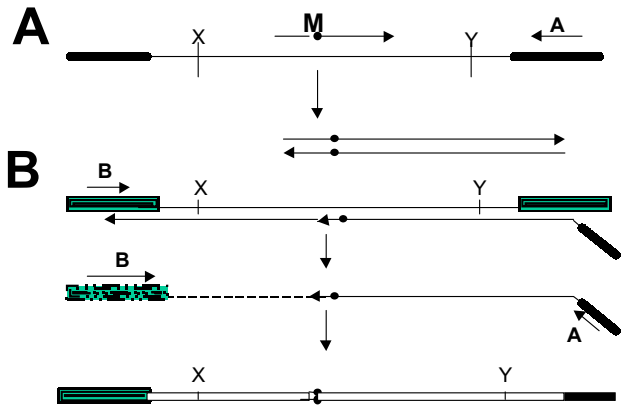

Fig. 11. Scheme of the mutagenesis procedure. A. First PCR reaction. **B.** Second PCR reaction.

3.3.5.1 Mutations of the truncated FTR: FTR mutants

Strategy for the production of the FTR mutants

A PCR to obtain megaprimers FTRΔ24 C27S and FTRΔ24 C84S mutants with SUBmin primer and SUAΔ24 C27S, SUAΔ24 C84S primers on truncated FTRΔ24 DNA template.
B PCR to obtain total cloning with SUBmeg primer for FTRΔ24 C27S and FTRΔ24 C84S mutants.
C PCR with two megaprimers C27S and C84S to obtain double mutant FTRΔ24 C27/84S.
D Cloning in pGEM®-T-Easy vector.
E Sequencing.
F Digestion with *Nde* I and *Bam* HI restriction enzymes for FTR mutants and pET 3d vector.
G Cloning in pET 3d vector.
H Minipreps, sequencing and transformation in BL21(DE3)pLysS cells.
I PCR on minipreps with T7 and T7 term primers of pET 3d vector.
J Sequencing of PCR fragments.

3.3.5.1.1 Fragment amplification by two single strand primers for FTRΔ24 C27S and C84S mutants.

DNA template	50 ng
Primer 1	1 μM
Mutant primer	1 μM
Nucleotide tri-phosphates	200 μM
Reaction buffer	1 X
TaqDNA polymerase (Boehringer Mannheim)	1 Unit
Reaction volume	50 μl

PCR program					
1)	95 °C	3 min	Initial denaturation		
2)	95 °C	30 sec	Denaturation		
3)	**48 °C**	**30 sec**	Hybridization		
4)	72 °C	1 min	Elongantion	Steps 2-4	10 cycles
5)	95 °C	30 sec	Denaturation		
6)	**60 °C**	**30 sec**	Hybridization		
7)	72 °C	1 min	Elongation	Steps 5-7	30 cycles
8)	10 °C				

3.3.5.1.2 Amplification with a double strand megaprimer containing the mutation and a single strand primer for FTRΔ24 C27S and C84S mutants

DNA template	50 ng
Megaprimer	30-50 ng
Primer 2	1 μM
Nucleotide tri-phosphates	200 μM
Reaction buffer	1 X
TaqDNA polymerase (Boehringer Mannheim)	1 Unit
Reaction volume	50 μl

PCR program					
1)	95 °C	3 min	Initial denaturation		
2)	95 °C	30 sec	Denaturation		
3)	**59 °C**	**30 sec**	Hybridization		
4)	72 °C	1 min	Elongation	Steps 2-4	30 cycles
5)	10 °C				

3.3.5.1.3 Amplification with a single strand primer containing the mutation for C84S mutant using the C27S megaprimer as template to obtain the double mutant

DNA template (mega C27S)	50 ng
Megaprimer C84S	30-50 ng
Primer 2 (SUB min)	1 μM
Nucleotide tri-phosphates	200 μM
Reaction buffer	1 X
TaqDNA polymerase (Boehringer Mannheim)	1 Unit
Reaction volume	50 μl

PCR program					
1)	95 °C	3 min	Initial denaturation		
2)	95 °C	30 sec	Denaturation		
3)	**59 °C**	**30 sec**	Hybridization		
4)	72 °C	1 min	Elongation	Steps 2-4	30 cycles
5)	10 °C				

3.3.5.2 Thioredoxin m_c C40S and C40A mutants

3.3.5.2.1 Fragment amplification by two single strand primers

DNA template	50 ng
Primer 1	1 μM
Mutant Primer	1 μM
Nucleotide tri-phosphates	200 μM
Buffer	1 X
TaqDNA polymerase (Boehringer Mannheim)	1 Unit
Reaction Volume	50 μl

PCR program					
1)	95 °C	3 min	Initial denaturation		
2)	95 °C	30 sec	Denaturation		
3)	**58 °C**	**30 sec**	Hybridization		
4)	72 °C	1 min	Elongantion	Steps 2-4	10 cycles
5)	95 °C	30 sec	Denaturation		
6)	**62 °C**	**30 sec**	Hybridization		
7)	72 °C	1 min	Elongation	Steps 5-7	30 cycles
8)	10 °C				

3.3.5.2.2 Amplification with a double strand megaprimer containing the mutation and a single strand primer

DNA template	50 ng
Megaprimer	30-50 ng
Primer 2	1 μM
Nucleotide tri-phosphates	200 μM
Reaction buffer	1 X
TaqDNA polymerase (Boehringer Mannheim)	1 Unit
Reaction volume	50 μl

PCR program					
1)	95 °C	3 min	Initial denaturation		
2)	95 °C	30 sec	Denaturation		
3)	**54 °C**	**30 sec**	Hybridization		
4)	72 °C	1 min	Elongation	Steps 2-4	10 cycles
5)	95 °C	30 sec	Denaturation		
6)	**58 °C**	**30 sec**	Hybridization		
7)	72	1 min	Elongation	Steps 5-7	30 cycles
8)	10 °C				

3.3.6 Expression system

The pET System process

Process	Detail
Prepare pET vector	1. Digest with restriction enzymes 2. Gel purify
↓	
Prepare insert DNA	1. Plasmid prep and/or PCR 2. Restriction digest 3. Gel purify
↓	
Clone insert into pET Vector	1. Ligate insert with pET vector 2. Transform into non-expression host (e.g. XL1) 3. Identify positive clones: colony PCR, miniprep,verify reading frame by sequencing
↓	
Transform into Expression Hosts	1. Transforming in BL21(DE3)pLysS Competent cells

Finally the selected colonies were tested by PCR with T7 and T7 term vector primers:

DNA template (colony)	20 ng
T7 primer	1 μM
T7 term primer	1 μM
Nucleotide tri-phosphates	200 μM
Reaction buffer	1 X
TaqDNA polymerase (Boehringer Mannheim)	1 Unit
Reaction volume	30 μl

PCR program					
1)	95 °C	3 min	Initial denaturation		
2)	95 °C	30 sec	Denaturation		
3)	**45 °C**	**30 sec**	Hybridization		
4)	72 °C	1 min	Elongation	Steps 2-4	30 cycles.
5)	10 °C				

3.4 Biochemical methods

3.4.1 Expression of the recombinant proteins

3.4.1.1 Culture medium

LB	Tryptone	10 g
	Yeast extract	5 g
	NaCl	10 g

Completed to 1 L, autoclave

3.4.1.2 Fermentors

Two different fermentors were used: a 1.5 L fermentor to work out optimal conditions for production and a 10 L fermentor to produce protein in large amounts. Small cultures were done at 37 °C in a Multigen, NewBrunswick Scientific Inc. fermentor with aeration (1.6 L/h) and stirring (500 rpm).
Large size cultures were done at 37 °C in a Bioengineering AG (Switzerland) fermentor sparged with air at 16 L/min^{-1} and stirred at 500 rpm.

3.4.1.3 Cell growth and harvest

The LB medium was inoculated with 1/20 of its volume by a saturated overnight preculture of the freshly transformed bacterial strain.
Appropriate antibiotics were added and bacteria were grown until an A_{600nm} of 0.6-1.0 was reached. Expression of the recombinant protein was then induced with isopropyl thio-β-D-galactoside (IPTG) (Biosynth AG®) as summarized in Table1.

Table 1. Cells growth conditions

Protein	Strain	Plasmid	Antibiotic	Antibiotic concentration	IPTG
FTR WT	BL21(DE3)pLysS	pET 3d	Amp/Chloram.	50 μg/ml/34μg/ml	0.1 mM
FTR mutants	BL21(DE3)pLysS	pET 3d	Amp/Chloram.	50 μg/ml/34μg/ml	0.1 mM
Trx m_c WT	BL21(DE3)	pET 3c	Ampicilline	100 μg/ml	1 mM
Trx m_c mutants	BL21(DE3)	pET 3c	Ampicilline	100 μg/ml	1 mM

Cells were harvested by centrifugation (5000 g and 4000 g at 4°C, for FTRs and thioredoxins respectively) after the culture had reached the end of exponential growth phase. Pellet was resuspended in 1/20 of the culture volume in the

following buffers; for FTRs 50 mM TEA-Cl pH 7.3, 0.1 mM PMSF, 14 mM 2-MET and for thioredoxins 20 mM Tris-Cl pH 8.0, 2.5 mM EDTA, 0.1 mM PMSF.
Thioredoxin containing cell suspensions were mixed with 1mg/ml of lysozyme (Merck) and incubated for 30 min at 25°C before freezing at –20°C; for thioredoxin mutants we added 10 mM Dithiothreitol (DTT) (Calbiochem®) in order to prevent the dimer formation. Cells were stored at –20°C until needed.

3.4.1.4 Analysis of protein expression: SDS-PAGE and Immunoblotting

To follow the expression by SDS-PAGE and immunoblotting 1 ml samples of culture were withdrawn at regular intervals. The cells were sedimented, washed with 500 µl of STE buffer (0.1 M NaCl, 10 mM Tris-Cl pH 8.0, 1 mM EDTA pH 8.0) and resuspended in 4 µl of H_2O/0.1 of A_{600nm}. Lysis was achieved by freezing for 15 min at –70°C and thawing (Johnson B.H. *et al*., 1994). One volume of double strength loading buffer (Laemmli U.K. *et al*., 1973) was added. The lysate was then vortexed for 5 min, heated for 3 min at 100 °C and finally centrifuged for 5 min at 16 000 g prior to separation by SDS-PAGE. The protein bands were transferred to nitrocellulose membrane by semidry blotting and immunodetected using a rabbit polyclonal antibody raised against the holoproteins. Immunocomplexes were detected using secondary antibodies (goat anti-rabbit IgG) coupled to peroxidase (Biorad) and visualized by chromogenic reaction with 4-chloro-1-naphthol.

3.4.2 Purification of the recombinant proteins: Chromatography

3.4.2.1 Chromatography columns used.

Chromatography colums used are summarize in Table 2.

Table 2. Chromatography columns

Column	Company	Type	Size
Phenyl-SepharoseFF	Amersham Pharmacia	Hydrophobic interaction	5.0 x 5.0 cm
Q-SepharoseFF	Amersham Pharmacia	Anion exchange	5.0 x 11.5 cm
Sephadex G-25	Amersham Pharmacia	Desalting column	5.0 x 25 cm
Sephadex G-50F	Amersham Pharmacia	Size exclusion	2.6 x 95 cm
Sephacryl S-100 HR	Amersham Pharmacia	Size exclusion	5.0 x 90 cm
Sephacryl S-200 HR	Amersham Pharmacia	Size exclusion	4.0 x 98 cm
*syn*Ferredoxin-Sepharose	Amersham Pharmacia	Affinity column	1.5 x 6.5 cm

3.4.2.2 Purification of FTR mutants

All preparation steps were performed at 4 °C. Protein concentration was assayed by the Lowry method. The purity of the FTR was assessed by calculating the A_{408} /A_{278} ratio (Droux *et al.,*1987, P. Schürmann,1981). Crude extract of FTR mutants was treated using the procedure set up for the wild-type protein as described in Gaymard *et al.*, 2000.
The chromatographic purification steps are summarized in Table 3.

Table 3. Purification steps of FTR mutants by chromatography

Protein	Column	Equilibration buffer	Elution buffer
FTR mutants	Phenyl-SepharoseFF	100 mM KPi buffer pH 7.3 1.0 M $(NH_4)_2SO_4$, 14 mM 2.0 2-MET	50 mM KPi buffer pH 7.3, 14 mM 2-MET
	Sephacryl S-100 HR	20 mM TEA-Cl pH 7.3, 200 mM NaCl, 0.05% NaN_3	idem
	Q-SepharoseFF	20 mM TEA-Cl pH 7.3, 100 mM NaCl, 14 mM 2-MET	2000 ml gradient from 100 to 500 mM NaCl in 20 mM TEA-Cl pH 7.3, 14 mM 2-MET
	syn-Ferredoxin-Sepharose	20 mM TEA-Cl pH 7.3	20 mM TEA-Cl pH 7.3, 500 mM NaCl

The pure proteins were concentrated and diafiltrated with 20 mM TEA-Cl pH 7.3 by ultrafiltration on YM-10 membrane and stored in liquid nitrogen.

3.4.2.3 Purification of Thioredoxins

All chromatograpic steps were performed at 4°C. Cells were thawed at 25°C and sonicated 6 x 30 sec. 2.5 U per ml of Benzonase (Merck, Darmstadt) and $MgCl_2$ to 10 mM were added. The extract was incubated at 25°C until no longer viscous. Then the lysate was centrifuged at 15 000 g for 20 min and the supernatant was recovered. In this supernatant $(NH_4)_2SO_4$ concentration was brought either to 1.0 M for the thioredoxin m_c wild type or to 1.5 M for mutants. For mutants, 10 mM DTT was then added and the extract was incubated at 25°C for 30 min. The precipitate was removed by centrifugation and the supernatant was clarified through a glass fiber filter (Whatman multigrade GMF 150, 1 μm) to remove lipoproteins. The clarified solution was chromatographed on a Phenyl-Sepharose column.
After hydrophobic interaction chromatography, active fractions were combined and the proteins concentrated with ammoniumsulfate at 90% saturation. The concentrated protein solution was clarified by centrifugation (48 000 g for 30 minutes) and chromatographed on Sephadex G-50F. Active fractions were combined and concentrated on a YM-10 membrane, diafiltrated with 20 mM Tris-Cl pH 8.3 (and 28 mM 2-MET for mutants) and loaded on a Q-Sepharose FF column. The active fractions were concentrated and diafiltred. Table 4 summarizes the purification of thioredoxins by chromatography.

Table 4. Purification steps of thioredoxin m_c and its mutants by chromatography

Protein	Column	Equilibration buffer	Elution buffer
Trx m_c wt	Phenyl-SepharoseFF	100 mM KPi buffer pH 7.0, 1.0 M $(NH_4)_2SO_4$	50 mM KPi buffer pH 7.0
	Sephadex G-50F	20 mM Tris-Cl pH 8.3, 200 mM NaCl, 0.05% NaN_3	idem
	Q-SepharoseFF	20 mM Tris-Cl pH 8.3	2000 ml gradient from 0 to 300 mM NaCl in 20 mM Tris-Cl pH 8.3
Trx m_c mutants	Phenyl-SepharoseFF	100 mM KPi buffer pH 7.0, 1.5 M $(NH_4)_2SO_4$, 28 mM 2-MET	50 mM KPi buffer pH 7.0, 28 mM 2-MET
	Sephadex G-50F	20 mM Tris-Cl pH 8.3, 200 mM NaCl, 0.05% NaN_3, 28 mM 2-MET	idem
	Q-SepharoseFF	20 mM Tris-Cl pH 8.3. 28 mM 2-MET	2000 ml gradient from 0 to 300 mM NaCl in 20 mM Tris-Cl pH 8.3, 28 mM 2-MET

3.4.2.4 Expression and purification of recombinant *Sorghum* NADP-MDH

Culture is performed at 37 °C. After transformation of the appropriate *E. coli* strain (BL21 for the pET plasmid), one colony is used to inoculate 500 ml of LB medium overnight. This culture is in turn used to inoculate 9.5 liters of LB medium in a 10 L fermentor. After 3 hr of culture (OD_{600} of 0.6), 100 μM IPTG is added and after an additional 4 hr, the cells are collected by centrifugation (5000 g, 10 min).The cell pellets are resuspended in 100 ml of extraction buffer consisting of 50 mM TEA-Cl pH 7.3, 1 mM EDTA and 100 μM PMSF. The bacterial extract was incubated 30 min at 25 °C with 1 mg/ml lysozyme before freezing. Protein purification is based on the method described by Jacquot *et al.*, 1995. The bacterial extract was sonicated 6 times at 3% power setting before incubating with 2.5 U per ml of Benzonase in 10 mM of $MgCl_2$ until disappearance of the viscosity. The cell debris are removed by centrifugation (10 min, 48 000 g). Solid ammonium sulfate (194 mg/ml) is slowly added to the protein solution to bring it to 35% of saturation. After 30 min of stirring at 4 °C, precipitating proteins are eliminated by centrifugation (30 min, 48 000 g) and solution was clarified through glass fibre filter (Whatman GMF 150, 2 μM, d=90 mm) with suction. The clarified solution was chromatographed on a Phenyl-Sepharose column. Solid ammonium sulfate is added to the combined fractions to bring them to 60 % of saturation. The NADP-MDH is recovered in the protein pellet obtained by centrifuging the solution for 20 min at 10 000 g and the proteins were dissolved in a minimal volume of Sephacryl S-200 column buffer, clarified and chromatographed on Sephacryl S-200. Active fractions were combined and then loaded on Q-Sepharose FF column. The combined fractions were concentrated and diafiltred with 20 mM TEA-Cl pH 7.3 buffer. Table 5 summarizes the purification of NADP-MDH by chromatography.

Table 5. Purification steps of NADP-MDH by chromatography.

Protein	Column	Equilibration buffer	Elution buffer
NADP-MDH	Phenyl-SepharoseFF	50 mM KPi buffer pH 7.3, 1.4 M $(NH_4)_2SO_4$; 1 mM EDTA	50 mM KPi buffer pH 7.3; 1 mM EDTA
	Sephacryl S-200	20 mM TEA-Cl pH 73, 100 mM NaCl, 0.02% NaN_3	idem
	Q-SepharoseFF	20 mM TEA-Cl pH 7.3; 100 mM NaCl	2000 ml gradient from 100 to 600 mM NaCl in 20 mM TEA-Cl pH 7.3

3.4.3 General methods

3.4.3.1 SDS-PAGE

SDS-PAGE was carried out essentially as described by Laemmli (Laemmli and Favre, 1973) using a mini PROTEAN II system (Biorad). Detection of separated protein bands was obtained by Coomassie blue staining.

3.4.3.2 Native-PAGE

Non-denaturing PAGE was performed using the same system as for SDS gels without the addition of detergent. Electrophoresis was run 15 min at 50V and then 45 min at 200V in migration buffer.

3.4.3.3 Protein blotting

Transfer of proteins to nitrocellulose membrane was accomplished by applying 2mA/cm^2 of gel in a solution of 20 mM Tris-HCl pH 7.5, 25 mM Glycine, 1.3 mM SDS, 20% methanol for 30 minutes. After transfer, the membrane was blocked with a solution of 5% powdered milk in TBS for 45 minutes at room temperature. The antibodies were diluted 1:1000 in TBS 1% powdered milk and were incubated with the nitrocellulose membrane overnight with agitation at room temperature. After washing twice with TBS plus 0.05 % Tween, the antigen-antibody complexes on the nitrocellulose paper were analyzed by goat anti-rabbit immunoglobulin G-peroxidase conjugate as described previously by Johnson *et al.*, 1994.

TBS (Tris Buffered Saline):	20 mM Tris-HCl pH 7.5; 500 mM NaCl
TTBS:	TBS; 0.05% Tween-20
Powdered milk-TBS 1 and 5%:	TBS; 1% and 5% of powdered milk
Color solution:	TBS; 500 μg/ml 4-chloro-1-naphtol (in methanol); 0.015% H_2O_2

3.4.3.4 Protein Concentration Measurements

The concentration of proteins was calculated based on their absorbance at 278, 279, 408 or 420 nm as summarized in Table 6.

Table 6. εM^{-1} cm^{-1} for Ferredoxin/Thioredoxin system components

	MW	nm	ε M^{-1} cm^{-1}
syn-Ferredoxin	10 400	420	9 680
so-Ferredoxin	10 500	420	9 680
syn- FTR	22 300	408	17 400
so-FTR	26 000	408	17 400
Trx *f* del	12 579	279	14 200
ECTM	13 400	279	20 500
rec Trx m_c	12 552	279	15 420
FBPase	160 000	278	144 000

3.4.3.5 Reaction of protein sulfhydryl groups with Ellman's reagent: DTNB-Test

The method described by Habeeb *et al.*,1972 was used. The amount of free SH-groups of thioredoxin and FTR was determined with 5,5'-dithiobis(2-nitrobenzoic acid) (DTNB). Proteins were incubated for 15 min in a solution of 100 mM Tris-HCl pH 8.0, 1 mM EDTA-Na with DTNB 0.008% and A_{412nm} was measured to monitor the release of TNB^-. A TNB^- extinction coefficient of 13,600 $M^{-1}cm^{-1}$ was used for the calculations.

3.4.3.6 Redox Titrations

Spinach thioredoxins *f* and *m* and spinach FTR were purified as described previously.
The reduced form of dithiothreitol (DTT) was obtained from Sigma Chemical Co, monobromobimane (mBBr) and the oxidized form of DTT were obtained from CalBiochem.
Oxidation-reduction titrations, using mBBr fluorescence to monitor the oxidation-reduction state of the disulfide/dithiol system, were carried out at room temperature under argon.

Fluorescence was measured using samples in microtiter plates (Costar Black Plate 3603) and a Bio_Tek model FL500 fluorescence plate reader with excitation at 360 nm and emission at 460 nm.
Trx *m*, Trx *f* and FTR, at a final concentration of 270 μg/ml, were incubated in 300 μl of 100 mM Bis-Tris-Cl buffer (Calbiochem) pH 7.0 , that contained DTT at a total concentration of 2 mM. After an incubation for 2 hours, excess mBBr was added and samples were prepared for fluorescence analysis.
Samples were allowed to equilibrate at ambient potentials (E_h) defined by different ratios of reduced:oxidized DTT to achieve the complete oxidation-reduction equilibrium. At the end of the equilibration period, aliquots were removed and exposed to mBBr under conditions causing this fluorescent probe to become covalently linked to thiol groups (Krimm *et al.*, 1998; Hutchison *et al.*, 1995 and Kosower *et al.*,1987).
For the mBBr titrations, a modification (Krimm *et al.*,1998) of the method of Hutchison and Ort was used in which protein precipitation with trichloroacetic acid (Fluka) replaced methylene chloride extraction (Hutchison *et al.*, 1995) as the method for separating the protein from other reactants and products.
Best-fit values for E_m were determined by fitting titration data to the Nernst equation using Kaleidagraph (Synergy Software) and setting the value of *n* in the Nernst equation at 2, the value expected for a disulfide/dithiol two electron-transfer process.
All E_m value calculations were based on a value of –330 mV for the E_m of DTT at pH 7.0 (Hutchison *et al.*,1995). The value used for the pH dependence of the E_m value of DTT was –59 mV/pH unit over the pH range from 5.5 to 8.2 (Hutchison *et al.,* 1995).

3.4.4 Specific assays for FTR

3.4.4.1 FTR activity determination

FTR activity was tested by its capacity to activate fructose 1,6-bisphosphatase in presence of thioredoxin *f.* FTR was routinely reduced by artificial electron donors (Schürmann *et al.*, 1995).

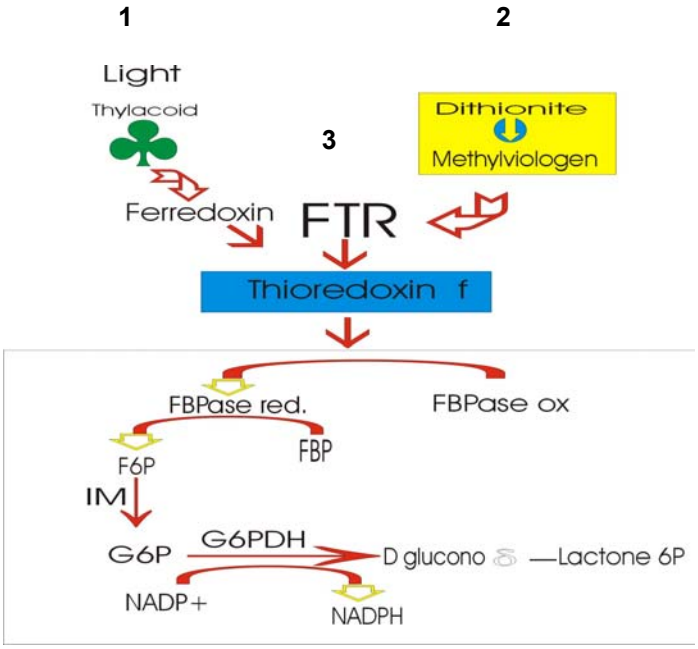

Fig. 12. Scheme of FTR test. **1** & **3**; **FTR reduction by light** (Schürmann and Jacquot,1979). **2** & **3**; **FTR reduction by artificial electron donors** (Dithionite-Methylviologen) (Schürmann *et al.*, 1995). Arrows represent electron transfer. FTR: ferredoxin:thioredoxin reductase. **FBPase: fructose 1,6-bisphosphatase;** F6P: fructose 6-phosphate; IM: phosphoglucose-isomerase; G6PDH: glucose 6-phosphate dehydrogenase.

The activation was performed in Eppendorf tubes at room temperature and the activation mixture contained in a final volume of 100 µl 100 mM Tris-Cl pH 7.9, 0.2 µM FTR, 1 µM of recombinant Trx *f,* 0.5 units FBPase, 1 µM methylviologen, 14 mM 2-mercaptoethanol. After 5 min under argon, 5 mM dithionite dissolved in 100 mM Tris-Cl pH 7.9 and kept under argon was added anaerobically with a Hamilton Microlab pipettor. After 5 min activation in presence of dithionite, an aliquot was withdrawn and injected into an 1 ml reaction mixture kept at 25 °C. The reaction mixture contained 100 mM Tris-Cl pH 7.9, 0.1 mM EGTA-Na, 1.5 mM $MgSO_4$, 1 mM fructose 1,6 bis-phosphate, 0.3 mM NADP, 1.75 units phosphoglucose isomerase, 0.7 units glucose 6-phosphate dehydrogenase and 14 mM 2-mercaptoethanol.

The reaction was followed at 340 nm and 25 °C in a Perkin-Elmer Lambda 16 spectrophotometer. Activities are expressed as nmol/min per total activation mixture volume.

3.4.4.2 Stability Test

FTR samples were incubated at concentrations which yielded an A_{408nm} of about 0.15 in a final volume of 700 μl in stoppered cuvettes at 25 °C in 20mM buffers in a pH range from 6.0 to 8.0. Spectra were recorded with a Perkin-Elmer Lambda 16 spectrophotometer at 30 min interval for a total period of 15 hours.

3.4.5 Specific assays for Thioredoxin *m*

3.4.5.1 NADP-MDH activation

Thioredoxin *m* activity was assayed by measuring its capacity to activate NADP-MDH for preincubation-periods of 5-30 minutes with 10-20 μM thioredoxin.

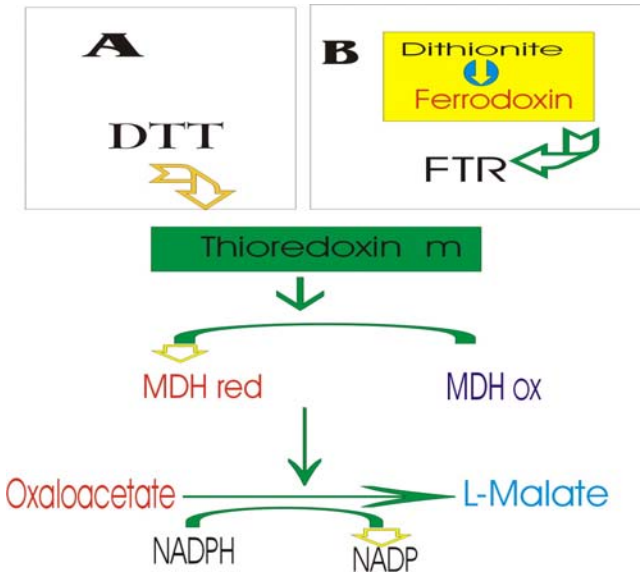

Fig. 13. NADP-MDH activation. A. DTT activation. DTT (Dithiotreitol); MDH (NADP-Malate dehydrogenase); **B. Ferredoxin/FTR activation.** Ferredoxin was reduced by dithionite; FTR (ferredoxin:thioredoxin reductase).

Thioredoxin was either reduced with DTT (Fig. 13 A) or by FTR reduced via ferredoxin (Fig.13 B).
NADP-MDH activity (0.1 U/μl) was followed spectrophotometrically as NADPH oxidation by recording the decrease of absorbance at 340 nm in the presence of 140 μM NADPH and 700 μM oxaloacetate in 100 mM Tris-HCl buffer pH 7.9 at 25 °C in a total volume of 1 ml. Activation was performed in Eppendorf tubes that were equilibrated with argon for 5 min. Half-saturation concentration values ($S_{0.5}$) for thioredoxins and V_{max} of the activated enzyme were determined by varying the concentration of thioredoxin while keeping the concentration of the FTR fixed.

3.4.5.2 Molar extinction coefficient determination for Trx *m*$_c$ WT

A sample of Trx *m*$_c$ WT was dialysed against 25 mM ammonium-formiate pH 8.0 during 48 hours. After recording the UV spectrum aliquots of the protein solution were distributed into dried, preweighed eppendorf tubes, frozen and lyophilized in a Speed Vac Concentrator. The dried samples were stored in a dessicator and the dry weight measured 5 times.
The extinction coefficient was calculated based on the absorbance maximum at 279 nm, the average dry weight and the molecular weight of thioredoxin *m*$_c$ (12 552 gr/mol).

3.4.5.3 Insulin test for thioredoxin *m*

Thioredoxins are disulfide reductase proteins and they are able to reduce disulfide bonds between subunits A and B of insulin. The method, described by Holmgren 1979, is a non specific test for thioredoxin where the reduction of insulin is followed by the increase of turbidity at 650 nm due to the precipitation of separated subunits of insulin.
The reaction mixture of 600 μl contained 600 μg/ml of insulin, 80 μM of DTT and thioredoxin. The reaction is characterized by the length of the lag phase until precipitation begins and the maximal ΔA_{650nm}/min.

3.4.6 Protein-protein complex formation studies

3.4.6.1 Measurements of Difference Spectra

Absorbance spectra were measured at 25 °C using a Perkin-Elmer Lambda 16 spectrophotometer. The spectrophotometer cells used for difference spectra measurements were dual compartment silica (tandem cuvette). The light path in each compartment was 0.44 cm. Measurements of the difference spectra between complexes of FTR plus one of its substrates were made as follows.
Equal volumes of a solution of FTR were pipetted into one compartment of sample and reference cuvette. Equal volumes of buffer were added to the other two compartments and baseline was recorded. Then Fd was added to the FTR in the measuring cuvette and to the buffer in the reference cuvette and the difference spectrum recorded. To dissociate the complex NaCl was added to each compartment.

4 Results and discussion

Molecular biology

4.1 Construction of the pET expression vector for the production of FTR mutants

4.1.1 Construction of the truncated form of spinach FTR variable subunit

To study possible functions of the long N-terminus present in the spinach FTR variable subunit, which has been demonstrated to be unstable (Tsugita *et al.*, 1991), we have constructed two mutants by removing parts of the N-terminal tail. The first truncation (FTRΔ16 mutant) starts at position 17, removes one positive and three negative charges and a number of clustered serine and proline residues resulting in a polypeptide of 11069 Da. The second truncation (FTRΔ24 mutant) starts at position 25, removes an additional seven residues containing four negative charges yielding a subunit of 10 214 Da (Fig. 14).

Fig. 14. Sequence alignment of truncated variable subunit of spinach FTR

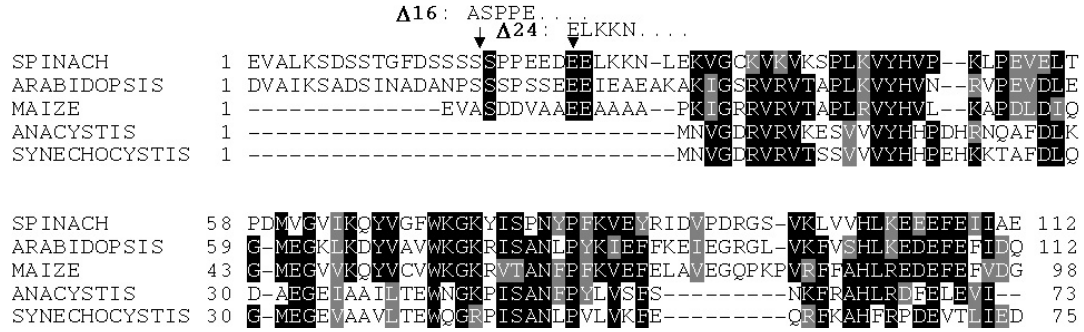

To truncate the N-terminus we designed a 31 bp upstream primer for FTRΔ16 mutant and a 39 bp primer for FTRΔ24 mutant. The downstream primer was the same as for FTR WT containing a *Kpn* I restriction site. Two fragments of 313 bp for FTRΔ16 and 290 bp for FTRΔ24 were obtained by PCR. The fragments were cloned in pBluescript SK+ vector and verified by sequencing. After sequencing the fragments were digested by *Nco* I and *Kpn* I and inserted in the *Nco* I/*Kpn* I digested pET 3d expression vector. Digestion with *Nco* I and *Bam* HI gave a

fragment including both subunits of FTR and confirms the truncation of the DNA (Fig. 15) by the presence of two different bands at 680 and 670 bp respectively for FTR∆16 and FTR∆24 truncations.

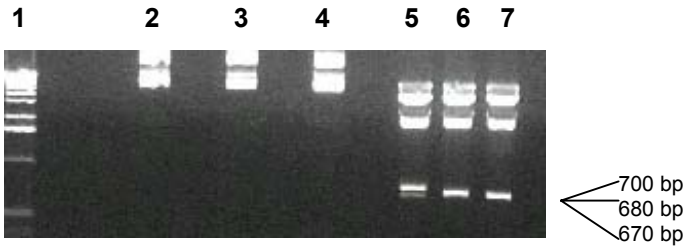

Fig. 15. Digestion of FTR and its mutants.
Lane 1. DNA ladder;
lane 2. FTR WT undigested;
lane 3. FTR∆16 undigested;
lane 4. FTR∆24 undigested;
lane 5. FTR WT digested with *Nco* I and *Bam* HI;
lane 6. FTR∆16 digested with *Nco* I and *Bam* HI;
lane 7. FTR∆24 digested with *Nco* I and *Bam* HI.

4.1.2 Construction of mutants: C27S, C84S and C27/84S from truncated FTR∆24 form

The plasmid used for further mutagenesis was the pET-3d-FTR∆24 construction. Three amplifications were needed to introduce the mutations into the template cDNA.
In the first step we obtained the two megaprimers:C27S and C84S of 242 bp
(Fig. 16).

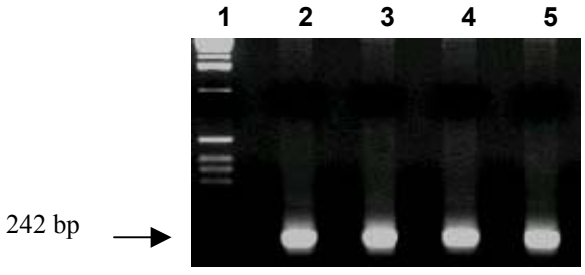

Fig. 16. PCR: megaprimers.
Lane 1. DNA ladder; lanes 2 & 3. C27S megaprimer obtained by PCR amplification with SUB min primer and FTR∆24 C27S primer antisense; lanes 4 & 5. C84S megaprimer obtained by SUB min primer and FTR∆24 C84S primer antisense.

In the second step the two megaprimers from the first step were used to amplify the double mutant and we obtained a fragment of 350 bp for FTR∆24 C27/84S (Fig. 17).

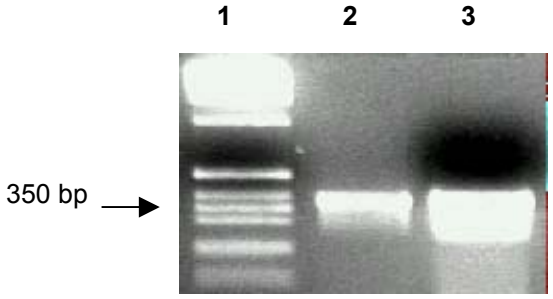

Fig. 17. Cloning of FTR∆24 double mutant. PCR amplification was perfomed using the megaprimer C27S sense with the megaprimer C84S antisense. Lane 1. DNA ladder; lanes 2 & 3; different quantity of FTR∆24 C27/84S DNA.

In the third PCR step we obtained the complete single mutants; the MegaC27S and SUB min primers were used to clone C27S mutant and the MegaC84S and SUB meg primers were used to clone C84S mutant. In both amplifications a fragment of 350 bp was obtained (Fig.18).

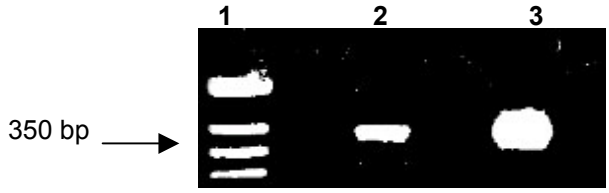

Fig. 18. Complete single mutants. Lane 1. DNA ladder; lane 2. FTR∆24 C27S mutant; Lane 3. FTR∆24 C84S mutant.

4.1.2.1 Cloning in expression system

30-50 ng of pGEM®-T-Easy-FTR mutant vectors were digested with 1U of *Nde* I & *Bam* HI and ligated in *Nde* I-*Bam* HI digested pET 3d plasmid. 1/3 ligation product was used to transform BL21(DE3)pLysS cells.
Clones were verified by PCR with T7 and T7 term primers (Fig. 19 A) and by digestion with *Nde* I and *Bam* HI (Fig. 19 B) enzymes, then sequenced to insure only desired mutations were present in the clones (Fig. 20).

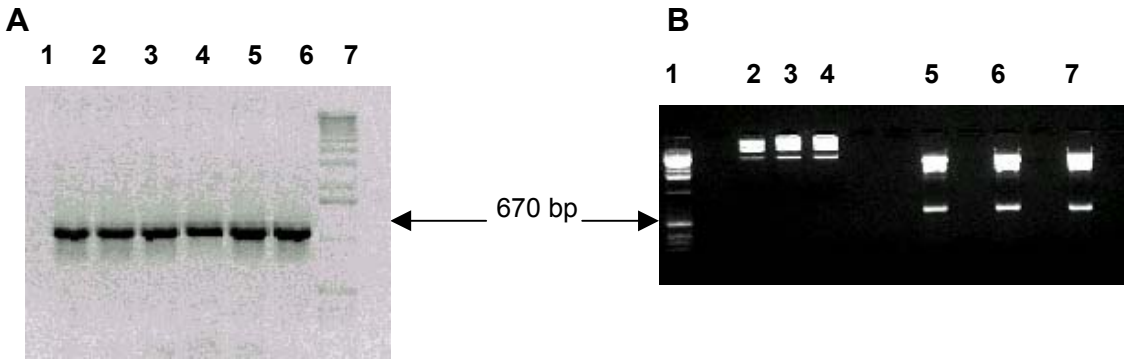

Fig. 19. A. PCR with T7 and T7 term primers (fragment of 670 bp). Lane 1&2. pET-C27S mutant; lanes 3&4. pET C84S mutant; lanes 5&6. pET-C27/84S mutant; lane 7. DNA ladder. **B. Digestion with *Nco* I and *Bam* HI (Fragment of 670 bp).** Lane 1. DNA ladder; lane 2. pET-C27S undigested; lane 3. pET-C84S undigested; lane 4. pET-C27/84S undigested; lane 5. pET-C27S digested; lane 6. pET-C84S digested; lane 7. pET-C27/84S digested.

Fig. 20. Sequence map of FTR active-site mutants. Position of mutation is in red

	1	27	84
FTRΔ24-SUB	MADPS.....	DTYFCVDK.....	MRERKECHCMLF.....VTSNM
FTRΔ24 C27S	MADPS.....	DTYFSVDK.....	MRERKECHCMLF.....VTSNM
FTRΔ24 C84S	MADPS.....	DTYFCVDK.....	MRERKECHSMLF.....VTSNM
FTRΔ24 C27/84S	MADPS.....	DTYFSVDK.....	MRERKECHSMLF..... VTSNM

4.1.2 Discussion

Sequence alignment of the different FTR enzymes shows a rather low conservation of the variable subunits (see Fig. 14), 46 to 60 % identity within the eukaryotes and 33 to 40% between eukaryotes and prokaryotes. The most striking difference between the FTR from spinach and *Synechocystis* (available in our laboratory) is the N-terminal extension in the spinach, rich in serine and proline

residues, which is rather long compared to the shorter N-terminus of *Synechocystis* FTR. This N-terminal extension was found to be unstable (Tsugita *et al.*, 1991), being degraded to shorter peptides.
In order to study the role of the N-terminus of spinach FTR we have removed parts of the N-terminus by truncation of the protein and thereby eliminated a series of serine and proline residues which were supposed to be responsible for the instability of the variable subunit of spinach FTR.
We have demonstrated that the shorter truncated mutant of spinach FTR (FTRΔ24) is the most stable, similar to the *Synechocystis* enzyme (see Chapter 5).
Since this truncation significantly stabilizes the spinach FTR, we used the shorter mutant, FTRΔ24, for all subsequent mutational studies on the catalytic subunit. Targets for these mutations were the accessible, conserved free Cys27 on the thioredoxin docking site and the inaccessible active site Cys84. For both mutations the megaprimer procedure was applied successfully. This procedure was preferred to amplification of the whole plasmid which could introduce additional mutations.

4.2 Construction of the pET expression vector for the production of Trx m_c wild type and its mutants

4.2.1 Spinach Trx m_c wild type

-

In previous work in our laboratory, the nucleotide sequence encoding spinach thioredoxin *mc* was subcloned into the pKK233-2 MTTL expression vector, resulting in an altered thioredoxin *m* with 6 additional N-terminal residues containing an *Eco* RI restriction site (Fig. 21) (May Morris, 1993, Diploma. University of Neuchâtel).

Fig. 21. Recombinant Thioredoxin *m* in pKK vector

	Start			**Fusion segment**							
pKK233-2-T*m*	**ATG**	TAC	TAT	TTA	**GAA**	**TTC**	GCT	AGT	GAA	GCT	GTC……
	M	Y	Y	L	E	F	A	S	E	A	V
Thioredoxin m_c							**A**	**S**	**E**	**A**	**V…..**

To avoid these alterations and likewise to make the native isomer *mc*, we have decided to subclone the gene into the pET system with *Nde* I and *Bam* HI restriction sites. The cloning of the spinach Trx *m* wild type sequence (which introduces the two restriction sites) was achieved by PCR with Trx m_c 1 and Trx m_c 2 primers on pKK233-2 Trx *m* MTTL plasmid and subcloned in pGEM® -T Easy vector.
pGEM® -T Easy-Trx m_c vector digested with *Nde* I and *Bam* HI restriction enzymes was then ligated in vector pET 3c digested with the same enzymes (Fig. 22). The Trx *m* fragment and digested pET 3c vector were separated and purified on a 1.2% agarose gel, followed by elution in an elutrap, ethanol precipitation and final dissolution in TE.

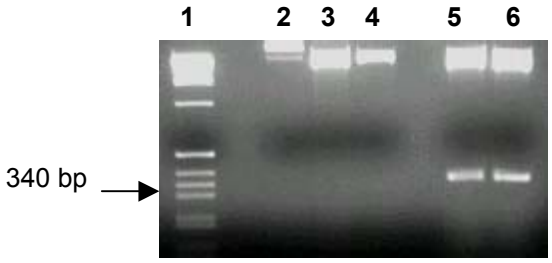

Fig. 22. Digestion. Lane1. DNA ladder; lane 2. pET 3c undigested; lanes 3&4. pET 3c digested with *Nde* I and *Bam* HI; lanes 5&6 pGEM® -T Easy-Trx m_c digested with *Nde* I *&* *Bam* HI enzymes.

After ligation, the pET 3c-Trx m_c construction containing a fragment coding for 342 bp (including the initiator methionine) was amplified by PCR in 30 cycles using Taq DNA polymerase and T7 and T7 term primers. We obtained a 542 bp nucleotide sequence (including pET 3c promotor) encoding thioredoxin m_c with a 5'terminal *Nde* I and a 3' terminal *Bam* HI restriction site (Fig. 23) which was sequenced in order to verify the correct cloning in pET vector.

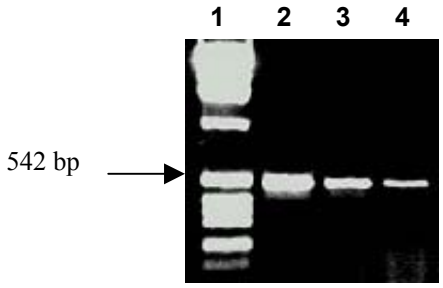

Fig. 23. Trx m_c WT in pET 3c system. Lane 1. DNA ladder; lanes 2&4. pET 3c-Trx m_c WT. The band of 542 bp includes the 342 bp fragment of thioredoxin plus the 200 bp of the pET 3c promotor.

The resulting sequence (Fig. 24) corresponds to the mature thioredoxin m_c in agreement with Wedel *et al.*, 1992.

Fig. 24. Sequence map of pET 3c-Trx m_c wild type

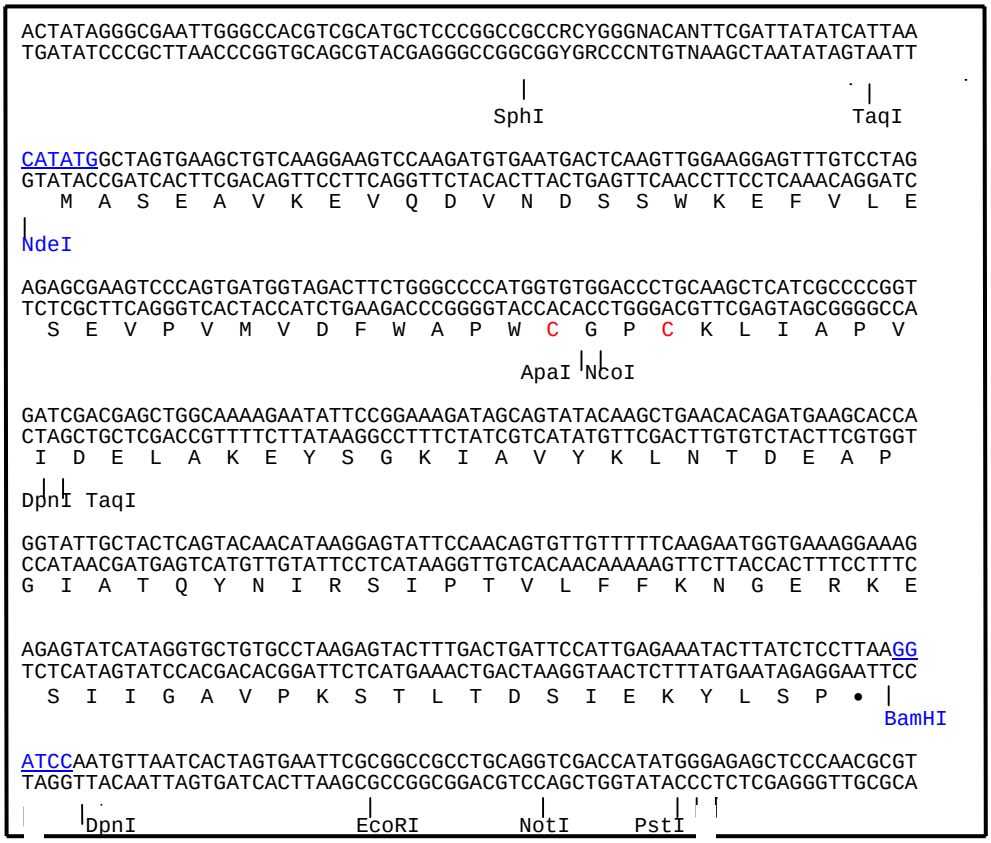

4.2.2 Spinach Trx m_c C40A and C40S mutants

The main objective of this study was the construction of stable mixed disulfides between FTR and thioredoxins. To stabilize these mixed disulfides it is necessary to use active site mutants of both proteins involved. A corresponding active site mutant of thioredoxin *f* was avaible in our lab, however, none of thioredoxin *m*. To obtain such a thioredoxin *m* mutant we replaced its inaccessible Cys40 by alanine and serine. The use of thioredoxin *m* for the production of mixed disulfides presents an additional advantage. Spinach thioredoxin *m* does not have a third, exposed Cys like thioredoxin *f*. Although this Cys73 in spinach thioredoxin *f* does not seem to be directly involved in the interaction with target proteins, it has been demonstrated in our lab that it can form dimers (del Val *et al.*, 1993; Balmer *et al.*, 2001) and might, under oxidizing conditions, interact nonspecifically with accessible Cys of other proteins.

4.2.2.1 Site-directed mutagenesis

Two PCR steps were necessary to obtain the mutated fragments: 1) a first PCR reaction using the primers Trx m_c 1 and Trx m_c C40S or Trx m_c C40A with the pET-3c-Trx m_c vector as a template to obtain megaprimers of 200 pb (Fig. 25 A); 2) a second PCR reaction using the megaprimer from the first PCR and the primer Trx m_c 2. This second reaction gave a 342 bp fragment for the C40S and C40A mutant respectively (Fig. 25 B).

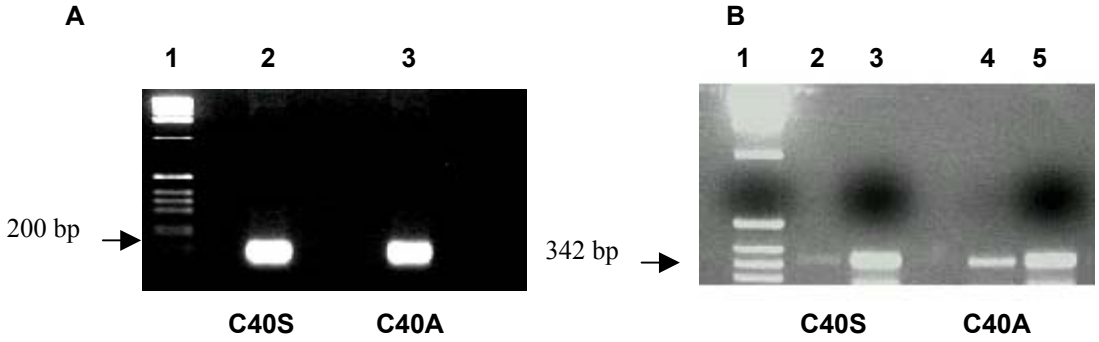

Fig. 25. A. First PCR: megaprimer. Lane1. DNA ladder; lane 2. Megaprimer of 200 bp for C40S mutant; lane 3. Megaprimer for C40A mutant. **B. Second PCR: mutant construction.** Lane 1. DNA ladder; lanes 2 & 3. Fragment of 342 bp coding for C40S mutant; lanes 4 & 5. Fragment of 342 bp coding for C40A mutant.

The *Nde* I-*Bam* HI fragment, obtained by PCR bearing the mutation was then ligated in pGEM® -T Easy vector. Ligation was verified by PCR, using Trx m_c 1 and Trx m_c 2 primers (Fig. 26 A) and by digestion with *Nde* I and *Bam* HI restriction enzymes (Fig. 26 B).

Fig. 26.A. PCR. Lane 1. DNA ladder; lanes 2&3. pGEM®-C40S mutant; lanes 4&5. pGEM®-C40A mutant. **B. Digestion.** Lanes 1&7. DNA ladder; lanes 2. pGEM® undigested vector; lanes 3&4. pGEM®-C40S mutant digested with *Nde* I and *Bam* HI; lanes 5&6. pGEM® -C40A mutant digested with *Nde* I and *Bam* HI.

The presence of the desired mutation was confirmed by sequence analysis of the clones (Fig. 27). DNA sequencing was performed with M13 and M13 reverse primers.

Fig. 27. Sequence map of WT and mutants of Thioredoxin m_c.
Position of mutation is in red.

Trx m_c wild type	ATG GCT….TGG TGT GGA CCC TGC AAG **M A W C G P C K**
Trx m_c C40S	ATG GCT….TGG TGT GGA CCC TCC AAG **M A W C G P S K**
Trx m_c C40A	ATG GCT….TGG TGT GGA CCC GCC AAG **M A W C G P A K**

The *Nde* I-*Bam* HI fragments of the mutated Trx m_c cDNA were transferred to pET 3c vector for production of the modified proteins. The pET 3c cloning was verified by PCR (Fig. 28 A) using vector specific primers and by digestion using *Nde* I & *Bam* HI restriction enzymes (Fig. 28 B).
We obtained a 542 bp nucleotide sequence (including pET 3c promotor) encoding thioredoxin m_c mutants with a 5'-terminal *Nde* I restriction site and a 3'-terminal *Bam* HI restriction site.

Fig. 28. A. PCR. Lane 1. DNA ladder; lane 2. pET-C40S amplified with T7 and T7 term primers; lane 3. pET-C40A amplified with the same enzymes. **B. Digestion.** Lane 1. DNA ladder; lane 2. pET-Trx m_c WT undigested; lane 3. pET-C40S digested with *Nde* I; lane 4. pET-C40A digested with *Bam* HI; lane 5. pET-C40S digested with *Nde* I and *Bam* HI; lane 6. pET-C40A digested with the same enzymes.

4.2.3 Discussion

The pET vector is a good expression system, but appears to be very sensitive to DNAses. We have observed during pET purification a partial or total degradation of the vector from mini or maxi-preparations. To avoid these problems of degradation, we routinely applied a phenol-chloroform extraction to purify the plasmid. This procedure provided a very clean DNA perfectly suited for all further operations.

5 Results and discussion

Biochemistry

5.1 FTR and its mutants

FTR is the central enzyme of the ferredoxin/thioredoxin system, the light-dependent regulatory system in oxygenic photosynthesis (Buchanan, 1991; Schürmann *et al*., 1995; Schürmann & Jacquot, 2000). The enzyme is composed of two subunits: a catalytic subunit highly conserved in different species (see Introduction) and a variable subunit that is not highly conserved and that, in spinach FTR, is unstable and gives rise to multiple peptides separable by SDS-PAGE.

5.1.1 Truncation mutants

We have constructed two mutants removing parts of the N-terminal chain. The first mutant, FTRΔ16, starts at position 17 with Ser17 been replaced by alanine and the second mutant, FTRΔ24, starts at position 25 with a conserved Asp25.
We were interested to test how the removal of the unstable region influences the expression, the stability and the catalytic properties of the spinach enzyme.

5.1.1.1 Expression and purification of truncation mutants

The truncation mutants were expressed in BL21(DE3)pLysS cells and small and large scale cultures were grown and induced with different concentrations of IPTG at different temperatures and with different concentrations of antibiotics in order to check the best level of expression. The expression was optimal when using 0.1 mM of IPTG, 37 °C and ampicilline and chloramphenicol at final concentrations of 50 μg/ml and 34 μg/ml respectively. The N-terminal truncation does not seem to influence the expression of the recombinant proteins because they were readily expressed at about the same level as the WT protein (the yields were about 1.5-2.0 mg pure protein per liter of bacterial culture) and could be purified by the same method used for WT FTR (Gaymard *et al.*, 2000). However, due to the removal of negative charges, both mutants were eluted earlier from the anion exchange column.

5.1.1.2 Characterization of FTR truncation mutants

5.1.1.2.1 Electrophoretic analysis

It was demonstrated that the variable subunit of spinach FTR is unstable and gives multiple bands under reducing SDS-PAGE due to degradation of the subunit into smaller peptides which migrate further (Tsugita *et al.*, 1991).
As expected, the electrophoretic analysis on purified WT FTR (Fig. 29 A, lane 1) reveals two bands of lower molecular weight (SUA' and SUA'') that are the degradation products of the full-length variable subunit (SUA). The purified truncated FTRs were then compared to WT (Fig. 29 A, lanes 2 and 3).

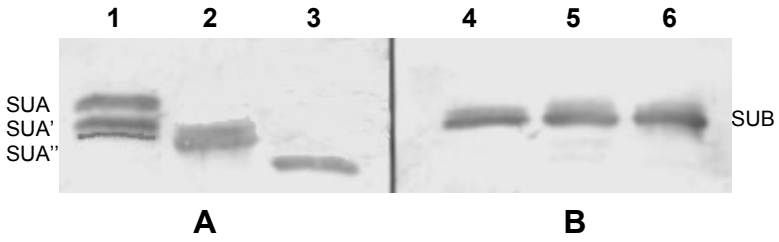

Fig. 29. Western blot of FTR WT and its mutants. A. Proteins were detected with antibodies against variable subunit. Lane 1. FTR WT; lane 2. FTR∆16; lane 3. FTR∆24. **B. Proteins were detected with antibodies against catalytic subunit.** Lane 4. FTR WT; lane 5. FTR∆16; lane 6. FTR∆24.

As shown in Fig. 29, the truncated subunits migrate further than the original peptide (SUA) as a consequence of the removal of either 16 (FTR∆16) or 24 residues (FTR∆24). The fact that we observe 2 bands for FTR∆16 suggests that this mutant is still unstable. In contrast, FTR∆24 migrates as a single band suggesting that it is stable. The truncation of the variable subunit of spinach FTR therefore clearly stabilizes the protein, especially for FTR∆24 truncation mutant (24 amino acids removed). The apparent molecular weight differences of the mutants are larger than the calculated differences in mass. This anomalous migration of the variable subunit of FTR in SDS-PAGE seems to be due to the peculiar amino acid sequence of the N-terminal tail with its clustered serine and proline residues as well as aspartates and glutamates.
For the catalytic subunit the migration pattern is identical for all three proteins (Fig. 29 B) suggesting that the truncation did not affect the dimer formation and SUB is always associated with SUA.

5.1.1.2.2 Spectral properties

The spectral properties of the truncated enzymes were compared with those of the unmodified enzyme. Fig. 30 shows that the spectra of truncated forms are identical to those of the spinach WT FTR. All mutants presented an A_{408}/A_{278} spectral ratio between 0.37-0.38 in agreement with published values. In addition both reduced mutants had very similar affinities for substrate as WT enzyme and they are not significantly different in their ability to catalyze the activation of fructose-1,6-bisphosphatase. This indicates that the functional properties are not substantially altered (see Chapter 9).

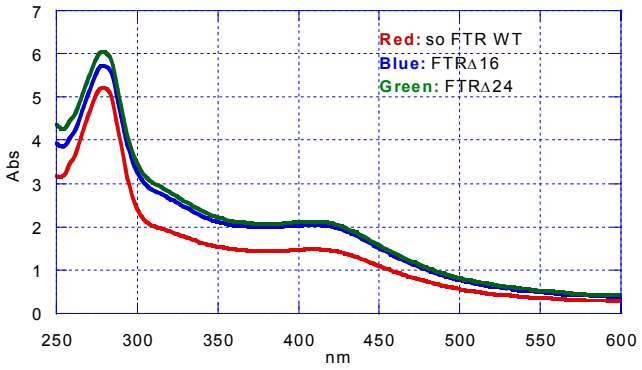

Fig. 30. UV spectral analysis of FTR WT and its truncation mutants. The absorbance was monitored in a range of 250-600 nm. The peak at 408 nm is due to the [4Fe-4S] cluster characteristic for all FTRs.

5.1.1.2.3 Stability

During the work with the WT FTR we observed a strong instability of the enzyme, which was most evident during freeze-thaw cycles. This instability was manifested by the decrease of the A_{408}/A_{278} ratio indicating a loss of the Fe-S cluster in the catalytic subunit. We observed a 40% decrease of the absorbance ratio after four freeze-thaw cycles (Table 7).

Table 7. Decrease of A_{408}/A_{278} ratio in freeze-thaw cycles for WT spinach FTR

Freeze-thaw cycles	A_{408}/A_{278} ratio	% initial ratio
Freshly prepared	0.3622	100
First cycle	0.3390	93
Second cycle	0.3085	85
Third cycle	0.2843	78
Fourth cycle	0.2297	63

In contrast, it was observed that the FTR from *Synechocystis*, which has a variable subunit with a shorter N-terminal sequence, more similar to our truncation mutants, is more stable than the spinach enzyme. To find out whether the pH, the type of buffer or the N-terminal tail was the prime responsible factor for the degradation of the spinach FTR, we incubated the *Synechocystis* and WT as well as mutant spinach FTR under various conditions and followed their visible absorbance as a measure for the intactness of the proteins. *Synechocystis* FTR showed quite good stability from pH 6.0 to 8.0 (Data not shown). When we compared spinach and *Synechocystis* FTR at pH 6.0 and 8.0 we observed a significantly larger decrease of A_{408} in spinach FTR than in *Synechocystis* FTR irrespective of the pH (Fig. 31). Similarly, in different types of buffers the WT spinach enzyme was always less stable (Data not shown). This suggests that the shorter N-terminus of *Synechocystis* FTR is advantageous for the stability of the protein.

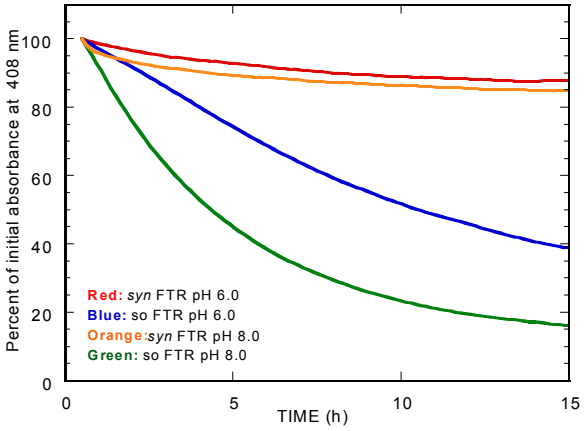

Fig. 31. Comparaison of stability of spinach and *Synechocystis* FTR at pH 6.0 and 8.0. Buffers used are: 20 mM bis-TRIS-HCl at pH 6.0 and 20 mM TRIS-HCl at pH 8.0. Temperature: 25 °C.

It was therefore of interest to compare the stability of the WT and truncated spinach FTRs with the *Synechocystis* enzyme. We tested all proteins in different buffers of a pH range from 6 to 8 and we observed a clearly improved stability of the truncation mutants compared to the WT protein. The shortest mutant, FTRΔ24, was the most stable, very similar to the *Synechocystis* FTR as shown in Fig. 32.

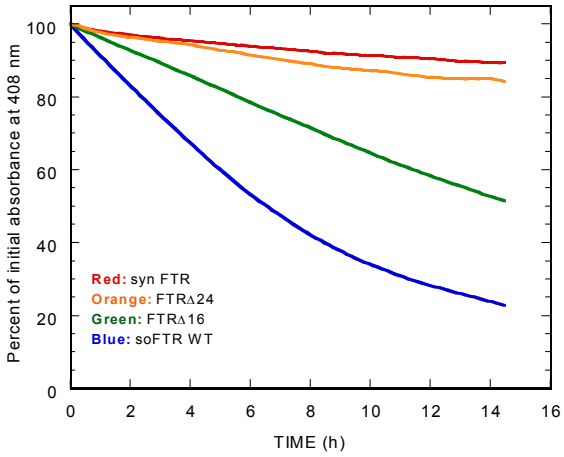

Fig. 32. Comparaison of stability of WT and truncated spinach FTR with *syn* FTR. The proteins at a concentration of 8.5 μM, were incubated in 20 mM TRIS-HCl buffer pH 8.0 in spectrophotometer cuvettes kept at 25 °C. Absorbance was recorded during 15 hours at 30 min intervals.

5.1.1.3 Discussion

The function of FTR involves the interaction between the catalytic and variable subunits. In order to elucidate the role of the variable subunit in the structure of the spinach enzyme we had the objective to obtain the crystal structure of FTR. Based on the results obtained by Tsugita *et al.*, 1991, which demonstrated the instability of variable subunit of spinach enzyme, the main objective was to stabilize the dimeric structure of the FTR.

We therefore generated truncated mutants of the variable subunit of spinach FTR with the objective to decrease its degradation and subsequently to increase the FTR stability. The two truncated mutants that we produced are readily expressed at about the same level than the WT protein and can be purified by the same method used for WT FTR. However, the deletion of the variable subunit removes N-terminal negatively charged residues, clustered serine and proline residues as well as aspartates and glutamates. Consequently, the mutants presented an overall charge slightly more positive and were eluted earlier from the anion exchange column than the WT.

Compared to the WT FTR the truncated mutants were more stable. After 14 hours of incubation in buffer there was about 4 times more FTRΔ24 compared to WT. This clearly indicates that the N-terminus of the variable subunit of spinach FTR causes a strong instability as we hypothesized.

We also had to make sure that the truncation introduced in the variable subunit did not affect the function of FTR. For this purpose, we tested the ability of mutants to catalyze the reduction of thioredoxins (see Chapter 9). We also found that the FTRΔ24 truncation mutant was significantly more stable than the mutant FTRΔ16 or WT and that it presents properties similar to *Synechocystis* FTR, which has a shorter N-terminus. To conclude, we succeeded in increasing spinach FTR stability and preserving FTR function, by truncating the variable subunit. The shorter mutant truncated by the 24 N-terminal amino acids could therefore provide a suitable material for further crystallization studies.

5.1.2 FTR∆24 mutants

5.1.2.1 C27S mutant

Oxidized catalytic subunit of spinach FTR contains one accessible cysteine (Cys27) which is exposed on the thioredoxin interaction side. In order to test a possible role of this free residue, we have replaced this cysteine by serine.

5.1.2.1.1 Expression and purification

Conditions of production of C27S mutant were as described in Materials and methods and the expression was tested by SDS-PAGE (Fig. 33 A) and Western blot analysis of the corresponding *E.coli* extracts. (Fig. 33 B).

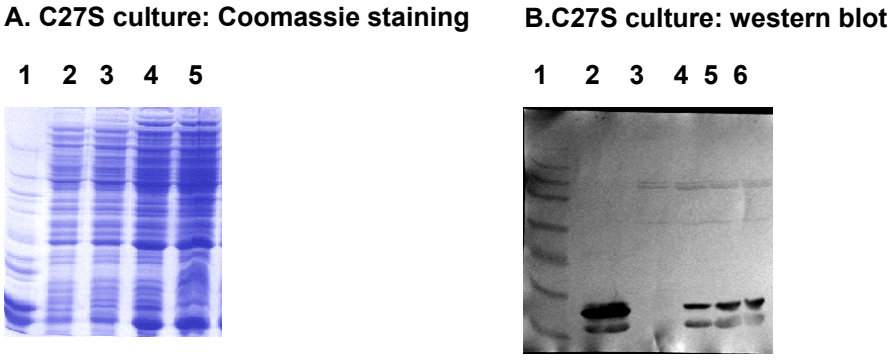

Fig. 33. A. SDS-PAGE analysis. Lane 1. Partially purified FTR; lane 2. Before IPTG; lane 3. After 60 min IPTG; lane 4. After 120 min IPTG; lane 5. After 180 min IPTG. **B. Western blot analysis.** Lane 1. HMW; Lane 2. Purified FTR; lane 3. Before IPTG; lane 4. After 60 min IPTG; lane 5. After 120 min IPTG; lane 6. After 180 min IPTG.

After various attempts we found that growing the cells at 37 °C in LB medium and inducing protein expression with 0.1 mM IPTG for 3 hours resulted in an accumulation of C27S mutant detected in the soluble fraction of the homogenate (see Fig. 33 A&B). This revealed that both subunits of mutant C27S are produced in soluble form.

The procedure for the isolation of spinach FTR∆24 C27S mutant from bacterial lysates is described in Materials and methods. The first purification step of this procedure was ammonium sulfate fractionation coupled to hydrophobic absorption on Phenyl-Sepharose column by which all nucleic acid contaminants are removed from FTR. Further, progress of the purification was monitored by the A_{408}/A_{278}

spectral ratio and revealed that already after anion-exchange chromatography on Q-Sepharose sufficiently pure FTR was obtained. The purification of recombinant FTRΔ24 C27S mutant is summarized in Table 8.

Table 8. Progress of purification of FTRΔ24 C27S mutant.

Step	Volume (ml)	Protein (mg) (Lowry)	Activity nmol/min/μl	Activity total U/total	$A_{408/278}$	Yield
Soluble extract	80	472	287.06	22965	-	- 100
Phenyl-Sepharose	182	324	112.04	20391	0.0541	89
Sephacryl S-100	92	153	208.02	19137	0.3586	83
Q-Sepharose	154	38	123.60	19034	0.3617	82

The recovery was estimated by the absorbance at 408 nm of the fractions. This is a good measure of the amount of FTR present in solution after each chromatographic step since it is due to the presence of the [4Fe-4S] cluster in FTR and no other proteins absorbing at 408 nm have been detected in the extract.
The absorption spectrum of purified C27S mutant is identical to that of WT FTR. An A_{408}/A_{278} spectral ratio of 0.36 can be calculated, in comparison with a published value of 0.37-0.38 for WT FTR (Schürmann, 1981; Droux *et al.*, 1987; Gaymard *et al.*, 2000). A yield of about 1.5-2 mg pure FTR per liter culture was usually obtained and the purity of the different fractions analyzed by SDS-PAGE is shown in Fig. 34.

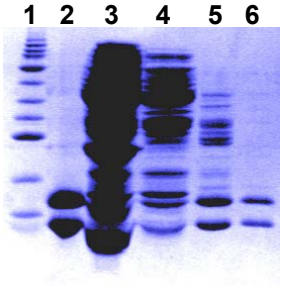

Fig.34. Progress of purification of FTRΔ24 C27S mutant as analyzed by 15% SDS-PAGE and protein staining by Coomassie blue. Lane1.HMW; lane 2. Purified FTRΔ24; lane 3. Crude extract; lane 4. After Phenyl-Sepharose (fractions combined); lane 5. After Sephacryl S-100 (fractions combined); lane 6. After Q-Sepharose (fractions combined).

5.1.2.1.2 Characterization: Thiol content of the FTRΔ24 C27S mutant

We have titrated the WT and FTRΔ24 C27S mutant with the thiol-specific reagent DTNB in order to verify whether Cys27 had been removed.
Structural analysis had indicated that two cysteines are accessible in the oxidized WT FTR (Chow *et al.*, 1995). The first one (Cys35) is located in the variable

subunit and the second one (Cys27) in the catalytic subunit of the spinach enzyme.

Titrations performed on freshly purified proteins gave a good agreement with the theoretical values. We determined 2 free –SH groups for WT and FTRΔ24 and only 1 free –SH group for the C27S mutant in agreement with our assumptions (Table 9).
Titrations done on protein stored for some time were more variable probably due to the degradation of the Fe-S cluster.

Table 9. Thiol Group Content of WT and mutant FTRs

FTR	Accessible –SH groups
WT	1.95
FTRΔ24	1.92
C27S	0.97

5.1.2.2 Discussion

The aim of this mutation was to test if the free, conserved, exposed cysteine 27 in the catalytic subunit of FTR plays a role in the function of the enzyme. For this purpose Cys27 has been replaced by mutagenesis with serine.
Replacing Cys27 by Ser in the catalytic subunit of FTR did not modify the production of the enzyme, since it was expressed at about the same level as the WT (1.5-2 mg/liter) and purified by the same procedure used for WT. The only difference observed between WT and C27S mutant was the rather easy purification of the latter, which, compared to WT, did not need the additional affinity chromatographic step.
In addition, the replacement of this free, accessible cysteine does not seem to affect the activity of the enzyme whose presence during purification could be followed by activity measurements (see Table 8).

5.1.3 Active-site mutants of FTR

5.1.3.1 Production

The active-site mutants of FTRΔ24, C84S and C27/84S, were produced under conditions comparable to the production of FTRΔ24 C27S.
According to the electrophoretic analysis of the bacterial extracts, the proteins are present in soluble form, however in a lower amount than the WT FTR (Fig. 35).

A. C84S culture: stained gel

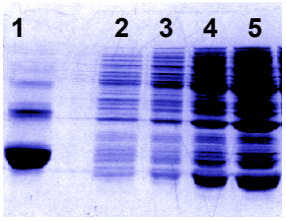

B. C84S culture: Western blot

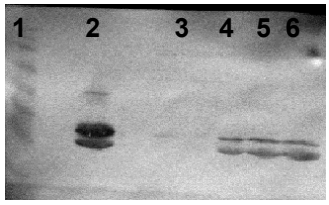

C.C27/84S culture: stained gel

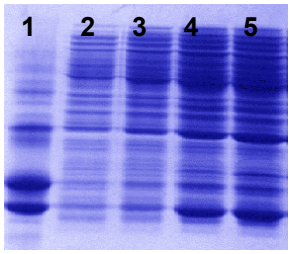

D.C27/84S culture: western blot

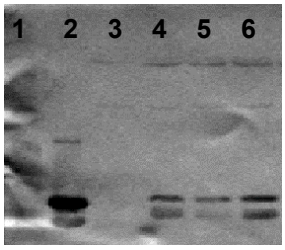

Fig. 35. A.C. SDS-PAGE analysis. Lane1. Partially purified FTR; lane 2. Before IPTG; lane 3. After 60 min IPTG; lane 4. After 120 min IPTG; lane 5. After 180 min IPTG. **B.D. Western blot analysis.** Lane 1. HMW; lane 2. Partially purified FTR; lane 3. Before IPTG; lane 4. After 60 min IPTG; lane 5. After 120 min IPTG; lane 6. After 180 min IPTG.

5.1.3.2 Purification

Since the active-site mutants were inactive, their presence during purification had to be followed using the antibodies.

Attempts to purify these mutants by our standard procedure turned out to be unsuccessful. Therefore, different modifications of the purification protocol were tested in the hope to obtain at least partially purified proteins.
In the following, we present only the results obtained for the C84S mutant.

5.1.3.2.1 Standard purification procedure

Upon addition of ammonium sulfate to 50% saturation (to prepare the bacterial extracts for hydrophobic interaction chromatography), it was observed that the mutant, unlike the WT protein, precipitated and virtually only the catalytic subunit of FTR could be detected in the supernatant as well as in the pellet with antibodies against the holoenzyme (Fig. 36 lanes 4 and 5).

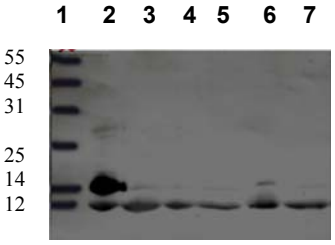

Fig. 36. Precipitation of FTR∆24 C84S by different concentrations of ammonium sulfate as detected by Western blotting. Lane 1. HMW; lane 2. 25% ammonium sulfate, supernatant; lane 3. 25% ammonium sulfate pellet; lane 4. 50% ammonium sulfate, supernatant; lane 5. 50 % ammonium sulfate, pellet; lane 6. 70% ammonium sulfate, supernatant; lane 7. 70% ammonium sulfate, pellet.

At an ammonium sulfate concentration above 50% saturation some variable subunit was detected in the supernatant (Fig. 36 lane 6) whereas the pellet seemed to contain only catalytic subunit (Fig. 36 lane 7). By contrast, at a lower ammonium sulfate concentration of 25% saturation, both subunits were found in the supernatant (Fig. 36 lane 2) in large amount compared to the pellet (Fig. 36 lane 3) and could be chromatographed on Phenyl-Sepharose (Fig. 37).

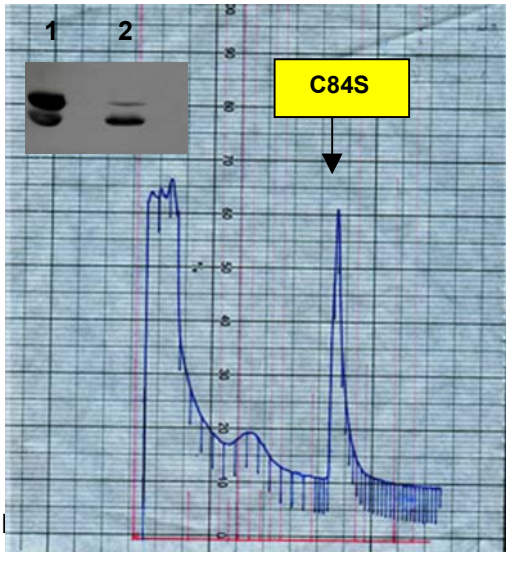

Fig. 37. Hydrophobic interaction chromatography of FTR∆24 C84S on Phenyl-Sepharose. The column was equilibrated in 100 mM KPi buffer pH 7.3 containing 0.6 M ammonium sulfate. After loading the proteins in the 25% ammonium sulfate supernatant, the column was washed with 100 mM KPi buffer containing 0.6 M ammonium sulfate and finally the FTR eluted with 50 mM KPi buffer pH 7.3.
The last peak contains the FTR mutant separated from nucleic acids. Western blot analysis confirms the presence of mutant in the last peak (lane 2). Lane 1. FTR WT control.

However, upon concentrating the separated protein fractions with ammonium sulfate at 90% saturation, before loading the size exclusion column, the mutant FTR could not be solubilized from the precipitate (Fig. 38).

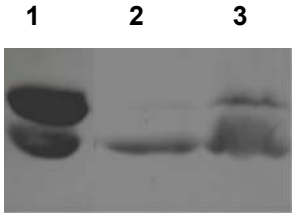

Fig. 38. C84S mutant after concentration with ammonium sulfate at 90 % saturation. Lane 1. FTR WT control; lane 2. Supernatant; lane 3. Pellet.

These observations indicate that the mutant structure is much more labile, particularly upon treatment with ammonium sulfate.

5.1.3.2.2 Ion exchange chromatography procedure

To avoid problems of instability in ammonium sulfate, ion exchange chromatography was tested as a first chromatographic step.
After removal of ribonucleo-proteins by precipitation with 2% Streptomycin sulfate the extract was loaded on a Q-Sepharose column and separated by a NaCl gradient from 50-500 mM. The analysis of the fractions revealed that certain contained both subunits whereas others contained only one of them (Fig. 39).

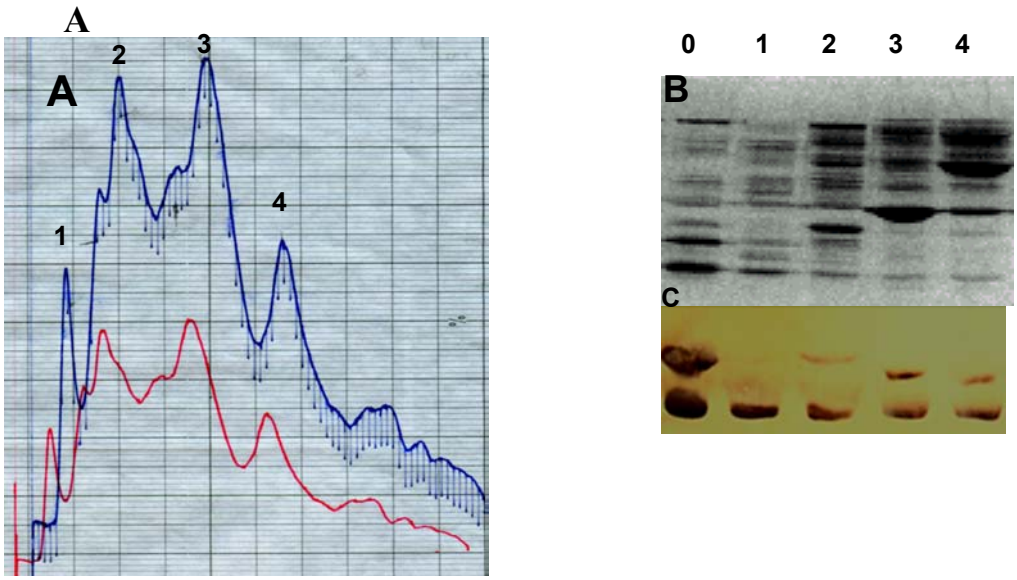

Fig. 39. Anion exchange chromatography of FTRΔ24 C84S on Q-Sepharose. A. Elution profile. B. SDS-PAGE. Lane 0. FTR WT control; lanes 1-4 correspond to the peaks labelled on the profile. **C. Western blot analysis.** Lane 0. FTR control; lanes 1-4 correspond to the peaks labelled on the profile.

Western blot analysis reveals that the mutant protein is eluted in peaks n° 3 and 4 on the anion exchange column (Fig. 39 C). Combined fractions of peaks 3 and 4 were concentrated by ultrafiltration and diafiltered to be loaded on Ferredoxin-sepharose. The affinity column failed to retain the mutant FTR that was detected by western blot analysis in the pass-through fractions (Data not shown).
These observations indicate that the mutation destabilizes the protein causing a conformational change, probably accompanied by the loss of the Fe-S cluster, which abolishes the affinity for ferredoxin.

5.1.3.2.3 Modification of the free thiols with DTNB

Since it is possible that the instability of the mutant protein is due to the presence of an accessible thiol at the active site, we tried to stabilize the mutant by modification of the accessible cysteines with Ellman's reagent in the bacterial extract.
After Benzonase and Streptomycin sulfate treatments the extract was treated with an excess of DTNB as described by Habeeb *et al.*, 1972 and excess reagent was removed through a G-25 desalting column.
Electrophoresis and western blot analysis showed that both subunit bands are present after modification (Fig. 40 A&B). The spectrum revealed a peak at 412 nm

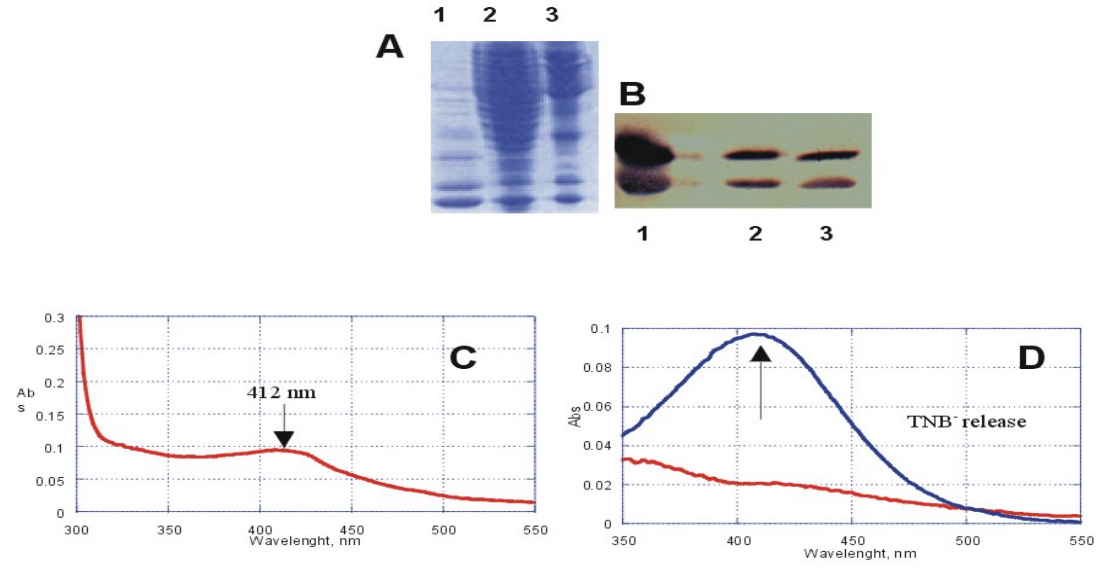

Fig. 40 A. SDS-PAGE analysis of C84S-TNB complex. Lane 1. Partially purified FTR; lane 2. Crude extract modified with DTNB; lane 3. C84S-TNB complex after G-25 column (combined fractions). **B. Western blot analysis.** Lane 1. FTR WT control; lane 2. crude extract modified with DTNB; lane 3. C84S-TNB complex after G-25 column (combined fractions). **C. Modification of C84S with DTNB.** Modification was obtained by Ellman's reagent and it was monitored following A_{412nm} (arrow) typical for TNB^- product. **D. C84S-TNB complex dissociation.** Dissociation of C84S-TNB complex was performed with DTT reagent and release of TNB^- was monitored following the A_{412nm} (arrow).

(Fig. 40 C), which was due to the attachment of TNB^- to free thiols (Fig. 40 C) as evidenced by the release of TNB^- after treatment with DTT (Fig. 40 D).
The modified extract was then chromatographed on the Q-Sepharose column under our standard conditions.
Anion-exchange separation caused the release of TNB^- from the modified protein. We observed that the C84S mutant did not contain TNB^- anymore and TNB^- was eluted from the column by 1M salt (Fig. 41 peak 7).
Western blot analysis (Fig. 41) showed that both subunits of C84S mutant were present in peak 5 on the Q-Sepharose elution profile. Combined fractions were then loaded on the Ferredoxin-sepharose column, but also in this case the C84S mutant was not retained on the affinity column and SDS-PAGE and western blot analysis of pass-through fractions confirmed that no chromatographic separation was obtained (Data not shown).

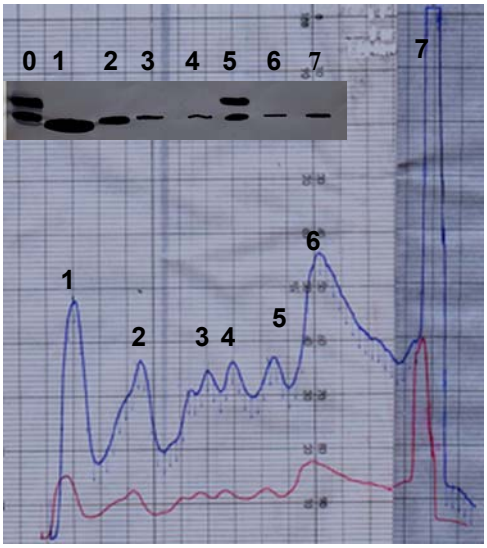

Fig. 41. Q-Sepharose profile of C84S-TNB modified FTR and western blot analysis of peak fractions. Lane 0 on western blot corresponds to purified FTR and lanes 1-7 to the peaks labelled on the profile.

5.1.3.2.4 Size exclusion procedure

A last strategy adopted to attempt a purification of the mutant consisted in a gel filtration step of the bacterial extract followed by affinity chromatography on Ferredoxin-sepharose.
The extract, treated with Benzonase and Streptomycin sulfate, was loaded on the Sephadex G-25 column to change buffer and concentrated by ultrafiltration before S-100 Sephacryl gel filtration (Fig. 42 A).

Analysis of the Sephacryl S-100 column fractions by immunoblotting (Fig. 42 B) revealed the presence of FTR in the fractions where WT FTR usually is eluted. This was also confirmed by the spectrophotometric analysis (Fig. 42 C).

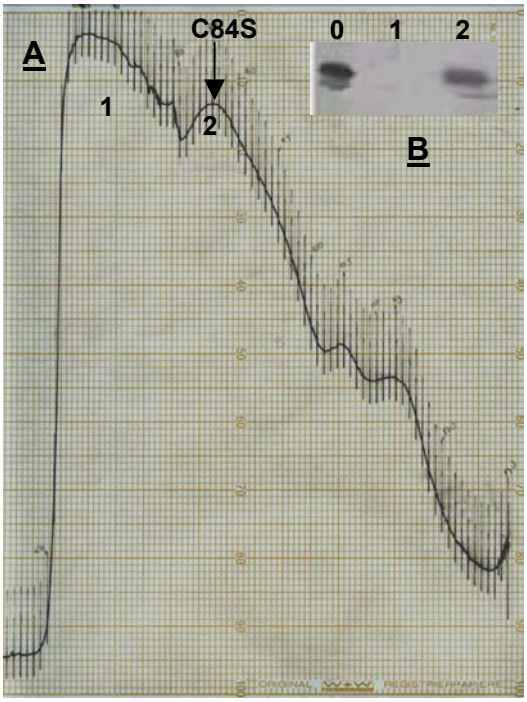

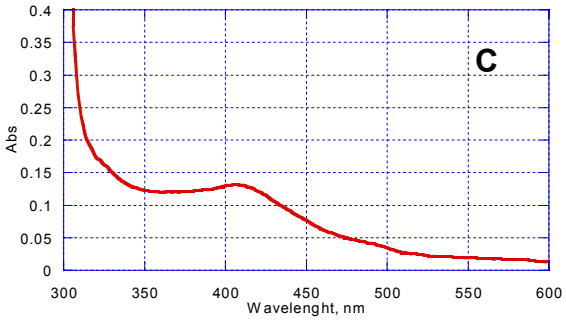

Fig. 42. A. Sephacryl S-100 elution profile of C84S mutant. Separation was performed with 20 mM TEA-HCl buffer pH 7.3 with 200 mM of NaCl. Arrow indicates the C84S mutant peak. **B. Western blot analysis.** Lane 0. Purified FTR WT; lane 1. Peak 1; lane 2. Peak 2. **C. Visible absorption spectrum of peak 2.**

The combined fractions of peak 2 were concentrated and diafiltered prior to loading on the Ferredoxin-sepharose column. At this stage, we observed partial precipitation of FTR, which must be due to the instability of the mutant protein. The concentrated fractions were then loaded on the Ferredoxin-sepharose column that failed to retain the mutant FTR since it eluted in the first fractions (Data not shown). This behavior indicates again a loss of affinity of the FTR mutant for ferredoxin.

5.1.3.3 Discussion

To be able to attempt the formation of stable mixed-disulfides between FTR and thioredoxins suitable for structural analyses, it was necessary to mutate the active site of the FTR by replacing the inaccessible Cys leaving the nucleophilic Cys

capable of forming the intermolecular disulfide bond. Based on discussions with the crystallographers and the fact they had been able to determine the structure of the reduced protein, where the active site disulfide was broken, we were rather confident that an active site mutant was stable enough to be produced and purified. We decided to replace Cys84 by Ser to obtain a single mutant and to construct also a double mutant where in addition Cys27 was replaced by Ser, to avoid possible nonspecific interactions with this exposed residue.

Our results show that *E.coli* produces both mutants, although in lower amounts compared to WT, and appear to be present in soluble form in the cells. However, during different attempts to purify the proteins the amount of dimer, which is the functional form of FTR, continuously decreased and the subunits were detected in different fractions indicating that the dimer was breaking apart. In addition, the typical color of the FTR, due to the Fe-S cluster, was very weak and disappeared during purification steps suggesting a loss of the cluster. These observations suggest that our active site mutation destabilizes the Fe-S cluster, which during purification disintegrates and as a consequence the two subunits separate. To explain the disintegration of the Fe-S cluster due to the mutation of the disulfide bridge we propose the following hypothesis (Fig. 43).

As a consequence of the mutation the remaining Cys54 becomes strongly electronegative and after nucleophilic attack forms a disulfide bridge with Cys82, which is only 6.44 Å away and which holds an Fe atom of the cluster at 3.4 Å distance (Fig. 43 B). The attack might still be helped by His83, which is very close to Cys54 and was proposed to increase its nucleophilicity. The internally formed disulfide bridge destabilizes the charge of the iron in the cluster leading to its oxidation from 2+ to 3+ and breakage of the bond between the iron and Cys82. As a consequence of these changes the cluster falls apart and the two subunits separate. Whether the formation of the disulfide between Cys54 and Cys82 precedes FeS cluster degradation or occurs briefly after dimer formation remain to be determined. The fact that, at a very early step of extraction, the bacterial extract presents either a weak absorbance at 408nm or none indicates that the degradation mechanism is extremely rapid and may even occurs shortly after the folding step of FTR subunits. Nevertheless, this absorbance at 408nm indicates that the bacteria are able to generate the Fe-S cluster. This was taken as an indication that the correct interaction between both subunits of FTR is possible even with the C84S mutation. Unfortunately, all our attempts to increase the yield of cluster-containing FTR at the level of protein synthesis failed. We therefore concentrated our efforts on preserving the small amount of FTR produced with an intact Fe-S cluster. It appeared that among the numerous modifications tested in the purification protocol, almost all of them failed to preserve correctly assembled FTR. These degradative processes might already operate during biosynthesis and explain the lower yield of mutant protein.

Fig. 43. A. The proposed mechanism of Fe-S cluster degradation of C84S mutant. B. Distance from Cys 54 to Cys 82 calculated with Weblab Viewer Lite 4.0 program.

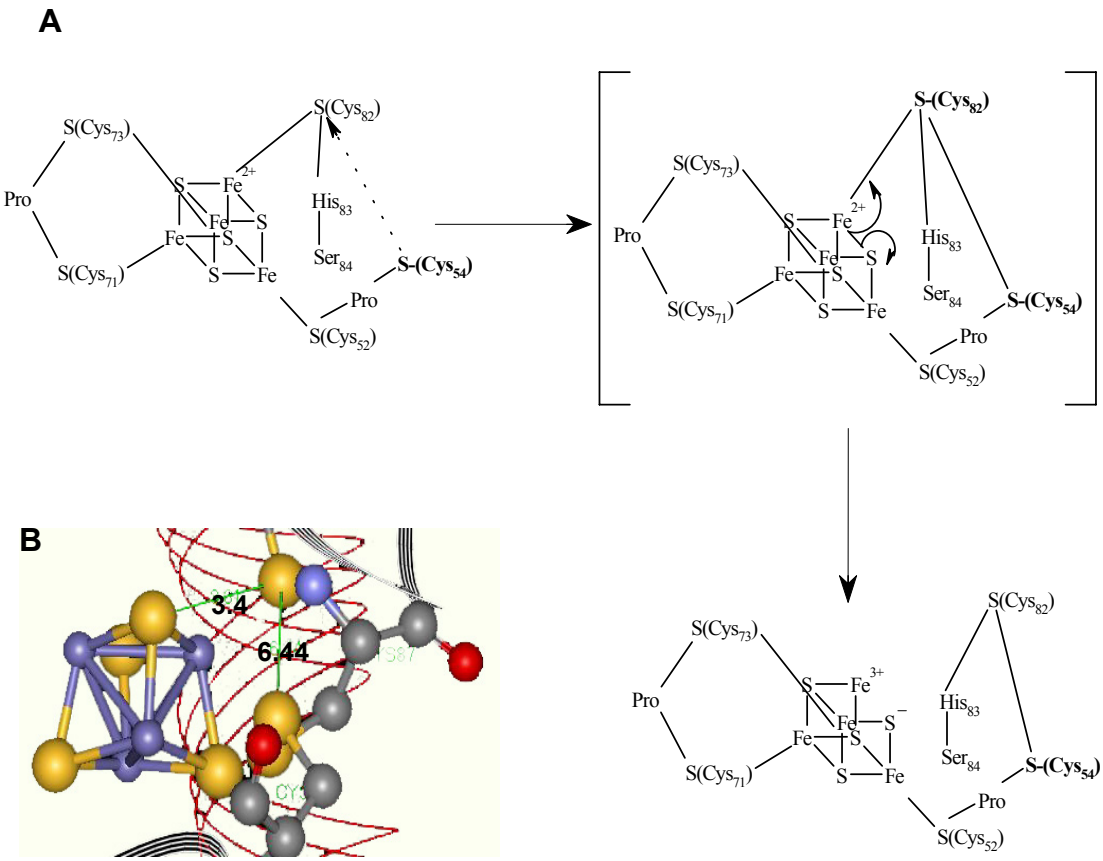

6 Results and discussion

Biochemistry

6.1 Expression, purification and characterization of Trx m_c WT and its mutants: C40S and C40A

6.1.1 Expression and purification

E.coli cells transformed with either WT or mutant plasmid displayed usual growth curves (Fig. 44 A) and readily expressed the recombinant thioredoxins. Yields of 30-50 mg pure protein were obtained from 10 L of culture.
The SDS-PAGE analysis of the cells expressing Trx *m* either in the pKK-system (Fig. 44 B, lane 1) or the pET-system (Fig. 44 B, lane 2) suggests that there is no large difference in the amount of recombinant protein produced between the two expression systems and that the mutations do not inhibit expression (Fig. 44 B, lanes 3&4). In addition, the intensity of the Trx bands indicates that thioredoxin represents the major protein present in the cellular extracts.

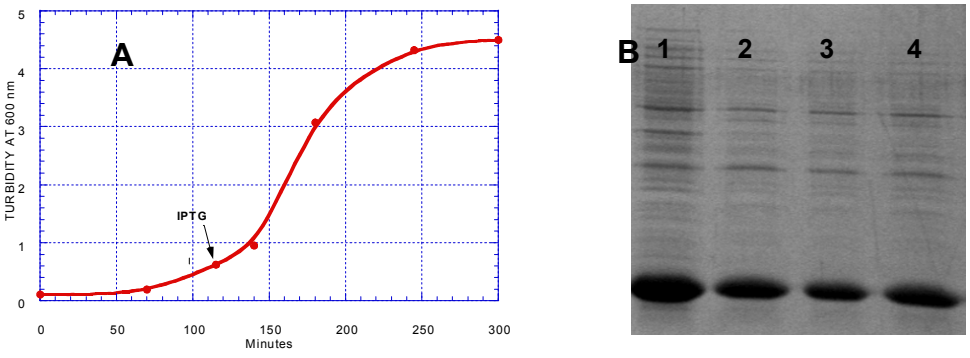

Fig. 44. A. Bacterial growth of Trx m_c WT before and after IPTG. Cell density was followed by measuring the absorbance at 600 nm and IPTG was added after 120 min of growth (arrow). Culture was stopped at the end of the exponential growth phase. **B. SDS-PAGE analysis of culture.** Lane 1. pKK-Trx *m*; lane 2. pET-Trx *m*; lane 3. pET-Trx m_c C40S; lane 4. pET-Trx m_c C40A. Cells were washed with STE buffer (see Material and methods) and lysed according to Johnson B.H. (1994).

All proteins were purified to homogeneity as described in Materials and methods. The purity of proteins was verified by SDS-PAGE after each purification step (Fig. 45).

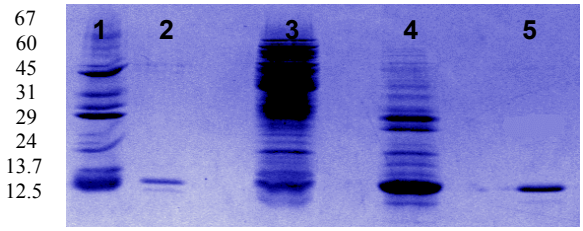

Fig. 45. Progress of purification of thioredoxin m_c by SDS-PAGE. Lane 1. HMW; lane 2. Purified Trx *m*; lane 3. After Phenyl-Sepharose; lane 4. After Sephadex G-50 FF; lane 5. After Anion exchange column.

Depending of the type of mutation, the yields were similar to those obtained with the wild type protein for the C40S mutant or systematically higher for the Ala mutant. This suggests that the structures of the mutant proteins be not altered.

6.1.2 Characterization of Trx m_c WT and its mutants

6.1.2.1 Molar extinction coefficient determination for Trx m_c WT

The molar extinction was obtained by a dry-weight determination of a thioredoxin solution of known UV absorbance. The dry-weight measured for several lyophilized aliquots of thioredoxin m_c are given in Table 10.

Table 10. Weight average of Trx m_c after lyophilization

Sample	mg of protein /400 μl	mg/ml
1	3.72	9.3
2	3.66	9.15
3	3.76	9.4
4	3.68	9.2
5	3.64	9.1
Average		**9.23**

UV spectral analysis of thioredoxin recorded before lyophilization has shown an A_{279} nm= 11.342 cm^{-1} (Fig. 46).

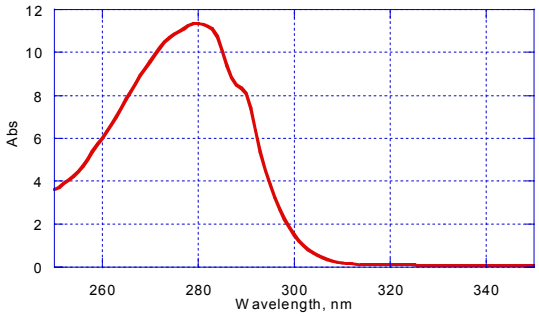

Fig. 46. UV spectrum of Trx m_c WT before lyophilization. Buffer was: 25 mM ammonium formiate pH 8.0. Pathlength = 0.1 cm

The molar extinction coefficient was 15 400 M^{-1} cm^{-1} and was calculated by the following formula:

$\varepsilon_{279\ nm}$ = Mr ($gr.mol^{-1}$) ∗ A (cm^{-1}) / C ($gr.l^{-1}$) = 12 552 ∗ 11.342 / 9.23 =

15 400 M^{-1} cm^{-1}

6.1.2.2 Reduction of mutant thioredoxin dimers

A problem encountered with the mutant thioredoxins, where only the solvent accessible cysteine of the disulfide bridge is present, is their tendency to dimerize (Fig. 47, lane 1). These dimers can be reduced by addition of DTT (1 mM) but not by 2-MET as shown in Fig. 47.
For this reason we have treated the protein fractions with 1 mM DTT before each chromatographic step and stored them in 28 mM of 2-MET.

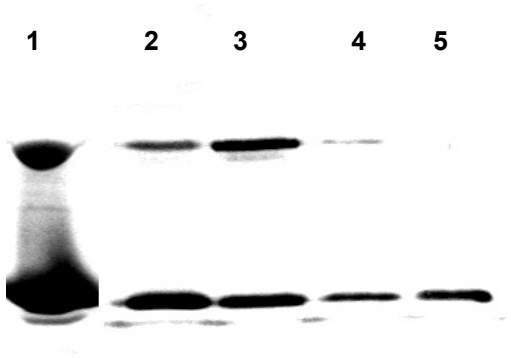

Fig. 47. Dimer formation of thioredoxin mutants. Western Blot analysis of Trx-dimer treated with 2-MET or DTT. Lane 1. Mutant not reduced; lane 2. C40S with 2-MET; lane 3. C40A with 2-MET; lane 4. C40S with DTT; lane 5. C40A with DTT.

6.1.2.3 Spectral and biochemical properties

The spectral properties of mutants thioredoxin m_c were similar to WT (Fig. 48 A), with absorbance maximal at 279 nm. However, active-site mutation influences the activity of mutant proteins since it eliminates the essential disulfide bridge.
We tested WT and mutant thioredoxins for their ability to activate NADP-MDH as a function of time. As shown in Fig. 48 B, NADP-MDH reached full activity after about 15 min when activated with 2 μM WT thioredoxin m_c, whereas the activity reached with the mutant thioredoxins was only about 5% of the maximum.

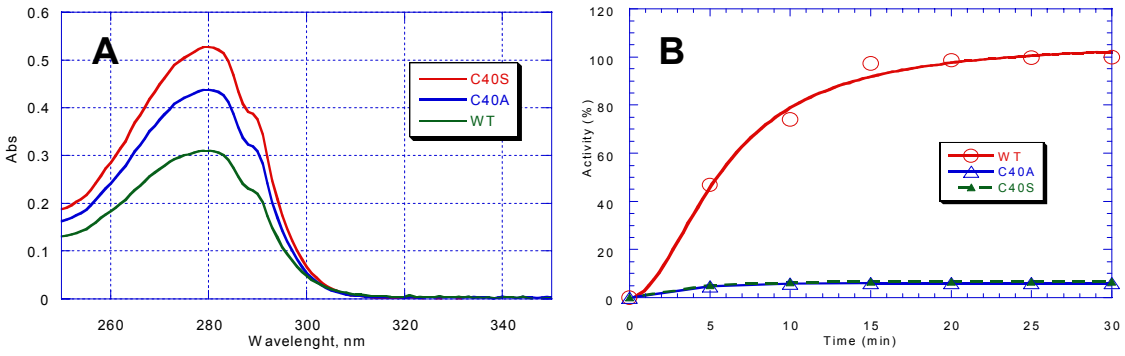

Fig. 48. A. UV spectra of Trx m_c and its mutants. The differences in absorbance are due to different concentrations. **B. Time course of NADP-MDH activation by DTT-reduced thioredoxins.** The activation conditions were as follows: 50 μl of the activation medium contained 100 mM Tris-Cl pH 7.9, 2.5 mM DTT; 0.5 U NADP-MDH, Trxs, 2 μM. 5 μl of activation mixture were used for the determination of the NADP-MDH activity.

If however much higher thioredoxin concentrations (100 μM or more) are used, MDH activation up to 50% of what is observed with the WT thioredoxin are measured by DTT reduction and only 30% by FTR reduction. (Data not shown).

6.1.2.4 Thiol content of mutant thioredoxins

The structural analysis of WT thioredoxin indicates that there is no accessible cysteine; by contrast removal of the inaccessible cysteine in the active site by mutagenesis forms a partially reduced protein with an accessible cysteine (Cys 37 in spinach). In order to check this, we have titrated the WT and mutant thioredoxins with DTNB as described in Materials and methods.
Table 11 summarizes the values obtained after DTNB-modification which are in agreement with the theoretical values; we obtained 0 –SH groups for WT and 1 for C40A and C40S, respectively.

Table 11. -SH groups content of thioredoxins

Trx	-SH groups
WT	0
C40A	0.83
C40S	0.87

6.1.3 Discussion

We generated two mutants of thioredoxin m_c with the objective of providing an inactive protein that should form a stable complex with FTR for crystallization purpose. We found that both mutants, C40S and C40A, were readily expressed and could be purified with good efficiency. In contrast to FTR mutational studies where the substitution of Cys with Ser was unsuccessful, we obtained stable mutants for thioredoxin. However, depending on the mutation introduced, the production yield varied. More precisely, the replacement of Cys40 with a hydrophobic aminoacid such as alanine, produced even more protein than WT recombinant thioredoxin. As expected, both mutants were practically inactive at low concentration (2 μM) which with the WT thioredoxin are sufficient to fully activate the enzyme. But when using 20-50 fold higher mutant concentrations up to 50% of

WT activity was obtained. One explanation for this is that the accepted thioredoxin reaction mechanism for modulating enzyme activities is not complete for thioredoxin mutants. This mechanism proposes that after the transfer of reducing equivalents from thioredoxin to the target enzyme, reduced enzyme and oxidized thioredoxin are liberated and that oxidized thioredoxin will be regenerated by FTR or DTT (see fig. 10 in the Introduction). In this way only catalytic amounts of thioredoxin are required to obtain fully activated target enzymes. The fact that with active site modified thioredoxins the activation of target enzymes requires high thioredoxin concentrations could be explained by protein-protein interactions. These interactions play a significant role in addition to disulfide/thiol exchange reaction in the regulation of plant enzymes by the various plant thioredoxins. In addition, it was demonstrated that high concentrations of monothiols such as 2-MET or dithiols like DTT can fully activate NADP-MDH (Scheibe *et al*., 1986). It is possible that our mutants behave like monothiol reagents, which can attack the disulfide of the target enzyme and form a mixed-disulfide. Either FTR or more efficiently by DTT can then reduce this mixed disulfide. Its smaller size and consequently better accessibility can explain the higher efficiency of DTT to the mixed disulfide bond.

A problem often encountered when the solvent accessible cysteine of the disulfide bridge is present is the tendency of these mutants to dimerize. Reduction of such dimers requires the presence of a strong reducing agent such as DTT.

Unfortunately, the DTT-mediated reduction is not stable since treatments such as removal of DTT by diafiltration or exposure to oxygen readily reform the dimer of mutant thioredoxin. This suggests that the efficient and spontaneous dimerization of mutant thioredoxin in non-reducing conditions could interfere with the generation of heterodimer with FTR, our final objective.

7 Results and discussion

Biochemistry

7.1 Interaction and affinity between Fd and FTR

The iron-sulfur protein ferredoxin (Fd) acts as the first soluble electron acceptor for PSI in oxygenic photosynthesis and, when reduced, serves as the electron donor for a variety of reductant-requiring reactions.
Complexes of Fd with reaction partners are stabilized by electrostatic interactions to which Fd contributes mainly negative charges. Mutational studies on isomer I of spinach Fd have shown that the acidic cluster, E92, E93, E94, plays an important role in the interaction between Fd and electron acceptor proteins (Piubelli *et al.*, 1996; Aliverti *et al.*, 1997). Moreover, based on differential chemical modification, residues D34, D65, E92, E93, E94 and A97 of spinach Fd were proposed to be located in the binding site for FTR (de Pascalis *et al.*, 1994). In addition, a report by Jacquot *et al,* 1997, based on mutagenesis indicated that the residue E91 of *Chlamydomonas reinhardtii* ferredoxin (E92 in spinach) is essential for electron transfer to FTR. It was therefore of interest to verify some of these propositions by studying the interaction of FTR with mutant ferredoxins in which acidic residues have been replaced. We have investigated the effects of two single mutations (E92K and E93A) and of two double mutations (E92/93A and E93/94A) in the C-terminal region of spinach ferredoxin, on the capacity of these mutants to transfer electrons to FTR and also studied the effects on the complex formation between Fd and FTR by spectral perturbation measurements. Professor Giuliana Zanetti, Department of Physiology and Biochemistry, University of Milan gently provided all ferredoxin mutants used in this study.

7.1.1 The role of the acidic cluster E92-94 of spinach Fd in FTR reduction

The effects of the various mutations on the reactivity with FTR are shown in Fig. 49.

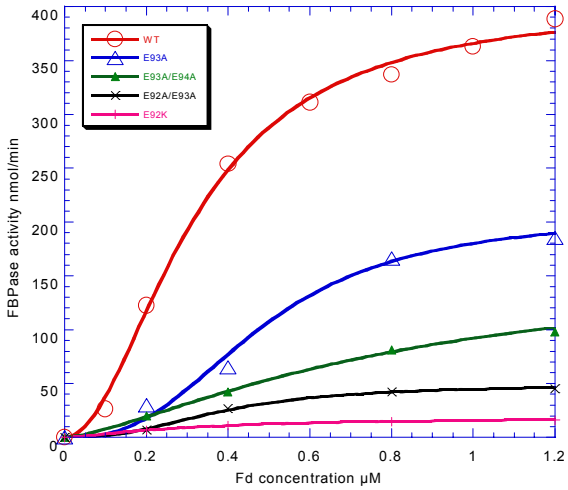

Fig. 49. Activation of FBPase as a function of ferredoxin concentration. Ferredoxin mutants were tested in a concentration range of 0.1 to 1.2 µM. The E92K mutant was tested at several concentrations, up to 250 µM, and was almost totally inactive through the whole range.

E92K mutant showed a very low activity as electron-donor for FTR (4.5% of maximal FBPase activity), in agreement with the results obtained by Jacquot *et al.*, when activating NADP-MDH. By contrast, neutralization of the charge in position 93 yielded a ferredoxin 50% less efficient than WT whereas Jacquot *et al.*, 1997 reported that the equivalent mutant of *Chlamydomonas* Fd was indistinguishable from WT. Elimination of the two acidic side-chains in position 92/93 produced a mutant Fd with very low activity in FTR reduction; the $S_{0.5}$ was increased and the V_{max} was decreased to 12% of WT Fd. The other double mutant obtained by replacing E93 and E94 with alanine showed a $S_{0.5}$ similar to that of the single mutant E93A (39% FBPase activity). The kinetic constants determined for FTR reduction with the various ferredoxin forms are reported in Table 12.

Table 12. Activation of spinach fructose 1,6-bis-phosphatase with WT and mutant ferredoxins. The activation mixture (100 µl) contained FTR (160 nmol), thioredoxin *f* (2 µM), recombinant spinach FBPase (0.5 U) in TRIS-Cl 100 mM pH 7.9. Ferredoxin was reduced by dithionite and Fd concentrations were in a range of 0.1-1 µM. Half-saturation concentrations ($S_{0.5}$) were calculated with a simplified Hill equation.

Mutation	$S_{0.5}$	V_{max}	% FBPase activity
WT	0.32 µM	403 nmol/min	100
E93A	0.40 µM	206 nmol/min	51
E93/94A	0.50 µM	159 nmol/min	39
E92/93A	0.70 µM	48 nmol/min	12
E92K	0.70 µM	18 nmol/min	4.5

7.1.1.1 Complex formation between WT and mutant ferredoxins with FTR

To investigate the role of residues E92-94 of ferredoxin in the complex formation with FTR we have measured the affinity between FTR and mutant ferredoxins by monitoring the spectral perturbations. The formation of complex between Fd and FTR is known to produce significant alterations in the absorbance spectra of the chromophores, which can be shown by difference spectra (Hirasawa *et al.*, 1988). Such absorbance changes were detected when oxidized ferredoxins were mixed with equal concentrations of FTR in 20 mM ionic strength buffer. Fig. 50 shows the difference spectra of the complex between FTR and mutant ferredoxins.

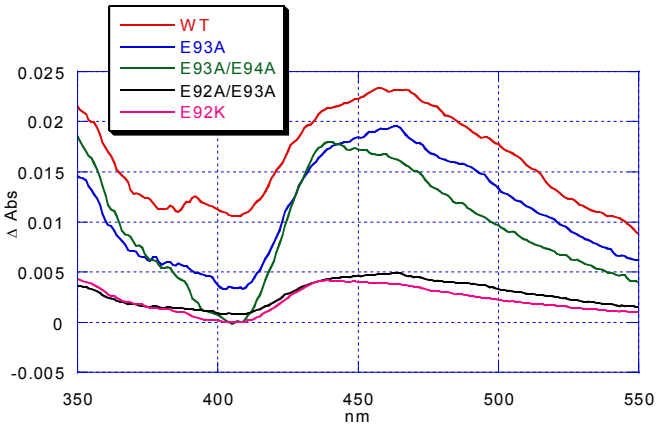

Fig. 50. Difference spectra of the complex between FTR and either WT Fd or mutants. The sample cuvette contained FTR at a concentration of 50 μM and equimolar amounts of ferredoxin in 20 mM TEA-Cl pH 7.3 in the same compartment. The reference cuvette contained the same components but with the ferredoxin and enzyme in separate compartments.

All spectra show maxima around 450 nm, which is probably due to changes in the environment of the Fe-S clusters. By contrast, the amplitude of the spectra show clear differences. The complexes with WT, mutants E93A and E93/94A show comparable differences between the absorbance maxima (around 450 nm) and minima (410 nm) suggesting similar affinities. The differences for the two other mutants, E92K and E92/93A, however, are much lower. This indicates that the interaction between FTR with these mutants is very weak and the complexes formed are unstable. Since in both of these ferredoxins the residue E92 has been replaced, it appears that it has not only an important function in electron transport, but also in the interaction, maybe by some structural changes. The complex formation is also strongly dependent on the ionic strength of the medium in which the reaction is carried out as has been reported in the literature (Hirasawa *et al.*,

1988). To probe the stability of the complexes we have increased the ionic strength by addition of NaCl and followed the disappearance of the difference spectra. Fig. 51 shows the effect of ionic strength on Fd/FTR complex dissociation.

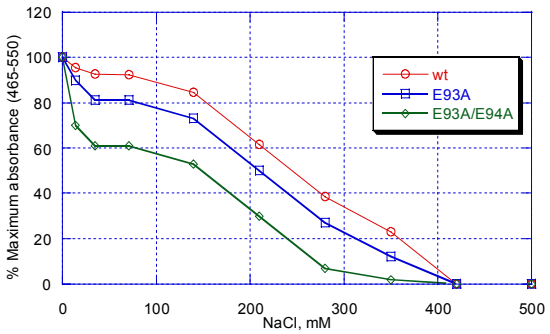

Fig. 51. Fd/FTR complex dissociation in function of NaCl concentration. Red: Fd WT; blue: E93A mutant; green: E93/94A mutant.

As we increase the ionic strength to 400 mM NaCl, the difference spectra decrease for all three complexes, however more pronounced for the mutants, especially for the double mutant. The complexes are completely dissociated at concentrations above 400 mM NaCl. These results show that the complexes with the mutants are less stable than with the WT ferredoxin and suggest that E94 plays also some role in the interaction since the double mutant dissociates faster.

7.1.2 Comparison of homologous and heterologous proteins.

Spinach ferredoxin has been shown to form a high affinity, electrostatically stabilized 1:1 complex with spinach FTR (Kd for ferredoxin $<1x10^{-7}$ M; Hirasawa *et al.*,1988) while spinach ferredoxin and *Synechocystis* FTR showed a Kd of $2x10^{-5}$ M (Schwendtmayer *et al.*, 1998) suggesting that despite the high degree of sequence similarity the charge complementarity between the two heterologous proteins is not optimal.
Here we compare the affinity between Fd and FTR from spinach and *Synechocystis*, in order to examine the electron-transfer ability of Fd in homologous and heterologous systems.
The ability to transfer electrons was analyzed by activation of FBPase as a function of varying amounts of Fd. As shown in Fig. 52 A, FTR from spinach can almost equally well be reduced by both Fds and the maximum activity (apparent V_{max}) obtained did not differ significantly when spinach (so) or *syn* Fd was used (Table

13). By contrast, the reduction of *Syn* FTR required at least 3-4 fold more of each Fd to reach half-maximal activity (Fig. 52 B) but showed comparable maximal activities.
A comparison of the calculated half-maximal saturation concentrations (Fig. 52 and Table 13) also shows that both FTRs have a slightly higher affinity for the homologous Fd.

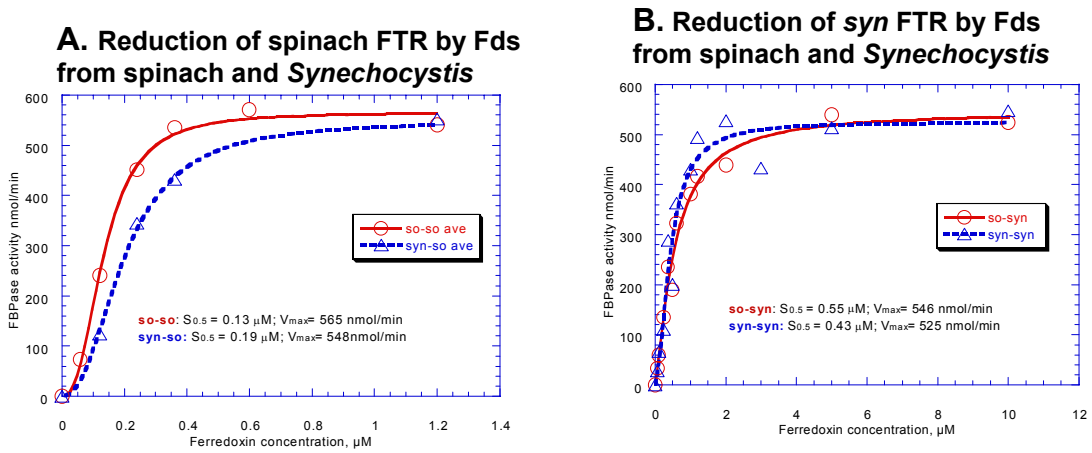

Fig. 52. Fd-dependent activation of FBPase. A. Spinach FTR reduced by spinach Fd (red) or by *syn* Fd (blue). **B.** *syn* FTR reduced by spinach Fd (red) or *syn* Fd (blue).The activities were measured after 5 min of activation with dithionite-reduced ferredoxin at 25 °C.

These data suggest that there may be only minimal structural differences between the two Fds, which affect their interaction with the two FTRs.

Table 13. Kinetic parameters of FTR reduction by Fd. The kinetic parameters have been calculated with a simplified Hill equation: $V= V_{max} [S]^n /(K' + [S]^n$. The curves are shown in Fig. 52. *syn* = *Synechocystis;* so = spinach.

Combination Fd/FTR	$S_{0.5}$	V_{max}
so/so	0.13 µM	565 nmol/min
syn/so	0.19 µM	548 nmol/min
so/*syn*	0.55 µM	546 nmol/min
syn/*syn*	0.43 µM	525 nmol/min

In all interactions the homologous system has a lower $S_{0.5}$ comparable to the heterologous system (Table 13). However, the *syn* FTR appears to have in general a lower affinity for both ferredoxins. This is not due to the use of spinach Trx *f* and FBPase for the activation as shown in Chapter 9, but must be due to structural differences on the Fd-interaction site of the FTR.

7.1.3 Discussion

Our results suggest that in the C-terminus of spinach ferredoxin, not only the residue E92 is essential for the interaction with FTR but also residues E93 and E94. Elimination of one or two acidic side-chains in the acidic cluster (Glu 92-94) of ferredoxin reduced the efficiency of the electron-transfer because these residues are located on the same surface of ferredoxin to the right of the [2Fe-2S] cluster where they form a semicircle around it. This conformation appears essential for interaction with the FTR and mutations do affect the capacity of Fd to transfer electrons to FTR, which results in a reduced activation of FBPase. In addition the mutation of neighboring E93 in spinach ferredoxin might cause further changes, like a conformational change due to the removal of a carboxyl group. As a consequence the mutation influences the affinity for ferredoxin and explains the 50% reduction of activity compared to wild type (see Table 12) and is not equally efficient as WT as reported by Jacquot *et al.* 1997, for the *Chlamydomonas* system.
The importance of the acidic cluster Glu92-94 in the interaction with FTR was also confirmed by difference spectra. When FTR was mixed with WT or mutant Fd in all cases difference spectra were observed however with different amplitudes. Ferredoxins in which E92 had been mutated showed much weaker interaction indicating that E92 is not only involved directly in the electron transport, but also in the protein-protein interaction.
Our results are in agreement with those of de Pascalis *et al.*, 1994, who showed that there is a recognition site for FTR in the C- terminus of ferredoxin, but they are in part in contrast with the results reported by Jacquot *et al*. 1997, who suggest that in the C-terminus of ferredoxin only residue E91 (E92 in spinach) is essential. We have demonstrated that this residue is also involved in the interaction with FTR and that residues E93, E94 influence the electron transport.
Our results suggest also that there is a slightly higher affinity between FTR and homologous ferredoxin, but that *syn* FTR has a generally lower affinity for ferredoxin. These differences could be due to differences in the Kd or to the electron-transfer route between the two proteins.

8 Results and discussion

Biochemistry

8.1 Redox potentials

Attempts to model the kinetics of activation and deactivation of various thioredoxin-regulated enzymes and to explain the differential effects of light intensity on these enzymes *in situ* require an accurate knowledge of the oxidation-reduction midpoint potentials (E_m) of the disulfide/dithiol couples involved in the regulatory pathway. In addition, it was interesting to re-determine the E_m for thioredoxin *f* and *m* in order to test if both chloroplast thioredoxins presented similar reducing power.
Previous work using cyclic voltammetry has provided the first published E_m values for spinach thioredoxins *f* and *m* and for spinach FTR (Salamon *et al.*, 1995). However, E_m values obtained by cyclic voltammetry for spinach thioredoxin *f* and *m* were significantly more positive than those obtained for maize thioredoxin *m* determined by enzyme activity (Rebeille *et al.*, 1986) and spinach thioredoxin *f* determined by mBBr (Hutchison, 1994).
In view of these discrepancies, it appeared important to reinvestigate the oxidation-reduction properties of these proteins using the mBBr labeling technique as described in Materials and methods. In addition, given the rise in the stromal pH from approximately pH 7.0 to 7.9, that occurs during illumination of chloroplasts, it was of interest to examine the pH dependence of the E_m values of FTR and thioredoxins all of which are soluble proteins located in the stromal space of chloroplasts. We report E_m values, measured over a range of pH values for thioredoxin *f*, thioredoxin *m* and FTR from spinach.

8.1.1 Redox titrations for thioredoxin *f* and *m*

Fig. 53 A & B shows the result of titrations of spinach thioredoxin *f* and *m* at pH 7.0. Multiple titrations of these spinach proteins gave average values for E_m, at pH 7.0, of –290 ± 10 mV and –300 ± 10 mV for thioredoxin *f* and *m*, respectively.

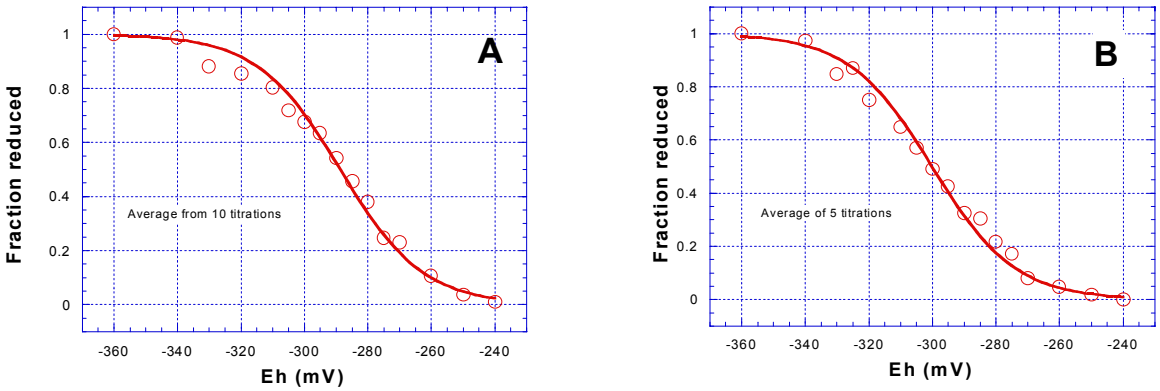

Fig. 53. Oxidation-reduction titrations of spinach thioredoxins *f* and *m* at pH 7.0.
Plots represent averages of 10 titrations (**A**) and 5 titrations (**B**) for thioredoxin *f* and *m* respectively.

The E_m values obtained for the two spinach chloroplast thioredoxins at pH 7.0 are 80-90 mV more negative than the values of –210 mV previously obtained by cyclic voltammetry for both spinach thioredoxins *f* and *m*. The more positive E_m found with cyclic voltammetry could be explained by conformational changes in the proteins due to interactions with the lipid bilayer at the surface of the electrode. By contrast the more reducing numbers obtained in this study from mBBr titrations are in good agreement with values reported for spinach thioredoxin *f* (Hutchison, 1994) and maize thioredoxin *m* (Rebeille *et al.*, 1986), in titrations that used either mBBr or enzyme activity measurements to monitor the reduction state of the active-site disulfides.

8.1.2 Redox titrations for FTR

Fig. 54 shows the results of titrations of the active-site disulfide of spinach FTR at pH 7.0. An average value of –320 ± 10 mV was obtained for the E_m value of the spinach enzyme at this pH.

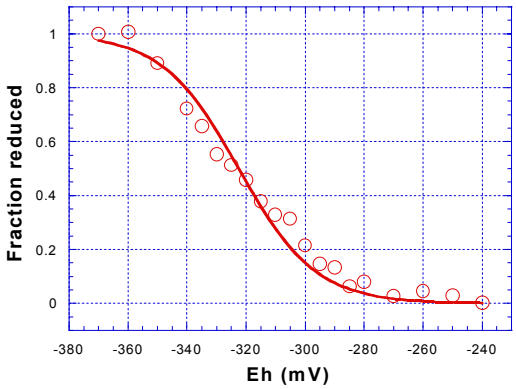

Fig. 54. Oxidation-reduction titration of spinach FTR at pH 7.0.
Titrations were carried out as in Materials and methods.
Plot represents the average of 9 titrations.

The E_m value at pH 7.0 obtained for spinach FTR is 90 mV more negative than that obtained by cyclic voltammetry and this difference is almost identical for all three of the proteins examined in the cyclic voltammetry measurements. This means that the thermodynamic driving force, at pH 7.0, of –30 mV estimated previously by Salamon *et al.*, 1995 for the reduction of the active-site disulfides of thioredoxin *f* and *m* by the two cysteines at the active site of reduced FTR is sufficient and correct.

8.1.2 pH dependency of the E_m values

Fig. 55 shows the pH dependency of the E_m values of thioredoxin *f* and *m*. Plots of E_m versus pH for both spinach thioredoxins *f* and *m* give good fits to straight lines with the –59 mV/pH unit dependence expected for a redox reaction that involves the uptake of two protons per two electrons over the pH range from 6.0 to 8.5. At pH values above the pK_a of the more acidic cysteine, where only one proton would be taken up per disulfide reduced, an E_m versus pH dependence of –30 mV/pH would be expected, and at pH values above the pK_a values of both cysteines, where no protons are taken up on reduction of the disulfide, the E_m would be expected to be independent of pH (Chivers *et al.*, 1997).

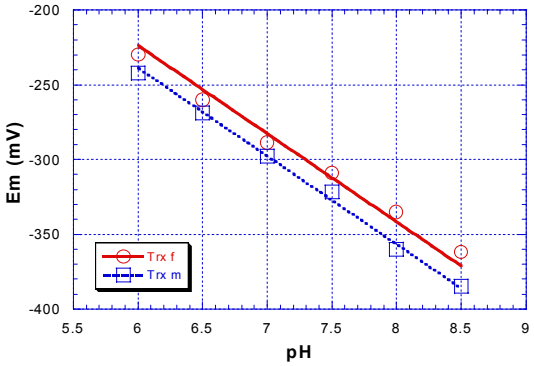

Fig. 55. Effect of the pH on the E_m values of spinach thioredoxins *f* and *m*. Buffers used were Bis-Tris-Cl (pH 6.0-7.0) and Tricine-NaOH (pH 7.5-8.5).

The explanation for the observation that both chloroplast thioredoxins *f* and *m* exhibit an E_m versus pH dependence that does not deviate from the –59 mV/pH unit value expected for the uptake of two protons per reduction of the active-site disulfide up to pH values of 8.5 or 9.0 is that neither of the active-site cysteines of these proteins have pK_a values significantly below 8.0.

8.2 Discussion

Oxidation-reduction midpoint potentials (E_m) for three components of the ferredoxin:thioredoxin system (FTR, thioredoxin *f* and *m*) have been determined and for the first time the dependence of the E_m values on pH for thioredoxins and FTR in the spinach system is now available. As a result of this study we have observed that the E_m values for the two chloroplast thioredoxins and for FTR as well exhibit -59-60 mV/pH unit dependence for the pH range over which the pH of the chloroplast stromal space increases during illumination. However, titrations of spinach FTR at pH 6.0 indicate that the enzyme also exhibits a –59 mV/pH unit dependence over the pH range between 6.0 and 7.0 (Data not shown). Although titrations of FTR at pH 8.0 suggest that this E_m versus pH unit dependence is also likely to extend to pH 8.0, the enzyme proved to be insufficiently stable at this pH to provide completely reliable E_m values at alkaline pH values. The 59-60 mV/pH unit dependence obtained in this study is in agreement with the previous results obtained by cyclic voltammetry and means that the driving force for reduction of either thioredoxin *f* and *m* by FTR will not change during illumination. Accordingly, we can continue our studies to test if FTR can reduce both thioredoxins with equal efficiency or, if there is a difference in affinity.

9 Results and discussion

Biochemistry

9.1 Interaction and affinity between FTR and Thioredoxins

Chloroplasts contain two types of thioredoxins, *f* and *m*, catalyzing identical reactions via FTR.
An open question still is whether FTR is capable of reducing both chloroplast thioredoxins with equal efficiency. We therefore measured the activation of FBPase and NADP-MDH under comparable conditions to obtain preliminary information on the affinity of FTR towards the two thioredoxins. The results presented in this work would be the basis for further studies in our laboratory to clarify the catalytic mechanism of FTR.

9.1.1 FBPase activation via FTR

Previous studies have shown that the two-stage assay is very convenient to analyze the activity of thioredoxin-dependent enzymes because it separates the conversion of the enzyme to a form with different kinetic properties from the transformation of substrates to product. Accordingly, we have tried to characterize the affinities between FTR (WT and mutants) and thioredoxins or ferredoxin by their $S_{0.5}$ values determined under standardized conditions.
Since spinach thioredoxin *f* is rather positively charged, a lower affinity for truncated FTR could be expected if the N-terminal tail with its negative charges is involved in the interaction. However, as shown in Fig. 56, the truncation of variable subunit of FTR does not seem to influence the ability of the FTR to reduce thioredoxin *f*, because the kinetic parameters (here represented by $S_{0.5}$ and V_{max}) for both mutants were essentially similar to the WT enzyme.

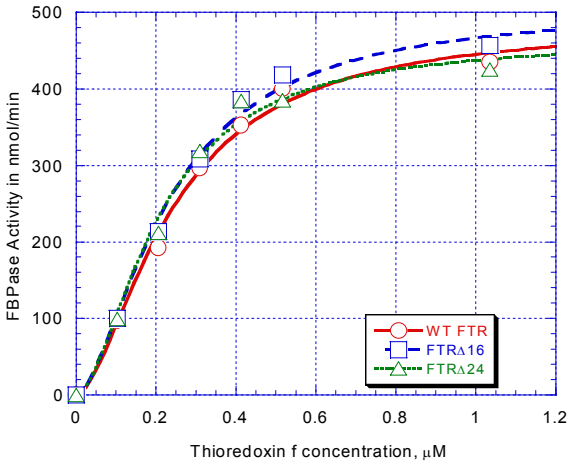

Fig. 56. Thioredoxin-concentration dependency of the activation of FBPase by WT and FTR mutants. FBPase (0.5 U) was activated during 5 min in presence of 5 mM Na-dithionite, 1 µM methylviologen, 200 nmol FTR and varying concentrations of thioredoxin *f*.

Likewise, when we reduced the active site disulfide of FTR with electrons donated by ferredoxin, we do not observe a significant change of the affinity between ferredoxin and wild type or mutant FTR (Fig. 57). It can be seen that the removal of the N-terminus of subunit A does not significantly alter the affinity for ferredoxin although the truncations remove a number of mainly negative charges making the protein more positive, which might favor the interaction with the negatively charged ferredoxin.

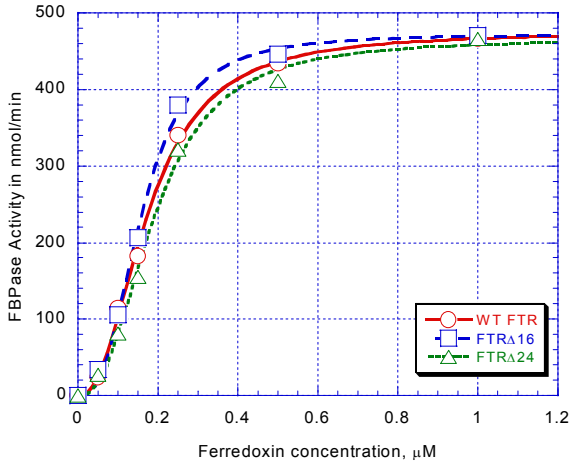

Fig. 57. Ferredoxin-concentration depedency of the activation of FBPase by WT and FTR mutants. FBPase (0.5 U) was activated by dithionite, varying concentrations of ferredoxin, 200 nmol FTR and 2 µM thioredoxin *f*.

Table 14 summarizes the kinetic parameters of the interaction between FTR and ferredoxin and thioredoxin *f* respectively.

Table 14. Comparison of the affinity between FTR and Fd or Trx *f*. Curves are shown in Figs. 56 and 57.

Protein	Ferredoxin affinity		Thioredoxin affinity	
	$S_{0.5}$	V_{max}	$S_{0.5}$	V_{max}
FTR	0.17 μM	475 nmol/min	0.24 μM	486 nmol/min
FTRΔ16	0.16 μM	472 nmol/min	0.23 μM	507 nmol/min
FTRΔ24	0.19 μM	466 nmol/min	0.21 μM	466 nmol/min

Based on these results we were also interested to compare the activation using *syn* FTR, which has an even shorter N-terminus in the variable subunit and spinach C27S mutant, which has a mutation on the thioredoxin-interaction side (Fig. 58).

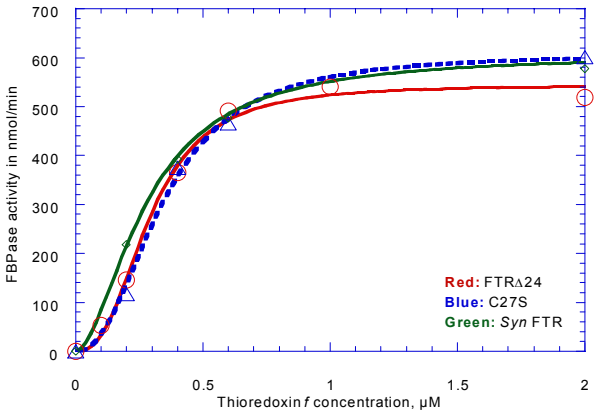

Fig. 58. Thioredoxin *f*-concentration dependency of the activation of FBPase with FTRΔ24, C27S mutant and *syn* FTR.
Red. FTRΔ24: $S_{0.5}$= 0.29 μM, V_{max}= 544 nmol/min.
Blue. C27S: $S_{0.5}$= 0.34 μM, V_{max}= 608 nmol/min.
Green. *syn* FTR: $S_{0.5}$= 0.28 μM, V_{max}= 607nmol/min.

As shown in Fig. 58, $S_{0.5}$ between *syn* and FTRΔ24 is rather similar although the system is not homologous. This means that *syn* FTR is able to reduce thioredoxin *f* with equal efficiency as spinach FTR, in agreement with the results obtained by Schwendtmayer *et al.*, 1998. The results that we obtained are also in agreement with the structural analysis of *syn* FTR, which showed that the thioredoxin docking area of FTR contains mainly hydrophobic residues and is less charged. The absence of charged groups make the FTR less selective and it could reduce different thioredoxins. By contrast, the replacement of a -SH group in C27S mutant increases slightly the $S_{0.5}$ (0.34 μM) but V_{max} is not substantially different from *syn*

FTR. We can hypothesize that this residue is not directly involved in the interaction with thioredoxin because the mutant is still able to fully activate FBPase after only 5 minutes, but the interaction is influenced. This is demonstrated by the lower affinity for C27S mutant compared to truncated mutant (FTRΔ24: 0.29 μM) where this residue is still present.

9.1.2 NADP-MDH activation via FTR

The activation of NADP-MDH was measured with different amounts of thioredoxin *m* and catalytic amount (0.2 μM) of FTR reduced by artificial electron donors as described in Materials and methods. All FTRs were able to reduce thioredoxin *m* while thioredoxin mutants (C40A and C40S) were inactive as expected for this active-site mutation.
In Fig. 59 A&B and in Table 15 we show the ability of FTR to reduce thioredoxin *m* expressed by the activation of NADP-MDH. We observed that the reduction ability of FTR truncation mutants was quite similar to the WT. This indicates that the removal of parts of the N-terminal tail of variable subunit of FTR does not influence the affinity of FTR in the interaction with thioredoxin *m* as observed previously in the reduction of thioredoxin *f*.

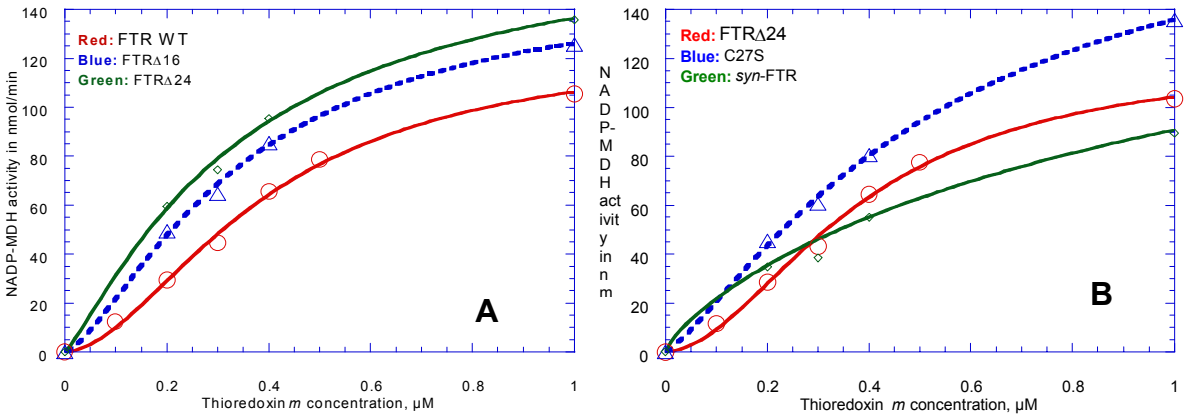

Fig. 59. Thioredoxin *m*-concentration dependency of the activation of NADP-MDH with WT, mutant and *syn* FTR. Reaction was performed as described in Materials and methods with Trx *m* in a range of 0.1 to 1 μM and with 0.2 μM of FTRs. **A.** Red: FTR WT; blue: FTRΔ16; green: FTRΔ24. **B.** Red: FTRΔ24; blue: C27S; green: *syn* FTR.

However, the replacement of Cys27 on the thioredoxin interaction-side of spinach FTR appears to reduce the affinity for thioredoxin *m* (Fig. 59 B), similar to what we observed with thioredoxin *f*. In addition using *syn* FTR in the activation system we observe an unexpected hyperbolic response to changing thioredoxin *m* concentrations. The $S_{0.5}$ value calculated based on this result suggests a significantly lower affinity for this heterologous, but prokaryotic type of thioredoxin.
Table 15 summarizes the kinetic parameters of the activation of FBPase and NADP-MDH by thioredoxin *f* and *m*, respectively**.**

Table 15. Summary of affinity between FTR, Trx *m* and Trx *f*. $S_{0.5}$ indicates the amount of Trxs necessary to obtain half of the maximum enzyme activity.

Protein	**FBPase activation**		**NADP-MDH activation**	
	$S_{0.5}$	**V_{max}**	**$S_{0.5}$**	**V_{max}**
WT	0.24 μM	486 nmol/min	0.39 μM	126 nmol/min
FTRΔ16	0.23 μM	507 nmol/min	0.35 μM	154 nmol/min
FTRΔ24	0.21 μM	466 nmol/min	0.35 μM	175 nmol/min
C27S	0.34 μM	608 nmol/min	0.54 μM	196 nmol/min
syn FTR	0.28 μM	607 nmol/min	1.7 μM	229 nmol/min

In conclusion, we observed that FTR seems to have a higher affinity for thioredoxin *f* than for thioredoxin *m* as suggested by the $S_{o.5}$ values.

9.2 Discussion

As already mentioned in the introduction, the aim of this study is to obtain preliminary information about the affinity of FTR for the two chloroplast thioredoxins. It was demonstrated that most thioredoxins have similar overall three-dimensional structure but significant differences in both the surface topology and the distribution of charges that surround the active site thereby non-covalent interactions at the exposed residues might contribute to the specificity of chloroplast thioredoxins for target enzymes (Capitani *et al.*, 2000). However, no evident conclusions can be proposed on the role of this different surface topology in the interaction with FTR.

For this purpose, we were interested to investigate the role of the N-terminal of the variable subunit of spinach FTR in the interaction with thioredoxin *f* and *m* and also the influence of the free accessible cysteine in the catalytic subunit of FTR, (Cys27), which is located in the thioredoxin-interaction side of FTR.
Our truncation mutational studies suggest that in vitro the N-terminus of variable subunit of spinach FTR does not have any significant function in the interaction between FTR and ferredoxin or thioredoxins. These results are in agreement with the structural analysis of the FTR from *Synechocystis* which revealed that all charged residues possibly involved in the interaction with ferredoxin are located on the catalytic subunit. We can also propose that the variable subunit of spinach FTR does not play a role in the interaction with thioredoxins because the removal of parts of the N-terminus did not affect the ability of FTR to reduce thioredoxins.
The replacement of the free, accessible, conserved residue (Cys27) does not alter significantly the ability of FTR to reduce thioredoxins, but the affinity for thioredoxin *m* appears to be slightly reduced. However, the maximal activities reached in each system are comparable. More information about the behaviour of the C27S mutant would be needed to draw definite conclusions about the role of Cys27 in the interaction with thioredoxins.
In conclusion, comparing the affinities of the WT and mutant FTRs with both chloroplast thioredoxins (Table 15), we have observed that, in general, the interaction of the enzyme with thioredoxin *m* seems to be less efficient than with thioredoxin *f* in the activation process. This could be explained by their specific surface structure, which would favor or prevent, respectively, the formation of the non covalent complex. In addition, given that both chloroplast thioredoxins have similar midpoint redox potentials for performing the thiol/disulfide exchange, non-covalent interactions appear responsible for the differences in their action with FTR. Obviously, the three dimensional structures of FTR/Trxs complexes could provide such information.

10 Conclusion

FTR is the key enzyme in the ferredoxin/thioredoxin system and transforms the redox signal from an electron to a disulfide signal to activate several FTR-dependent enzymes in the photosynthetic regulatory pathway.
The structure of the FTR from *Synechocystis* was recently solved (Dai, 1998) and a mechanism of action was proposed for the transformation of a light signal into a redox signal (Dai *et al.*, 2000).
The structure of FTR is ideally suited for this task because FTR is an unusually flat molecule where the Fe-S cluster is accessible from one side and the disulfide bridge, constituting the active site, is accessible from the other side.
This double accessibility should allow simultaneous docking of ferredoxin and thioredoxin to the FTR.
In order to get detailed information about the interaction of FTR it would be helpful to crystallize a triple-protein-complex between FTR, ferredoxin and thioredoxin, the principal aim in this thesis.

In contrast to *syn* FTR, spinach FTR was less stable. Comparing the aminoacid sequences between both FTRs we observed a longer N-terminal tail for the variable subunit of spinach FTR. Since this additional N-terminal sequence is rich in serine and proline residues, we supposed that these residues were responsible for the instability of the spinach enzyme. We therefore removed parts of the spinach FTR N-terminus with the objective to obtain a stable pure protein for crystallization studies. The truncated mutants showed indeed a higher stability than the unmodified enzyme, especially the shortest mutant whose behaviour was similar to *Synechocystis* enzyme.

Based on these positive results, we then introduced mutations in order to stabilize a triple-complex Fd/FTR/Trx. Since this complex remains only transiently in its wild type conformation, we chose to modify the active-site of both spinach FTR and thioredoxin *m* by mutating the respective non accessible Cys resulting in a nucleophilic accessible thiol on each protein.
Unfortunately, while this active-site mutagenesis approach produced two stable mutants for thioredoxin *m* (C40S and C40A), we failed to obtain mutant FTR. The failure to obtain a stable active-site mutant for FTR could be explained by the fact that mutagenesis presents some limitations. In fact, the theoretical assumption that Serine and Alanine are equivalent in replacing the Cysteine residue is not true. In our specific case, we have clearly demonstrated that the mutation on Cys84 on the active site of spinach FTR with Ser, produced an unstable mutant that disintegrates the Fe-S cluster. This result is also confirmed by active-site mutagenesis on *syn* FTR where the equivalent mutant produces the same effect. By contrast, the

substitution of the inaccessible Cys87 on the active site of *syn* FTR with a hydrophobic residue such as Ala does yield a stable mutant (preliminary results obtained in our lab by a student).
Since the catalytic subunit of spinach FTR presents a free, accessible and well-conserved cysteine (Cys27) which is located on the thioredoxin-interaction side, we also mutated this cysteine to a serine. This mutation did not seem to produce relevant functional effects on FTR, but the route of electron transfer is influenced as demonstrated by affinity studies between FTR and thioredoxins in this work. Obviously, more information about the properties of C27S mutant would be needed such as the effects produced by mutation on the structure of FTR and especially the role of this free residue in the interaction with thioredoxin, before we can draw a definite conclusion.

The preliminary studies on the capacity of FTR to reduce both chloroplastic thioredoxins revealed that FTR seems to be more efficient in the reduction of thioredoxin *f* than thioredoxin *m* although the E_m is rather similar for both thioredoxins.

The re-investigation of the redox potentials of the three proteins involved in the regulatory pathway, (FTR, thioredoxin *f* and *m*), studied in this thesis, has shown a E_m for thioredoxin *f* and *m* of –290 mV and –300 mV respectively, whereas the E_m value at pH 7.0 for spinach FTR is –320 mV. This means that the difference of –30 mV for the reduction of the active-site disulfides of thioredoxin *f* and *m* by the two cysteines at the active site of reduced FTR is sufficient to reduce both thioredoxins efficiently.

Our very preliminary results on the affinity between FTR and thioredoxins suggest that the affinities are not equal. This can be explained by the differences in the interaction area of the two thioredoxins, as reported by crystallization studies (Capitani *et al.*, 2000). Considering these studies, it is evident that there is a different charge distribution on the FTR-interaction area of the thioredoxins and this might play an essential role. We have shown that the hydrophobic residues of thioredoxin *f* are important, since the interaction site of FTR is rather hydrophobic. This could explain the difference in affinities between FTR and thioredoxin *f* or *m.* To clarify this, it will be interesting to produce mutations on the principal residues of thioredoxins that were proposed to be responsible in orienting thioredoxins correctly in the interaction with FTR.
However, we do not dismiss the possibility that the approach we have used to investigate the affinity of FTR with thioredoxins, is not entirely conclusive because other factors can influence the interaction (i.e. pH, target enzymes, methylviologen). In addition, as both FTR and thioredoxin possess reducible disulfide bridges, no direct measurement of thioredoxin reduction by the enzyme

has been possible so far, and the complete demonstration of this hypothesis will require additional experiments.
Future perspectives involve the measurement of the direct electron transfer between FTR and thioredoxins by reduction of FTR with methylviologen or by light-reduced deazaflavine.
Although the interaction between FTR and thioredoxins occurs via the formation of a mixed disulfide heterodimer, the complex between FTR and ferredoxin (the first electron transfer step in ferredoxin/thioredoxin system) is stabilized by electrostatic interactions to which Fd contributes mainly the negative charges. In this interaction, mutational studies demonstrated that the residue E92 in the acidic cluster of Fd (E92-94) is essential in electron transfer (Jacquot *et al*., 1997). The results obtained by Jacqout *et al*., 1997 have shown that in *Chlamydomonas* only this residue is involved in the electron transfer. We have demonstrated that in spinach ferredoxin all three acidic residues are essential and their replacement reduces the efficiency of electron transport as well as the affinity in the interaction between the two proteins. However, to corroborate these results, it would be interesting to investigate, by mutational studies, the role of other residues on FTR involved in the interaction with ferredoxin.

In conclusion, the principal goal consisting in obtaining a triple complex was not reached. However, several of our results can give a precious help to understand the complexity of the ferredoxin/thioredoxin system and could provide new approaches in order to deepen the knowledge of this interesting regulatory system.

11 References

Aguilar, F., Brunner, B., Gardet-Salvi, L., Stutz, E. and Schürmann, P. (1992). Biosynthesis of active spinach-chloroplast thioredoxin *f* in transformed *E.coli*. Plant Mol.Biol. 20: 301-306.

Aliverti, A. and Zanetti, G. (1997). A three-domain iron-sulfur flavoprotein obtained through gene fusion of ferredoxin and ferredoxin-$NADP^+$ reductase from spinach leaves. Biochemistry 36: 14771-14777.

Aliverti, A., Livraghi, A., Piubelli, L. and Zanetti, G. (1997). On the role of the acidic cluster Glu 92-94 of spinach ferredoxin I. Biochimica et Biophysica Acta: Protein Structure and Molecular Enzymology 1342: 45-50.

Balmer, Y. and Schürmann, P. (2001). Heterodimer formation between thioredoxin *f* and fructose 1,6-bisphosphatase from spinach chloroplasts. FEBS Letters 492: 58-61.

Balmer, Y., Stritt-Etter, A.-L., Hirasawa, M., Jacquot, J.-P., Keryer, E., Knaff, D.B. and Schürmann, P. (2001). Oxidation-reduction and activation properties of chloroplast fructose 1,6-bisphosphatase with mutated regulatory site. Biochemistry 40: 15444-15450.

Barettino, D., Feigenbutz, M., Valcàrel, R. and Stunnenberg, H.G. (1994). Improved method for PCR-mediated site-directed mutagenesis. Nucleic Acids Research 22: 541-542.

Beinert, H., Holm, R.H. and Munck, E. (1997). Iron-sulfur clusters: nature's modular, multipurpose structures. Science 277: 653-659.

Binda, C., Coda, A., Aliverti, A., Zanetti, G. and Mattevi, A. (1998). Structure of Mutant E92K of [2Fe-2S] Ferredoxin I from *Spinacia oleracea* at 1.7 Å Resolution. Acta Crystallographica D54: 1353-1358.

Buchanan, B.B. (1980). Role of light in the regulation of chloroplast enzymes. Annu.Rev.Plant Physiol.Plant Mol.Biol. 31: 341-374.

Buchanan, B.B. (1991). Regulation of CO_2 assimilation in oxygenic photosynthesis: The ferredoxin/thioredoxin system: Perspective on its discovery, present status, and future development. Arch.Biochem.Biophys. 288: 1-9.

Buchanan, B.B., Schürmann, P., Decottignies, P. and Lozano, R.M. (1994). Thioredoxin: a multifunctional regulatory protein with a bright future in technology and medicine. Arch.Biochem.Biophys. 314: 257-260.

Buchanan, B.B., Schürmann, P. and Jacquot, J.-P. (1994). Thioredoxin and metabolic regulation. Seminars in Cell Biology 5: 285-293.

Capitani, G., Markovic-Housley, Z., del Val, G., Morris, M., Jansonius, J.N. and Schürmann, P. (2000). Crystal structures of two functionally different thioredoxins in spinach chloroplasts. J.Mol.Biol. 302: 135-154.

Carr, P.D., Verger, D., Ashton, A.R. and Ollis, D.L. (1999). Chloroplast NADP-malate dehydrogenase: Structural basis of light-dependent regulation of activity by thiol oxidation and reduction. Structure 7: 461-475.

Chiadmi, M., Navaza, A., Miginiac-Maslow, M., Jacquot, J.-P. and Cherfils, J. (1999). Redox signalling in the chloroplast: structure of oxidized pea fructose-1,6-bisphosphate phosphatase. EMBO J. 18: 6809-6815.

Chivers, P.T., Prehoda, K.E., Volkman, B.F., Kim, B.M., Markley, J.L. and Raines, R.T. (1997). Microscopic pK_a values of *Escherichia coli* thioredoxin. Biochemistry 36: 14985-14991.

Chivers, P.T., Prehoda, K.E. and Raines, R.T. (1997). The CXXC motif: A rheostat in the active site. Biochemistry 36: 4061-4066.

Chow, L.-P., Iwadate, H., Yano, K., Kamo, M., Tsugita, A., Gardet-Salvi, L., Stritt-Etter, A.-L. and Schürmann, P. (1995). Amino acid sequence of spinach ferredoxin:thioredoxin reductase catalytic subunit and identification of thiol groups constituting a redox active disulfide and a [4Fe-4S] cluster. Eur.J.Biochem. 231: 149-156.

Dai, S., Schwendtmayer, C., Ramaswamy, S., Eklund, H. and Schürmann, P. (1998). Crystallization and crystallographic investigations of ferredoxin:thioredoxin reductase from *Synechocystis* sp.PCC6803. In: *Photosynthesis: Mechanisms and Effects* (Garab, G., ed.), Vol. 3, pp. 1931-1934. Kluwer Academic Publishers, Dordrecht.

Dai, S. (1998). Structural and Functional Studies of NADPH and Ferredoxin Dependent Thioredoxin Reductases. Thesis/Dissertation. Swedish University of Agricultural Sciences, Uppsala

Dai, S., Schwendtmayer, C., Schürmann, P., Ramaswamy, S. and Eklund, H. (2000). Redox signaling in chloroplasts: Cleavage of disulfides by an iron-sulfur cluster. Science 287: 655-658.

Dai, S., Schwendtmayer, C., Johansson, K., Ramaswamy, S., Schürmann, P. and Eklund, H. (2000). How does light regulate chloroplast enzymes? Structure - function studies of the ferredoxin/thioredoxin system. Quarterly Reviews of Biophsics 33: 67-108.

De La Torre, A., Lara, C., Yee, B.C., Malkin, R. and Buchanan, B.B. (1982). Physiochemical properties of ferralterin, a regulatory iron-sulfur protein functional in oxygenic photosynthesis. Arch.Biochem.Biophys. 213: 545-550.

De Pascalis, A.R., Schürmann, P. and Bosshard, H.R. (1994). Comparison of the binding sites of plant ferredoxin for two ferredoxin-dependent enzymes. FEBS Letters 337: 217-220.

del Val, G., Maurer, F., Stutz, E. and Schürmann, P. (1999). Modification of the reactivity of spinach chloroplast thioredoxin *f* by site-directed mutagenesis. Plant Science 149: 183-190.

Droux, M., Jacquot, J.-P., Miginiac-Maslow, M., Gadal, P., Huet, J.C., Crawford, N.A., Yee, B.C. and Buchanan, B.B. (1987). Ferredoxin-thioredoxin reductase, an iron-sulfur enzyme linking light to enzyme regulation in oxygenic photosynthesis: purification and properties of the enzyme from C3, C4, and cyanobacterial species. Arch.Biochem.Biophys. 252: 426-439.

Fukuyama, K., Ueki, N., Nakamura, H., Tsukihara, T. and Matsubara, H. (1995). Tertiary structure of [2Fe-2S] ferredoxin from *Spirulina platensis* refined at 2.5 Å resolution: Structural comparisons of plant-type ferredoxins and an electrostatic potential analysis. J.Biochem.(Tokyo) 117: 1017-1023.

Gardemann, A., Schimkat, D. and Heldt, H.W. (1986). Control of CO_2 fixation. Regulation of stromal fructose-1,6-bisphosphatase in spinach by pH and Mg^{2+} concentration. Planta 168: 536-545.

Gaymard, E. and Schürmann, P. (1995). Cloning and expression of cDNAs coding for the spinach ferredoxin:thioredoxin reductase. In: *Photosynthesis: from Light to Biosphere* (Mathis, P., ed.), Vol. 2, pp. 761-764. Kluwer Academic Publishers, Dordrecht.

Gaymard, E., Franchini, L., Manieri, W., Stutz, E. and Schürmann, P. (2000). A dicistronic construct for the expression of functional spinach chloroplast ferredoxin:thioredoxin reductase in *E.coli*. Plant Science 158: 107-113.

Geck, M.K., Larimer, F.W. and Hartman, F.C. (1996). Identification of residues of spinach thioredoxin *f* that influence interactions with target enzymes. J.Biol.Chem. 271: 24736-24740.

Geck, M.K. and Hartman, F.C. (2000). Kinetic and mutational analyses of the regulation of phosphoribulokinase by thioredoxins. J.Biol.Chem. 275: 18034-18039.

Goyer, A., Decottignies, P., Lemaire, S., Ruelland, E., Issakidis-Bourguet, E., Jacquot, J.-P. and Miginiac-Maslow, M. (1999). The internal Cys207 of sorghum leaf NADP-malate dehydrogenase can form mixed disulfides with thioredoxin. FEBS Letters 444: 165-169.

Goyer, A., Decottignies, P., Issakidis-Bourguet, E. and Miginiac-Maslow, M. (2001). Sites of interaction of thioredoxin with sorghum NADP-malate dehydrogenase. FEBS Letters 505: 405-408.

Habeeb, A.F.S.A. (1972). Reaction of protein sulfhydryl groups with Ellman's reagent. In: *Enzyme Structure, Part B* (Hirs, C.H.W. and Timasheff, S.N., eds.), Methods in Enzymology, Vol. 25, pp. 457-464. Academic Press, New York, London.

Hermoso, R., Lázaro, J.J., Chueca, A., Sahrawy, M. and López-Gorgé, J. (1999). Purification and binding features of a pea fructose-1,6-bisphosphatase domain involved in the interaction with thioredoxin *f*. Physiologia Plantarum 105: 756-762.

Hirasawa, M., Droux, M., Gray, K.A., Boyer, J.M., Davis, D.J., Buchanan, B.B. and Knaff, D.B. (1988). Ferredoxin-thioredoxin reductase: Properties of its complex with ferredoxin. Biochim.Biophys.Acta 935: 1-8.

Hirasawa, M., Schürmann, P., Jacquot, J.-P., Manieri, W., Jacquot, P., Keryer, E., Hartman, F.C. and Knaff, D.B. (1999). Oxidation-reduction properties of chloroplast thioredoxins, ferredoxin:thioredoxin reductase and thioredoxin *f*-regulated enzymes. Biochemistry 38: 5200-5205.

Holmgren, A. (1979). Thioredoxin catalyzes the reduction of insulin disulfides by dithiothreitol and dihydrolipoamide. J.Biol.Chem. 254: 9627-9632.

Huppe, H.C., Lamotte-Guéry, F.d., Jacquot, J.-P. and Buchanan, B.B. (1990). The ferredoxin-thioredoxin system of a green alga, *Chlamydomonas reinhardtii*. Identification and characterization of thioredoxins and ferredoxin-thioredoxin reductase components. Planta 180: 341-351.

Hutchison, R.S. (1994). Thioredoxin-mediated reduction of photosynthetic carbon production enzymes following chilling in the light. Thesis/Dissertation. University of Illinois

Hutchison, R.S. and Ort, D.R. (1995). Measurement of equilibrium midpoint potentials of thiol/disulfide regulatory groups on thioredoxin-activated chloroplast enzymes. In: *Biothiols Part B; Glutathione and Thioredoxin: Thiols in Signal Transduction and Gene Regulation* (Packer, L., ed.), Methods in Enzymology, Vol. 252, pp. 220-228. Academic Press, San Diego.

Hutchison, R.S., Groom, Q. and Ort, D.R. (2000). Differential effects of low temperature induced oxidation on thioredoxin mediated activation of photosynthetic carbon reduction cycle enzymes. Biochemistry 39: 6679-6688.

Issakidis, E., Saarinen, M., Decottignies, P., Jacquot, J.-P., Crétin, C., Gadal, P. and Miginiac-Maslow, M. (1994). Identification and characterization of the second regulatory disulfide bridge of recombinant sorghum leaf NADP-malate dehydrogenase. J.Biol.Chem. 269: 3511-3517.

Issakidis, E., Lemaire, M., Decottignies, P., Jacquot, J.-P. and Miginiac-Maslow, M. (1996). Direct evidence for the different roles of the N- and C-terminal regulatory disulfides of sorghum leaf NADP-malate dehydrogenase in its activation by reduced thioredoxin. FEBS Letters 392: 121-124.

Iwadate, H., Tsugita, A., Chow, L.-P., Kizuki, K., Stritt-Etter, A.-L., Li, J. and Schürmann, P. (1996). Amino acid sequence of the maize ferredoxin:thioredoxin reductase variable subunit. Eur.J.Biochem. 241: 121-125.

Iwadate, H., Kizuki, K., Schürmann, P. and Tsugita, A. (1998). Primary structure of maize ferredoxin:thioredoxin reductase catalytic subunit. Research Communications in Biochemistry, Cell and Molecular Biology 2: 105-112.

Jacquot, J.-P., Issakidis, E., Decottignies, P., Lemaire, M. and Miginiac-Maslow, M. (1995). Analysis and manipulation of target enzymes for thioredoxin control. In: *Biothiols, Part B* (Packer, L., ed.), Methods in Enzymology, Vol. 252, pp. 240-252. Academic Press, San Diego, USA.

Jacquot, J.-P., Stein, M., Suzuki, K., Liottet, S., Sandoz, G. and Miginiac-Maslow, M. (1997). Residue Glu-91 of *Chlamydomonas reinhardtii* ferredoxin is essential for electron transfer to ferredoxin-thioredoxin reductase. FEBS Letters 400: 293-296.

Johansson, K., Ramaswamy, S., Saarinen, M., Lemaire-Chamley, M., Issakidis-Bourguet, E., Miginiac-Maslow, M. and Eklund, H. (1999). Structural basis for light activation of a chloroplast enzyme. The structure of sorghum NADP-malate dehydrogenase in its oxidized form. Biochemistry 38: 4319-4326.

Johnson, B.H. and Hecht, M.H. (1994). Recombinant proteins can be isolated from *E.coli* cells by repeated cycles of freezing and thawing. BioTechnology 12: 1357-1360.

Kamo, M., Tsugita, A., Wiessner, Ch., Wedel, N., Bartling, D., Herrmann, R.G., Aguilar, F., Gardet-Salvi, L. and Schürmann, P. (1989). Primary structure of spinach-chloroplast thioredoxin *f* . Protein sequencing and analysis of complete cDNA clones for spinach-chloroplast thioredoxin *f*. Eur.J.Biochem. 182: 315-322.

Kosower, E.M. and Kosower, N.S. (1995). Bromobimane probes for thiols. In: *Biothiols, Part A* (Packer, L., ed.), Methods in Enzymology, Vol. 251, pp. 133-148. Academic Press, San Diego, USA.

Krimm, I., Lemaire, S., Ruelland, E., Miginiac-Maslow, M., Jaquot, J.P., Hirasawa, M., Knaff, D.B. and Lancelin, J.M. (1998). The single mutation Trp35-->Ala in the 35-40 redox site of *Chlamydomonas reinhardtii* thioredoxin *h* affects its biochemical activity and the pH dependence of C36-C39 ^{1}H-^{13}C NMR. European Journal of Biochemistry 255: 185-195.

Laemmli, U.K. and Favre, M. (1973). Maturation of the head of bacteriophage T 4. J.Mol.Biol. 80: 575-599.

Lamotte-Guéry, F.d., Miginiac-Maslow, M., Decottignies, P., Stein, M., Minard, P. and Jacquot, J.-P. (1991). Mutation of a negatively charged amino acid in thioredoxin modifies its reactivity with chloroplastic enzymes. Eur.J.Biochem. 196: 287-294.

Lancelin, J.-M., Stein, M. and Jacquot, J.-P. (1993). Secondary structure and protein folding of recombinant chloroplastic thioredoxin Ch2 from the green alga *Chlamydomonas reinhardtii* as determined by ^{1}H NMR. J.Biochem.(Tokyo) 114: 421-431.

López-Jaramillo, J., Chueca, A., Jacquot, J.-P., Hermoso, R., Lázaro, J.J., Sahrawy, M. and Gorgé, J.L. (1997). High-yield expression of pea thioredoxin *m* and assessment of its efficiency in chloroplast fructose-1,6-bisphosphatase activation. Plant Physiology 114: 1169-1175.

Maeda, K., Tsugita, A., Dalzoppo, D., Vilbois, F. and Schürmann, P. (1986). Further characterization and amino acid sequence of m-type thioredoxins from spinach chloroplasts. Eur.J.Biochem. 154: 197-203.

Mora-García, S., Ballícora, M.A. and Wolosiuk, R.A. (1996). Chloroplast fructose-1,6-bisphosphatase: Modification of non-covalent interactions promote the activation by chimeric *Escherichia coli* thioredoxins. FEBS Letters 380: 123-126.

Mora-García, S., Rodriguez-Suárez, R.J. and Wolosiuk, R.A. (1998). Role of electrostatic interactions on the affinity of thioredoxin for target proteins. Recognition of chloroplast fructose-1,6-bisphosphatase by mutant *Escherichia coli* thioredoxins. J.Biol.Chem. 273: 16273-16280.

Morris, M. (1993). Genetic Construction, Expression and Comparative Analysis of Reciprocal Hybrids of Spinach Thioredoxins f and m. Diploma. University of Neuchâtel

Ocón, E., Hermoso, R., Chueca, A. and Lázaro, J.J. (2001). Cross-linking between chloroplast fructose-1,6-bisphosphatase and thioredoxin *f*. Physiologia Plantarum 113: 452-460.

Piubelli, L., Aliverti, A., Bellintani, F. and Zanetti, G. (1996). Mutations of Glu92 in ferredoxin I from spinach leaves produce proteins fully functional in electron transfer but less efficient in supporting $NADP^+$ photoreduction. Eur.J.Biochem. 236: 465-469.

Prado, F.E., Lázaro, J.J., Hermoso, R., Chueca, A. and Gorgé, J.L. (1992). Purification and properties of pea (*Pisum sativum* L.) thioredoxin *f*, a plant thioredoxin with unique features in the activation of chloroplast fructose-1,6-bisphosphatase. Planta 188: 345-353.

Rebeille, F. and Hatch, M.D. (1986). Regulation of NADP-malate dehydrogenase in C4 plants: effect of varying NADPH to NADP ratios and thioredoxin redox state on enzyme activity in reconstituted systems. Arch.Biochem.Biophys. 249: 164-170.

Rebeille, F. and Hatch, M.D. (1986). Regulation of NADP-malate dehydrogenase in C4 plants: relationship among enzyme activity NADPH to NADP ratios and thioredoxin redox states in intact maize mesophyll chloroplasts. Arch.Biochem.Biophys. 249: 171-179.

Reche, A., Lázaro, J.J., Hermoso, R., Chueca, A. and Gorgé, J.L. (1997). Binding and activation of pea chloroplast fructose-1,6-bisphosphatase by homologous thioredoxins *m* and *f*. Physiologia Plantarum 101: 463-470.

Ruelland, E., Johansson, K., Decottignies, P., Djukic, N. and Miginiac-Maslow, M. (1998). The autoinhibition of sorghum NADP malate dehydrogenase is mediated by a C-terminal negative charge. J.Biol.Chem. 273: 33482-33488.

Salamon, Z., Tollin, G., Hirasawa, M., Knaff, D.B. and Schürmann, P. (1995). The Oxidation-Reduction Properties of Spinach Thioredoxins f and m and of Ferredoxin:Thioredoxin Reductase. Biochim.Biophys.Acta 1230: 114-118.

Sambrook, J., Maniatis, T. and Fritsch, E.F. (1989). Molecular cloning: A laboratory manual. Cold Spring Harbor Laboratory Press, New York.

Scheibe, R. and Jacquot, J.-P. (1983). NADP regulates the light activation of NADP-dependent malate dehydrogenase. Planta 157: 548-553.

Scheibe, R., Fickenscher, K. and Ashton, A.R. (1986). Studies on the mechanism of the reductive activation of NADP- malate dehydrogenase by thioredoxin m and low-molecular-weight thiols. Biochim.Biophys.Acta 870: 191-197.

Scheibe, R. (1991). Redox-modulation of chloroplast enzymes. A common principle for individual control. Plant Physiol. 96: 1-3.

Schürmann, P. and Wolosiuk, R.A. (1978). Studies on the regulatory properties of chloroplast fructose 1,6-bisphosphatase. Biochim.Biophys.Acta Enzymology 522: 130-138.

Schürmann, P. and Jacquot, J.-P. (1979). Improved in vitro light activation and assay systems for two spinach chloroplast enzymes. Biochim.Biophys.Acta Enzymology 569: 309-312.

Schürmann, P. (1981) The ferredoxin/thioredoxin system of spinach chloroplasts. Purification and characterization of its components. In: *Photosynthesis* (Akoyunoglou, G., ed.), Vol. 4, pp. 273-280. Balaban Intern. Sci. Services, Philadelphia, Pa.

Schürmann, P., Maeda, K. and Tsugita, A. (1981). Isomers in thioredoxins of spinach chloroplasts. Eur.J.Biochem. 116: 37-45.

Schürmann, P., Stritt-Etter, A.-L. and Li, J. (1995). Reduction of Ferredoxin:Thioredoxin Reductase by Artificial Electron Donors. Photosynth.Res. 46: 309-312.

Schürmann, P. (1995). The Ferredoxin/Thioredoxin System. In: *Biothiols Part B; Glutathione and Thioredoxin: Thiols in Signal Transduction and Gene*

Regulation (Packer, L., ed.), Methods in Enzymology, Vol. 252, pp. 274-283. Academic Press, Orlando, Florida 32887.

Schürmann, P. and Jacquot, J.-P. (2000). Plant thioredoxin systems revisited. (Jones, R.L., Bohnert, H.J., and Delmer, D.P., eds.), Annu.Rev.Plant Physiol.Plant Mol.Biol., Vol. 51, pp. 371-400. Annu.Reviews, Inc., Palo Alto, USA.

Schwendtmayer, C., Manieri, W., Hirasawa, M., Knaff, D.B. and Schürmann, P. (1998). Cloning, expression and characterization of ferredoxin:thioredoxin reductase from *Synechocystis* sp. PCC6803. In: *Photosynthesis: Mechanisms and Effects* (Garab, G., ed.), Vol. 3, pp. 1927-1930. Kluwer Academic Publishers, Dordrecht.

Staples, C.R., Ameyibor, E., Fu, W., Gardet-Salvi, L., Stritt-Etter, A.-L., Schürmann, P., Knaff, D.B. and Johnson, M.K. (1996). The nature and properties of the iron-sulfur center in spinach ferredoxin:thioredoxin reductase: a new biological role for iron-sulfur clusters. Biochemistry 35: 11425-11434.

Staples, C.R., Gaymard, E., Stritt-Etter, A.L., Telser, J., Hoffman, B.M., Schürmann, P., Knaff, D.B. and Johnson, M.K. (1998). Role of the [Fe_4S_4] cluster in mediating disulfide reduction in spinach ferredoxin: thioredoxin reductase. Biochemistry 37: 4612-4620.

Stout, C.D., Stura, E.A. and McRee, D.E. (1998). Structure of *Azotobacter vinelandii* 7Fe ferredoxin at 1.35 Å resolution and determination of the [Fe-S] bonds with 0.01 Å accuracy. J.Mol.Biol. 278: 629-639.

Towbin, H., Staehelin, T. and Gordon, J. (1979). Electrophoretic transfer of proteins from polyacrylamide gels to nitrocellulose sheets: Procedures and some applications. Proc.Natl.Acad.Sci.USA 76: 4350-4354.

Tsugita, A., Yano, K., Gardet-Salvi, L. and Schürmann, P. (1991). Characterization of spinach ferredoxin-thioredoxin reductase. Protein Seq.Data Anal. 4: 9-13.

Walker, M.C., Pueyo, J.J., Navarro, J.A., Gómez-Moreno, C. and Tollin, G. (1991). Laser flash photolysis studies of the kinetics of reduction of ferredoxins and ferredoxin-$NADP^+$ reductases from *Anabaena* PCC 7119 and spinach: Electrostatic effects on intracomplex electron transfer. Arch.Biochem.Biophys. 287: 351-358.

Wedel, N., Clausmeyer, S., Herrmann, R.G., Gardet-Salvi, L. and Schürmann, P. (1992). Nucleotide sequence of cDNAs encoding the entire precursor

polypeptide for thioredoxin *m* from spinach chloroplasts. Plant Mol.Biol. 18: 527-533.

Wolosiuk, R.A., Crawford, N.A., Yee, B.C. and Buchanan, B.B. (1979). Isolation of three thioredoxins from spinach leaves. J.Biol.Chem. 254: 1627-1632.